

1 **Impact of Timanian thrust systems on the late**
2 **Neoproterozoic–Phanerozoic tectonic evolution of the**
3 **Barents Sea and Svalbard**

4

5 Jean-Baptiste P. Koehl^{1,2,3,4}, Craig Magee⁵, Ingrid M. Anell⁶

6 ¹Centre for Earth Evolution and Dynamics (CEED), University of Oslo, PO Box 1028 Blindern, N-0315 Oslo,
7 Norway.

8 ²Department of Geosciences, UiT The Arctic University of Norway in Tromsø, N-9037 Tromsø, Norway.

9 ³Research Centre for Arctic Petroleum Exploration (ARCEX), UiT The Arctic University of Norway in Tromsø, N-
10 9037 Tromsø, Norway.

11 ⁴CAGE – Centre for Arctic Gas Hydrate, Environment and Climate, UiT The Arctic University of Norway in
12 Tromsø, N-9037 Tromsø, Norway.

13 ⁵School of Earth Science and Environment, University of Leeds, Leeds, LS2 9JT, United Kingdom.

14 ⁶Department of Geosciences, University of Oslo, P.O. Box 1047 Blindern, N-0316 Oslo, Norway.

15 **Correspondence:** Jean-Baptiste P. Koehl (jean-baptiste.koehl@uit.no)

16

17 **Abstract**

18 The Svalbard Archipelago ~~is composed~~consists of three basement terranes that record a
19 complex Neoproterozoic–Phanerozoic tectonic history, including four contractional events
20 (Grenvillian, Caledonian, Ellesmerian, and Eurekan) and two episodes of collapse- to rift-related
21 extension (Devonian–Carboniferous and late Cenozoic). ~~These Previous studies suggest these~~ three
22 terranes ~~are thought to have~~likely accreted during the early–mid Paleozoic Caledonian and
23 Ellesmerian orogenies. Yet recent geochronological analyses show that the northwestern and
24 southwestern terranes of Svalbard both record an episode of amphibolite (–eclogite) facies
25 metamorphism in the latest Neoproterozoic, which may relate to the 650–550 Ma Timanian
26 Orogeny identified in northwestern Russia, northern Norway and the Russian Barents Sea.
27 However, discrete Timanian structures have yet to be identified in Svalbard and the Norwegian
28 Barents Sea. Through analysis of seismic reflection, and regional gravimetric and magnetic data,
29 this study demonstrates the presence of continuous, several kilometers thick, NNE-dipping, deeply
30 buried thrust systems that extend thousands of kilometers from northwestern Russia to northeastern
31 Norway, the northern Norwegian Barents Sea, and the Svalbard Archipelago. The consistency in

32 orientation and geometry, and apparent linkage between these thrust systems and those recognized
33 as part of the Timanian Orogeny in northwestern Russia and Novaya Zemlya suggests that the
34 mapped structures are likely Timanian. If correct, these findings would ~~indicate~~imply that
35 Svalbard's three basement terranes and the Barents Sea were accreted onto northern Norway during
36 the Timanian Orogeny and should, hence, be attached to Baltica and northwestern Russia in future
37 Neoproterozoic–early Paleozoic plate tectonics reconstructions. In the Phanerozoic, the study
38 suggests that the interpreted Timanian thrust systems represented major preexisting zones of
39 weakness that were reactivated, folded, and overprinted by (i.e., controlled the formation of new)
40 brittle faults during later tectonic events. These faults are still active at present and can be linked
41 to folding and offset of the seafloor.

42

43 **Introduction**

44 Recognizing and linking tectonic events across different terranes is critical to plate
45 reconstructions. In the latest Neoproterozoic (at ca. 650–550 Ma), portions of northwestern Russia
46 (e.g., Timan Range and Novaya Zemlya) and the Russian Barents Sea were accreted to northern
47 Baltica by top-SSW thrusting during the Timanian Orogeny (Olovyanishnikov et al., 2000;
48 Kostyuchenko et al., 2006). Discrete Timanian structures with characteristic WNW–ESE strikes
49 are sub-orthogonal to the N–S-trending Caledonian grain formed during the closure of the Iapetus
50 Ocean (Gee et al., 1994; Witt-Nilsson et al., 1998; Johansson et al., 2004; 2005). Thus far,
51 Timanian structures have only been identified in onshore–nearshore areas of northwestern Russia
52 and northeastern Norway and offshore in the Russian Barents Sea and southeasternmost Norwegian
53 Barents Sea (Barrère et al., 2009, 2011; Marelló et al., 2010; Gernigon et al., 2018; Hassaan et al.,
54 2020a, 2020b). Therefore, the nature of basement rocks in the northern and southwestern
55 Norwegian Barents Sea remains debatable. Some studies suggest a NE–SW-trending Caledonian
56 suture within the Barents Sea (Gudlaugsson et al., 1998; Gee and Teben'kov, 2004; Breivik et al.,
57 2005; Gee et al., 2008; Knudsen et al., 2019), whereas others argue for a swing into a N–S trend
58 and merging of Norway and Svalbard's Caledonides, which ~~are expected to~~probably continue into
59 northern Greenland (Ziegler, 1988; Gernigon and Brönnér, 2012; Gernigon et al., 2014).
60 Regardless, these models solely relate basement structures in the northern and southwestern
61 Norwegian Barents Sea to the Caledonian Orogeny, implying that Laurentia and Svalbard were not
62 involved in the Timanian Orogeny and were separated from Baltica by the Iapetus Ocean in the

63 latest Neoproterozoic (Torsvik and Trench, 1991; Cawood et al., 2001; Cocks and Torsvik, 2005;
64 Torsvik et al., 2010; Merdith et al., 2021).

65 Nonetheless, geochronological data yielding Timanian ages suggest that deformation and
66 metamorphism contemporaneous of the Timanian Orogeny affected parts of the Svalbard
67 Archipelago and Laurentia and, possibly, all Arctic regions (Estrada et al., 2018; Figure 1
68 4a): (1) eclogite facies metamorphism (620–540 Ma; Peucat et al., 1989; Dallmeyer et al., 1990b)
69 and eclogite facies xenoliths of mafic–intermediate granulite in Quaternary volcanic rocks are
70 found in northern Spitsbergen (648–556 Ma; Griffin et al., 2012); (2) amphibolite facies
71 metamorphism (643 ± 9 Ma; Majka et al., 2008, 2012, 2014; Mazur et al., 2009) and WNW–ESE-
72 striking shear zones like the Vimsodden–Kosibapasset Shear Zone (VKSZ; Figure 1
73 b–c) occur in southwestern Spitsbergen (600–537 Ma; Manecki et al., 1998; Faehnrich et al., 2020); and (3)
74 xenoliths of the subduction-related Midtkap igneous suite in northern Greenland yield Timanian
75 ages (628–570 Ma; Rosa et al., 2016; Estrada et al., 2018). In addition, several recent studies also
76 show the presence of NW–SE- to E–W-trending basement grain in the Norwegian Barents Sea,
77 which could possibly represent Timanian fabrics and structures (Figure 1
78 4b; Barrère et al., 2009, 2011; Marelllo et al., 2010; Klitzke et al., 2019). Following these developments, a few paleo-
79 plate reconstructions now place Svalbard together with Baltica in the latest Neoproterozoic–
80 Paleozoic (e.g., Vernikovsky et al., 2011), and imply that the Norwegian Barents Sea and Svalbard
81 basement may contain Timanian structures overprinted during later (e.g., Caledonian) deformation
82 events.

83 To test the origin of basement grain in the northern Norwegian Barents Sea and Svalbard,
84 the present study focuses on several kilometers deep structures identified on 2D seismic reflection
85 data and correlated using regional gravimetric and magnetic data. These newly identified structures
86 trend WNW–ESE, i.e., parallel to the Timanian structural grain in northwestern Russia and
87 northern Norway (Figure 1
88 4a–c). The structures are described and interpreted based on their
89 geometry and potential kinematic indicators, and are compared to well-known examples of
90 Caledonian and Timanian fabrics and structures elsewhere, e.g., onshore Norway (e.g., NNE-
91 dipping Trollfjorden–Komagelva Fault Zone – TKFZ; Siedlecka and Siedlecki, 1967; Siedlecka,
92 1975), in Svalbard (e.g., gently north-plunging Atomfjella Antiform – AA; Witt-Nilsson et al.,
93 1998), in northwestern Russia (NNE-dipping Central Timan Fault – CTF; Siedlecka and Roberts,
1995; Olovyanishnikov et al., 2000; Kostyuchenko et al., 2006), and in the southern Norwegian

Formatted: Font: 12 pt, Not Bold

Formatted: Font: 12 pt, Not Bold, Not Italic

Formatted: Font: 12 pt, Not Bold

Formatted: Font: 12 pt, Not Bold, Not Italic

Formatted: Font: 12 pt, Not Bold

Formatted: Font: 12 pt, Not Bold, Not Italic

Formatted: Font: 12 pt, Not Bold

Formatted: Font: 12 pt, Not Bold, Not Italic

94 Barents Sea (Barrère et al., 2011; Gernigon et al., 2014) and the Russian Barents Sea (NNE-dipping
95 Baidaratsky fault zone – BaFZ; Lopatin et al., 2001; Korago et al., 2004; Figure 1b–c). The present
96 contribution proposes Aa scenario involving several episodes of deformation starting in the
97 ~~(~~Timanian Orogeny, and involving reactivation and overprinting of Timanian structures during the
98 Caledonian Orogeny, Devonian–Carboniferous extension, Triassic extension, Eurekan tectonism,
99 and present-day tectonism), ~~is proposed and~~ Having established that Timanian structure may be
100 present across the Barents Sea and Svalbard, we briefly discuss the potential implications for the
101 tectonic evolution of the Barents Sea and the Svalbard Archipelago and associated basins (e.g., Ora
102 and Olga basins; Anell et al., 2016) ~~are discussed~~.

Formatted: Font: 12 pt, Not Bold

Formatted: Font: 12 pt, Not Bold, Not Italic

103 Should our interpretation of discrete Timanian structures throughout the Norwegian
104 Barents Sea and Svalbard be validated by future research, it would support accretion of these
105 terranes to Baltica in the late Neoproterozoic and place the Caledonian suture farther west than is
106 commonly suggested (e.g., Breivik et al., 2005; Gernigon et al., 2014), thus leading to a major
107 revision of plate tectonics models. In addition, constraining the extent and reactivation history of
108 such faults may shed some light on their influence on younger tectonic events, such as Caledonian,
109 Ellesmerian and Eurekan contraction, Devonian–Carboniferous collapse–rifting, and late Cenozoic
110 breakup and ongoing extension.

111

112 **Geological setting**

113 *Timanian Orogeny*

114 The Timanian Orogeny corresponds to a ca. 650–550 Ma episode of NNE–SSW
115 contractional deformation that affected northwestern Russia and northeastern Norway. During this
116 tectonic episode, crustal-scale, WNW–ESE-striking, NNE-dipping thrusts systems with south-
117 southwestwards transport direction (top-SSW; Siedlecka and Siedlecki, 1967; Siedlecka, 1975;
118 Figure 1~~Figure 1b~~), accreted portions of the Russian Barents Sea and northwestern Russia onto
119 northeastern Baltica, including Novaya Zemlya, Severnaya Zemlya, the Kanin Peninsula, the
120 Timan Range, and the Kola Peninsula (Siedlecka and Roberts, 1995; Olovyaniishnikov et al.,
121 2000; Roberts and Siedlecka, 2002; Gee and Pease, 2004; Kostyuchenko et al., 2006; Lorenz et al.,
122 2008; Marelllo et al., 2013) and the Varanger Peninsula in northeastern Norway (Siedlecka and
123 Siedlecki, 1967; Siedlecka, 1975; Roberts and Olovyaniishnikov, 2004; Herrevold et al., 2009;
124 Drachev, 2016; Figure 1~~Figure 1a~~). Major Timanian thrusts include the NNE-dipping Baidaratsky

Formatted: Font: 12 pt, Not Bold

Formatted: Font: 12 pt, Not Bold, Not Italic

Formatted: Font: 12 pt, Not Bold

Formatted: Font: 12 pt, Not Bold, Not Italic

125 fault zone in the Russian Barents Sea and Novaya Zemlya (~~Figure 1~~Figure 1a–b; Eldholm and
126 Ewing, 1971, their figure 4 profile C–D; Lopatin et al., 2001; Korago et al., 2004; Drachev, 2016),
127 the NNE-dipping Central Timan Fault on the Kanin Peninsula and the Timan Range (Siedlecka
128 and Roberts, 1995; Olovyanishnikov et al., 2000; Kostyuchenko et al., 2006), and the NNE-dipping
129 Trollfjorden–Komagelva Fault Zone in northern Norway (Siedlecka and Siedlecki, 1967;
130 Siedlecka, 1975; Herrevold et al., 2009).

Formatted: Font: 12 pt, Not Bold

Formatted: Font: 12 pt, Not Bold, Not Italic

132 *Accretion of Svalbard basement terranes in the early Paleozoic*

133 The Svalbard Archipelago consists of three Precambrian basement terranes (Figure 2),
134 some of which show affinities with Greenland (northwestern and northeastern terranes), whereas
135 others are possibly derived from Pearya (southwestern terrane; Harland and Wright, 1979; Ohta et
136 al., 1989; Gee and Teben'kov, 2004; Labrousse et al., 2004; Piepjohn et al., 2013; Fortey and
137 Bruton, 2013). These terranes ~~are inferred to have possibly~~ accreted during the mid-Paleozoic
138 Caledonian (collision of Greenland with Svalbard and Norway at ca. 460–410 Ma; Horsfield, 1972;
139 Dallmeyer et al., 1990a; Johansson et al., 2004, 2005; Faehnrich et al., 2020) and Late Devonian
140 Ellesmerian orogenies (Piepjohn, 2000; Majka and Kosminska, 2017). In these models, accretion
141 was facilitated via hundreds of kilometers of displacement along (arcuate) N–S-striking strike-slip
142 faults, such as the Billefjorden Fault Zone (BFZ – Harland, 1969; Harland et al., 1992; Labrousse
143 et al., 2008) and the Lomfjorden Fault Zone (LFZ – Piepjohn et al., 2019; ~~Figure 2~~Figure 2),
144 although other studies suggest more limited strike-slip displacement (Lamar et al., 1986; Manby
145 and Lyberis, 1992; Manby et al., 1994; Lamar and Douglass, 1995). Some previous workers
146 assumed that ~~t~~These large (strike-slip?) faults ~~are assumed to have~~ extended thousands of
147 kilometers southwards and ~~to~~represented the continuation of Caledonian faults in Scotland (Norton
148 et al., 1987; Dewey and Strachan, 2003). Caledonian contraction resulted in the formation of large
149 fold and thrust complexes, such as the N–S-trending, gently north-plunging Atomfjella Antiform
150 in northeastern Spitsbergen (Gee et al., 1994; Witt-Nilsson et al., 1998) and the N–S-trending
151 Rjippdalen Anticline in Nordaustlandet (Johansson et al., 2004; 2005; Dumais and Brönnner, 2020),
152 whereas Ellesmerian tectonism ~~is thought to may~~ have formed narrow N–S-trending fold and thrust
153 belts, like the Dickson Land and Germaniahelvøya fold-thrust zones (McCann, 2000; Piepjohn,
154 2000; Dallmann and Piepjohn, 2020).

Formatted: Font: 12 pt, Not Bold

Formatted: Font: 12 pt, Not Bold, Not Italic

155 In northern Norway, Timanian thrusts were reactivated–overprinted in subsequent tectonic
156 events (e.g., Caledonian Orogeny and late–post-Caledonian collapse–rifting) as dominantly strike-
157 to oblique-slip faults (Siedlecka and Siedlecki, 1971; Roberts et al., 1991; Herrevold et al., 2009;
158 Rice, 2014). A notable example is the folding and reactivation of Timanian fabrics and structures
159 (e.g., [NNE-dipping](#) Trollfjorden–Komagelva Fault Zone) during the Caledonian Orogeny
160 (Siedlecka and Siedlecki, 1971; Herrevold et al., 2009) and intrusion of Mississippian dolerite
161 dykes along steeply dipping WNW–ESE-striking brittle faults that overprint the Trollfjorden–
162 Komagelva Fault Zone onshore–nearshore northern Norway (Roberts et al., 1991; Lippard and
163 Prestvik, 1997; Nasuti et al., 2015; Koehl et al., 2019).

164

165 *Late Paleozoic post-Caledonian collapse and rifting*

166 In the latest Silurian–Devonian, extensional collapse of the Caledonides led to the
167 deposition of several kilometers thick sedimentary basins such as the Devonian Graben in northern
168 Spitsbergen (Gee and Moody-Stuart, 1966; Friend et al., 1966; Friend and Moody-Stuart, 1972;
169 Murascov and Mokin, 1979; Manby and Lyberis, 1992; Manby et al., 1994; Friend et al., 1997;
170 McCann, 2000; Dallmann and Piepjohn, 2020). In places, N–S-trending basement ridges
171 potentially exhumed as metamorphic core complexes along bowed, reactivated detachments, such
172 as the Keisarhjelmen Detachment in northwestern Spitsbergen (Braathen et al., 2018).

173 In the latest Devonian–Mississippian, coal-rich sedimentary strata of the Billefjorden
174 Group were deposited within normal fault-bounded basins throughout Spitsbergen (Cutbill and
175 Challinor, 1965; Harland et al., 1974; Cutbill et al., 1976; Aakvik, 1981; Koehl and Muñoz-Barrera,
176 2018; Koehl, 2020a) and the Norwegian Barents Sea (Koehl et al., 2018a; Tonstad, 2018). As rift-
177 related normal faulting evolved, Pennsylvanian sedimentation was localized into a few, several
178 kilometers deep, N–S-trending basins like the Billefjorden Trough (Cutbill and Challinor, 1965;
179 Braathen et al., 2011; Koehl et al., 2021 in review) and the [E–W-trending](#) Ora Basin (Anell et al.,
180 2016). In the Permian, rift-related faulting stopped and platform carbonates were deposited
181 throughout Svalbard (Cutbill and Challinor, 1965) and the Barents Sea (Larssen et al., 2005).

182 Overall, the several kilometers thick, late Paleozoic sedimentary succession deposited
183 during late–post-Caledonian extension buried Proterozoic basement rocks. As a result, these rocks
184 are sparsely exposed and, thus, difficult to study.

185

186 ***Mesozoic sedimentation and magmatism***

187 In the Mesozoic, Svalbard and the Barents Sea remained tectonically quiet and were only
188 affected by minor Triassic normal faulting (e.g., Anell et al., 2013; Osmundsen et al., 2014; Ogata
189 et al., 2018; Smyrak-Sikora et al., 2020). In the Early Cretaceous, Svalbard was affected by a
190 regional episode of magmatism recorded by the intrusion of numerous dykes and sills of the
191 Diabasodden Suite (Senger et al., 2013).

192
193 ***Early Cenozoic Eurekan tectonism***

194 The opening of the Labrador Sea and Baffin Bay between Greenland and Arctic Canada in
195 the early Cenozoic (Chalmers and Pulvercraft, 2001; Oakey and Chalmers, 2012) led to the
196 collision of northern Greenland with Svalbard and the formation of a fold-and-thrust belt with top-
197 east thrusts and east-verging folds in western Spitsbergen (Dallmann et al., 1993). In eastern
198 Spitsbergen, this deformation event is characterized by dominantly thin-skinned deformation
199 structures, including décollements, some of which showing westwards transport directions
200 (Andresen et al., 1992; Haremo and Andresen, 1992). Notably, the N–S-striking Agardhbukta
201 Fault, a major splay/segment of the **N–S-striking** Lomfjorden Fault Zone, accommodated reverse
202 and, possibly, strike-slip movements during this event (Piepjohn et al., 2019).

203
204 ***Late Cenozoic opening of the Fram Strait***

205 After the end of extension in the Labrador Sea and Baffin Bay, the Fram Strait started to
206 open in the earliest Oligocene (Engen et al., 2008). Tectonic extension and break-up in the Fram
207 Strait resulted in the formation of two major, NW–SE-striking transform faults (Lowell, 1972;
208 Thiede et al., 1990; **Figure 1Figure 1b**).

209
210 **Methods and datasets**

211 Seismic surveys from the DISKOS database (see **Figure 1Figure 1b–c** and supplement S1
212 for location) were used to interpret basement-seated structures and related, younger, brittle
213 overprints (**Figure 3Figure 3a–f** and **Figure 4Figure 4a–h** and supplement S2). Other features of
214 interest include potential dykes, which commonly appear as high positive reflections on seismic
215 data. The geology interpreted from onshore seismic data was directly correlated to geological maps
216 of the Norwegian Polar Institute (e.g., Dallmann, 2015). Where possible, interpretation of offshore

Formatted: Font: 12 pt, Not Bold

Formatted: Font: 12 pt, Not Bold, Not Italic

Formatted: Font: 12 pt, Not Bold

Formatted: Font: 12 pt, Not Bold, Not Italic

Formatted: Font: 12 pt, Not Bold

Formatted: Font: 12 pt, Not Bold, Not Italic

Formatted: Font: 12 pt, Not Bold

Formatted: Font: 12 pt, Not Bold, Not Italic

217 seismic data was tied to onshore geological maps and to exploration wells Raddedalen-1 and
218 Plurdalen-1 on Edgeøya (Bro and Shvarts, 1983; Harland and Kelly, 1997) and to the Hopen-2 well
219 on Hopen (Anell et al., 2014; ~~Figure 1~~Figure 1c and supplement S3). The Raddedalen-1 well
220 penetrated 2823 meters of Upper Permian to Mississippian or Ordovician strata, the Plurdalen well
221 2351 meters of Middle Triassic to (pre-?) Devonian strata, and the Hopen-2 well 2840 meters of
222 Middle–Upper Triassic to Pennsylvanian strata (Bro and Shvarts, 1983; Harland and Kelly, 1997;
223 Anell et al., 2014; Senger et al., 2019). Note that the present contribution favors interpretation of
224 lower Paleozoic (Ordovician–Silurian) rocks in the Raddedalen-1 well by Bro and Shvarts (1983)
225 ~~is preferred~~ to that of upper Paleozoic (Upper Devonian–Mississippian) by Cambridge Svalbard
226 Exploration (see contrasting interpretations in Harland and Kelly, 1997). This is based on the more
227 detailed lithological, palynological and paleontological analyses by the former, and on the strong
228 contrast of the lithologies described in the well with Devonian–Mississippian successions on
229 Svalbard (Cutbill and Challinor, 1965; Cutbill et al., 1976; Friend et al., 1997; Dallmann and
230 Piepjohn, 2020).

231 The present contribution Only includes a few examples of seismic sections ~~are included~~
232 ~~in the present contribution~~. However, more interpreted and uninterpreted seismic data are available
233 as supplements (supplements S1–2) and from the Norwegian Petroleum Directorate (DISKOS
234 database). None of the seismic sections were depth-converted, and ~~the thicknesses are~~ therefore
235 appear discussed in seconds (Two-Way Time; TWT). However, local time conversion was
236 performed to tie seismic wells onshore Edgeøya to seismic section in Storfjorden and depth
237 conversion was performed locally to evaluate fault displacement. Velocities of Gernigon et al.
238 (2018) were used in these conversions. ~~Details related to these conversions are shown in~~
239 Ssupplement S3 includes further details related to these conversions.

240 The correlation of kilometer-thick structures discussed in the present contribution was also
241 tested using gravimetric and magnetic data in cross section (~~Figure 3~~Figure 3a–f) and regional
242 magnetic and gravimetric data in the northern Norwegian Barents Sea and Svalbard (Figure
243 5~~Figure 5~~ and supplement S4) from the Federal Institute for Geosciences and Natural Resources in
244 Germany in map view (Klitzke et al., 2019). Regional gravimetric and magnetic data are also used
245 to interpret deep basement fabrics and structures, e.g., regional folds (gravimetric highs commonly
246 associated with major anticlines of thickened dense basement (i.e., Precambrian) rocks and
247 gravimetric lows with synclines with less dense sedimentary basins) and large faults that commonly

Formatted: Font: 12 pt, Not Bold

Formatted: Font: 12 pt, Not Bold, Not Italic

Formatted: Font: 12 pt, Not Bold

Formatted: Font: 12 pt, Not Bold, Not Italic

Formatted: Font: 12 pt, Not Bold

Formatted: Font: 12 pt, Not Bold, Not Italic

248 correlate with elongated gravimetric and/or magnetic anomalies (e.g., Koehl et al., 2019), and to
249 discuss the relationship of the described structures with known structural trends in onshore
250 basement rocks in Russia, Norway and Svalbard.

251

252 **Results and interpretations**

253 First, the interpretation of seismic data are described by area, including (1) Storfjorden
254 (between Edgeøya and Spitsbergen) and the northeastern part of the Norwegian Barents Sea (east
255 of Edgeøya), (2) Nordmannsfonna to Sassenfjorden onshore–nearshore the eastern–central part of
256 Spitsbergen, and (3) the northwestern part of the Norwegian Barents Sea between Bjørnøya and
257 Spitsbergen (Figure 1b–c). Description in each area starts with deep Precambrian basement
258 rocks and shallow sedimentary rock units, and ends with deep brittle–ductile structures and with
259 shallow brittle faults. Then, potential field data and regional gravimetric and magnetic anomalies
260 in the Barents Sea and Svalbard are described, and compared and correlated to seismic data and to
261 major Timanian and Caledonian fabrics and structures onshore northwestern Russia, Svalbard and
262 Norway. Please see high resolution versions of all the figures and supplements on DataverseNO
263 (doi.org/10.18710/CE8RQH).

264

265 *Structures in the northwestern–northeastern Norwegian Barents Sea, Storfjorden and central–* 266 *eastern Spitsbergen*

267 *Storfjorden and northeastern Norwegian Barents Sea*

268 Folded Precambrian–lower Paleozoic basement rocks

269 Seismic facies at depths of 2–6 seconds (TWT) typically comprise successions of laterally
270 discontinuous (< three kilometers long), sub-horizontal, moderately curving–undulating,
271 moderate–high-amplitude seismic reflections that alternate with packages of highly-disrupted
272 and/or curved low-amplitude seismic reflections (see yellow lines within pink and purple units in
273 Figure 3a and Figure 4a). The curving geometries of the moderate–high amplitude
274 reflections display a typical kilometer- to hundreds of meter-scale wavelength and are commonly
275 asymmetric, seemingly leaning/verging towards the south/SSW (see yellow lines in Figure 4
276 4b). Based on ties with well bores on Edgeøya (Raddedalen-1 well; Bro and Shvarts, 1983; Harland
277 and Kelly, 1997), these asymmetric, undulate features most likely correspond to SSW-verging
278 folds in Precambrian–lower Paleozoic basement rocks. In places, apparent reverse offsets of these

Formatted: Font: 12 pt, Not Bold

Formatted: Font: 12 pt, Not Bold, Not Italic

Formatted: Font: 12 pt, Not Bold

Formatted: Font: 12 pt, Not Bold, Not Italic

Formatted: Font: 12 pt, Not Bold

Formatted: Font: 12 pt, Not Bold, Not Italic

Formatted: Font: 12 pt, Not Bold

Formatted: Font: 12 pt, Not Bold, Not Italic

279 undulate reflections align along moderately–gently north- to NNE-dipping surfaces (see red lines
280 in Figure 4 ~~Figure 4~~a and c), which are therefore interpreted as minor, top-south/SSW, brittle
281 thrusts.

Formatted: Font: 12 pt, Not Bold

Formatted: Font: 12 pt, Not Bold, Not Italic

282 Upper Paleozoic–Mesozoic sedimentary successions

283 In Storfjorden and the northwestern Norwegian Barents Sea, shallow (0–3 seconds TWT)
284 seismic reflections above folded and thrust Precambrian–lower Paleozoic basement rocks show
285 significantly more continuous patterns (>> five kilometers), gently curving–undulating geometries
286 and only local disruptions by shallow, dominantly NNE-dipping, high-angle listric disruptions (see
287 yellow lines within orange unit in Figure 3 ~~Figure 3~~a and c). In the northeastern Barents Sea, these
288 reflections are largely flat-lying (see yellow lines within orange unit in Figure 3 ~~Figure 3~~b and d).

Formatted: Font: 12 pt, Not Bold

Formatted: Font: 12 pt, Not Bold, Not Italic

289 Based on field mapping campaigns and well-bores in adjacent onshore areas of Spitsbergen,
290 Edgeøya, Hopen and Bjørnøya (see location in Figure 1 ~~Figure 1~~b), these continuous reflections are
291 interpreted as mildly folded upper Paleozoic–Mesozoic (–Cenozoic?) sedimentary strata
292 (Dallmann and Krasil’scikov, 1996; Harland and Kelly, 1997; Worsley et al., 2001; Dallmann,
293 2015). The Permian–Triassic boundary was correlated throughout the northern Norwegian Barents
294 Sea and Storfjorden by using the tie of Anell et al. (2014) to the Hopen-2 well.

Formatted: Font: 12 pt, Not Bold

Formatted: Font: 12 pt, Not Bold, Not Italic

Formatted: Font: 12 pt, Not Bold

Formatted: Font: 12 pt, Not Bold, Not Italic

Formatted: Font: 12 pt, Not Bold

Formatted: Font: 12 pt, Not Bold, Not Italic

295 Deep thrust systems

296 The packages of sub-horizontal, moderately curving–undulating (folded Precambrian–
297 lower Paleozoic basement) reflections alternate laterally from north to south with 20–60 kilometers
298 wide, up to four seconds thick (TWT), upwards-thickening, wedge-shaped packages (areas with
299 high concentrations of black lines in Figure 3 ~~Figure 3~~a and d). These wide upwards-thickening
300 packages consist of two types of reflections. First, they include planar, continuous, gently–
301 moderately north- to NNE-dipping, sub-parallel, high-amplitude reflections that commonly merge
302 together downwards and that can be traced and correlated on several seismic sections in Storfjorden
303 (black lines in Figure 3 ~~Figure 3~~a). Upwards, these reflections terminate against high-amplitude
304 convex-upwards reflections interpreted as intra- Precambrian–lower Paleozoic basement
305 reflections (fuchsia lines in Figure 3 ~~Figure 3~~a and c) or continue as moderately NNE-dipping
306 disruption surfaces that offset these intra-basement reflections top-SSW (e.g., offset intra-
307 Precambrian unconformities in Figure 3 ~~Figure 3~~a and c and Figure 4 ~~Figure 4~~d).

Formatted: Font: 12 pt, Not Bold

Formatted: Font: 12 pt, Not Bold, Not Italic

Formatted: Font: 12 pt, Not Bold

Formatted: Font: 12 pt, Not Bold, Not Italic

Formatted: Font: 12 pt, Not Bold

Formatted: Font: 12 pt, Not Bold, Not Italic

Formatted: Font: 12 pt, Not Bold

Formatted: Font: 12 pt, Not Bold, Not Italic

Formatted: Font: 12 pt, Not Bold

Formatted: Font: 12 pt, Not Bold, Not Italic

308 Second, sub-parallel, high-amplitude reflections bound wedge-shaped, upwards-thickening
309 packages of asymmetric, curved, south- to SSW-leaning, moderately north- to NNE-dipping,

310 moderate-amplitude reflections showing narrow (< one kilometer wide) upwards-convex
311 geometries (Figure 4d). These asymmetric reflections also commonly appear as gently
312 north- to NNE-dipping packages of Z-shaped reflections bounded by sub-parallel, planar, high-
313 amplitude reflections (see yellow lines in Figure 4e). Asymmetric, south- to SSW-leaning,
314 convex-upwards reflections are interpreted as south- to SSW-verging fold anticlines reflecting
315 relatively low amounts of plastic deformation of layered rocks.

316 The alternation of packages of layered rocks folded into SSW-verging folds (yellow lines
317 in Figure 3a-c) with packages of planar, NNE-dipping, sub-parallel, high-amplitude
318 reflections (black lines in Figure 3a-c) suggest that the latter reflection packages represent
319 zones where initial layering was destroyed and/or possibly reoriented, i.e., areas that
320 accommodated larger amounts of deformation and tectonic displacement. Thus, planar, gently-
321 moderately north- to NNE-dipping, high-amplitude reflections (black lines in Figure 3a-
322 c) are interpreted as low-angle brittle-ductile thrust systems. We name these thrust systems (from
323 north to south) the Steiløya-Krylen (SKFZ), Kongsfjorden-Cowanodden (KCFZ),
324 Bellsundbanken (BeFZ), and Kinnhøgda-Daubjørnpynten fault zones (KDFZ; Figure 3a
325 and supplement S2a-b; see Figure 1c for location of the thrusts).

326 The relatively high-amplitude character of planar, NNE-dipping reflections within the
327 thrusts suggest that these tectonic structures consist of sub-parallel layers of rocks and minerals
328 with significantly different physical properties. A probable explanation for such laterally
329 continuous and consistently high-amplitude reflections is partial recrystallization of rocks layers-
330 mineral bands into rocks and minerals with significantly higher density along intra-thrust planes
331 that accommodated large amounts of displacement (e.g., mylonitization; Fountain et al., 1984;
332 Hurich et al., 1985). In places, packages of aggregates of Z-shaped reflections bounded upwards
333 and downwards by individual low-angle thrust surfaces are interpreted as forward-dipping duplex
334 structures (e.g., Boyer and Elliott, 1982) reflecting relatively strong plastic deformation between
335 low-angle, brittle-ductile (mylonitic?) thrusts (see yellow lines in Figure 4e).

336 The Kongsfjorden-Cowanodden, Bellsundbanken, and Kinnhøgda-Daubjørnpynten fault
337 zones can be traced east-southeast of Edgeøya as a similar series of 20-60 kilometers wide, up to
338 four seconds thick (TWT), upwards-thickening packages (e.g., black lines in Figure 3d
339 and supplements S2a). However, their imaging along NNW-SSE-trending seismic sections is
340 much more chaotic and it is more difficult to identify smaller structures (like south-verging folds

Formatted: Font: 12 pt, Not Bold

Formatted: Font: 12 pt, Not Bold, Not Italic

Formatted: Font: 12 pt, Not Bold

Formatted: Font: 12 pt, Not Bold, Not Italic

Formatted: Font: 12 pt, Not Bold

Formatted: Font: 12 pt, Not Bold, Not Italic

Formatted: Font: 12 pt, Not Bold

Formatted: Font: 12 pt, Not Bold, Not Italic

Formatted: Font: 12 pt, Not Bold

Formatted: Font: 12 pt, Not Bold, Not Italic

Formatted: Font: 12 pt, Not Bold

Formatted: Font: 12 pt, Not Bold, Not Italic

Formatted: Font: 12 pt, Not Bold

Formatted: Font: 12 pt, Not Bold, Not Italic

Formatted: Font: 12 pt, Not Bold

Formatted: Font: 12 pt, Not Bold, Not Italic

Formatted: Font: 12 pt, Not Bold

Formatted: Font: 12 pt, Not Bold, Not Italic

341 and minor thrusts) within each thrust system (e.g., supplement S2a). This suggests that these three
342 thrust systems strike oblique to NNW–SSE-trending seismic sections (supplement S2a), whereas
343 they are most likely sub-orthogonal to N–S- to NNE–SSW-trending seismic sections in Storfjorden
344 (Figure 3a). The only orientation that reconciles these seismic facies variations (i.e., well-
345 imaged on NNE–SSW-trending seismic sections and poorly imaged by NNW–SSE-trending
346 seismic sections; Figure 3a and supplement S2a) is an overall WNW–ESE strike.

347 South of each 20–60 kilometers wide packages of thrust surfaces and related fold and
348 duplex structures, seismic reflections representing Precambrian–lower Paleozoic basement rocks
349 typically appear as gently curved, convex-upwards, relatively continuous reflections showing sub-
350 horizontal seismic onlaps (see white arrows in Figure 3a–f). This suggests that
351 Precambrian–lower Paleozoic basement rocks most likely consist (meta-) sedimentary rocks
352 (analogous to those observed in northeastern Spitsbergen and Nordaustlandet; Harland et al., 1993;
353 Stouge et al., 2011) that were deposited in foreland and piggy-back basins ahead of each 20–60
354 kilometers wide packages (Figure 3a–f).

355 Hence, based on the upwards-thickening geometry of the packages of south- to SSW-
356 verging folds and of forward-dipping duplexes, on the top-SSW reverse offsets of intra-basement
357 reflections by low-angle brittle–ductile thrust surfaces, on the upwards truncation of these low-
358 angle thrusts by intra-basement reflections, and on the overlapping geometries of (meta-)
359 sedimentary basement rocks south of each set of top-SSW thrust surfaces, the 20–60 kilometers
360 wide, upwards-thickening, wedge-shaped packages are interpreted as crustal-scale, several
361 kilometers thick, north- to NNE-dipping, top-SSW, brittle–ductile thrust systems (see fault zones
362 with high concentration of black lines in Figure 3a–f). These thrust systems include low-
363 angle, brittle–ductile, mylonitic thrust surfaces (black lines in Figure 4d–e) separating
364 upwards-thickening thrust sheets that consist of gently to strongly folded basement rocks and
365 forward-dipping duplex structures (yellow lines in Figure 4d–e). These thrust sheets are
366 interpreted to reflect accretion and stacking from the north or north-northeast. The interpreted thrust
367 systems are comparable in seismic facies and thickness to kilometer-thick mylonitic shear zones in
368 the Norwegian North Sea (Phillips et al. 2016) and southwestern Norwegian Barents Sea (Koehl et
369 al., 2018).

370 N–S-trending folds

Formatted: Font: 12 pt, Not Bold

Formatted: Font: 12 pt, Not Bold, Not Italic

Formatted: Font: 12 pt, Not Bold

Formatted: Font: 12 pt, Not Bold, Not Italic

Formatted: Font: 12 pt, Not Bold

Formatted: Font: 12 pt, Not Bold, Not Italic

Formatted: Font: 12 pt, Not Bold

Formatted: Font: 12 pt, Not Bold, Not Italic

Formatted: Font: 12 pt, Not Bold

Formatted: Font: 12 pt, Not Bold, Not Italic

Formatted: Font: 12 pt, Not Bold

Formatted: Font: 12 pt, Not Bold, Not Italic, Check spelling and grammar

Formatted: Font: 12 pt, Not Bold

Formatted: Font: 12 pt, Not Bold, Not Italic, Check spelling and grammar

371 On E–W seismic cross sections, reflections of the Kongsfjorden–Cowanodden,
372 Bellsundbanken, and Kinnhøgda–Daudbjørnpynten fault zones define large, 50–100 kilometers
373 wide, U-shaped, symmetrical depressions (black lines in [Figure 3Figure 3b](#)) on the edge of which
374 they are truncated at a high angle and overlain by folded lower Paleozoic and mildly folded to flat-
375 lying upper Paleozoic (meta-) sedimentary rocks (purple and orange units with associated yellow
376 lines in [Figure 3Figure 3b](#)). In addition, within these U-shaped depressions, the thrust systems show
377 curving up and down, symmetrical geometries with 5–15 kilometers wavelength (yellow lines
378 within the pink unit in [Figure 3Figure 3b](#) and [Figure 4Figure 4f](#)). Also notice the kilometer- to
379 hundreds of meter-scale undulating pattern of 5–15 kilometers wide curved geometries (yellow
380 lines in [Figure 4Figure 4f](#)). Based on the truncation and abrupt upward disappearance of high-
381 amplitude seismic reflections characterizing the thrust systems, the high-angle truncation of the
382 thrusts is interpreted as a major erosional unconformity (dark blue line in [Figure 3Figure 3b](#) and
383 pink line in [Figure 4Figure 4f](#)), and the large U-shaped depressions as large N–S- to NNE–SSW-
384 trending, upright regional folds (black lines in [Figure 3Figure 3b](#)). Furthermore, the 5–15
385 kilometers wide, symmetrical, curved geometries and associated, kilometer- to hundreds of meter-
386 scale, undulating pattern of seismic reflections within the thrusts are interpreted as similarly (N–S-
387 to NNE–SSW-) trending, upright, parasitic macro- to meso-scale folds (yellow lines in [Figure](#)
388 [3Figure 3b](#) and [Figure 4Figure 4f](#)).

389 Shallow brittle faults

390 In places, near the top of the 20–60 kilometers wide thrust systems (Kongsfjorden–
391 Cowanodden, Bellsundbanken, and Kinnhøgda–Daudbjørnpynten fault zones), low-angle brittle–
392 ductile thrust surfaces merge upwards with high-angle to vertical, listric, north- to NNE-dipping
393 disruption surfaces at depths of c. 2–3 seconds (TWT; see red lines in [Figure 3Figure 3a](#) and d).
394 These listric disruption surfaces truncate shallow, laterally continuous reflections that display
395 gently curved, symmetric geometries in Storfjorden (yellow lines in [Figure 3Figure 3a](#)) and flat-
396 lying geometries in the northeastern Norwegian Barents Sea (yellow lines in [Figure 3Figure 3d](#)).
397 Notably, they show minor, down-NNE normal offsets, and related minor southwards thickening
398 (towards the disruption) of seismic sub-units within Devonian–Carboniferous (–Permian?)
399 sedimentary strata in the north, both in Storfjorden and the northeastern Barents Sea ([Figure](#)
400 [3Figure 3a–d](#) and white double arrows in [Figure 4Figure 4g](#)). In addition, they display minor
401 reverse offsets and associated gentle upright folding of shallow continuous reflections potentially

Formatted: Font: 12 pt, Not Bold

Formatted: Font: 12 pt, Not Bold, Not Italic

Formatted: Font: 12 pt, Not Bold

Formatted: Font: 12 pt, Not Bold, Not Italic

Formatted: Font: 12 pt, Not Bold

Formatted: Font: 12 pt, Not Bold, Not Italic

Formatted: Font: 12 pt, Not Bold

Formatted: Font: 12 pt, Not Bold, Not Italic

Formatted: Font: 12 pt, Not Bold

Formatted: Font: 12 pt, Not Bold, Not Italic

Formatted: Font: 12 pt, Not Bold

Formatted: Font: 12 pt, Not Bold, Not Italic

Formatted: Font: 12 pt, Not Bold

Formatted: Font: 12 pt, Not Bold, Not Italic

Formatted: Font: 12 pt, Not Bold

Formatted: Font: 12 pt, Not Bold, Not Italic

Formatted: Font: 12 pt, Not Bold

Formatted: Font: 12 pt, Not Bold, Not Italic

Formatted: Font: 12 pt, Not Bold

Formatted: Font: 12 pt, Not Bold, Not Italic

Formatted: Font: 12 pt, Not Bold

Formatted: Font: 12 pt, Not Bold, Not Italic

Formatted: Font: 12 pt, Not Bold

Formatted: Font: 12 pt, Not Bold, Not Italic

Formatted: Font: 12 pt, Not Bold

Formatted: Font: 12 pt, Not Bold, Not Italic

Formatted: Font: 12 pt, Not Bold

Formatted: Font: 12 pt, Not Bold, Not Italic

Formatted: Font: 12 pt, Not Bold

Formatted: Font: 12 pt, Not Bold, Not Italic

402 representing upper Mesozoic (–Cenozoic?) sedimentary deposits in Storfjorden (Figure 3a–c and e, and orange lines in Figure 4h). Note that flat-lying Mesozoic (–Cenozoic?)
403 sedimentary rocks are not offset in the northeastern Norwegian Barents Sea (Figure 3d).

404
405 Based on the observed normal offsets and southwards-thickening of Devonian–
406 Carboniferous (–Permian?) sedimentary strata north of these disruption surfaces (e.g., white double
407 arrows in Figure 4g), these are interpreted as syn-sedimentary Devonian–Carboniferous
408 normal faults. The minor reverse offsets and associated gentle upright folding of Mesozoic (–
409 Cenozoic?) sedimentary rocks in Storfjorden (e.g., orange lines in Figure 4h) suggest that
410 these normal faults were mildly inverted near Svalbard in the Cenozoic. However, it is unclear
411 whether inversion in Storfjorden initiated in the early Cenozoic or later. Nonetheless, minor reverse
412 offset and folding of the seafloor clearly indicate ongoing inversion along these faults (Figure
413 3a and c, and Figure 4h). Furthermore, considering the merging relationship
414 between these high-angle listric disruption surfaces and underlying shear zones (i.e., merging black
415 and red lines in Figure 3a and c–d), we propose that the formation of Devonian–
416 Carboniferous normal faults was controlled by the crustal-scale, north- to NNE-dipping (inherited)
417 thrust systems (Kongsfjorden–Cowanodden, Bellsundbanken, and Kinnhøgda–Daudbjørnpynten
418 fault zones).

419
420 *Nordmannsfunna–Sassenfjorden (eastern–central Spitsbergen)*
421 Deep thrust system and N–S-trending folds

422 Seismic data from Nordmannsfunna to Sassenfjorden in eastern Spitsbergen (see Figure
423 1c for location) show reflection packages including both planar, continuous, moderately-
424 dipping high-amplitude reflections and upwards-curving, moderate-amplitude reflections (black
425 and yellow lines in Figure 3e–f). These two sets are similar to reflection packages
426 interpreted as low-angle, brittle–ductile mylonitic thrusts bounding packages of south- to SSW-
427 verging folds in Storfjorden and the northeastern Norwegian Barents Sea (black and yellow lines
428 in Figure 3a and d, and supplement S2a). In addition, they are located at similar depths (>
429 2 seconds TWT) and seem to align with the Kongsfjorden–Cowanodden fault zone in Storfjorden
430 along a WNW–ESE-trending axis. Hence, we interpret the deep, continuous, high-amplitude
431 reflections in eastern Spitsbergen as the western continuation of the top-SSW Kongsfjorden–
432 Cowanodden fault zone. This thrust can be traced on seismic data as gently NNE-dipping, high-

Formatted: Font: 12 pt, Not Bold

Formatted: Font: 12 pt, Not Bold, Not Italic

Formatted: Font: 12 pt, Not Bold

Formatted: Font: 12 pt, Not Bold, Not Italic

Formatted: Font: 12 pt, Not Bold

Formatted: Font: 12 pt, Not Bold, Not Italic

Formatted: Font: 12 pt, Not Bold

Formatted: Font: 12 pt, Not Bold, Not Italic

Formatted: Font: 12 pt, Not Bold

Formatted: Font: 12 pt, Not Bold, Not Italic

Formatted: Font: 12 pt, Not Bold

Formatted: Font: 12 pt, Not Bold, Not Italic

Formatted: Font: 12 pt, Not Bold

Formatted: Font: 12 pt, Not Bold, Not Italic

Formatted: Font: 12 pt, Not Bold

Formatted: Font: 12 pt, Not Bold, Not Italic

Formatted: Font: 12 pt, Not Bold

Formatted: Font: 12 pt, Not Bold, Not Italic

Formatted: Font: 12 pt, Not Bold

Formatted: Font: 12 pt, Not Bold, Not Italic

Formatted: Font: 12 pt, Not Bold

Formatted: Font: 12 pt, Not Bold, Not Italic

433 amplitude reflections in Sassendalen and Sassenfjorden–Tempelfjorden (supplement S2c–d), and
434 possibly in Billefjorden (Koehl et al., 2021 in review, their figure 9a–b).

435 In Nordmannsonna, ~~the Kongsfjorden–Cowanodden fault zone (black lines in Figure 3e–~~
436 ~~f) is truncated upwards by~~ the base-Pennsylvanian unconformity (white line in ~~Figure 3~~Figure 3e–
437 f; tied to onshore geological maps; Dallmann, 2015) ~~truncates the Kongsfjorden–Cowanodden fault~~
438 ~~zone (black lines in Figure 3e–f) upwards and the fault~~ shows pronounced variations in dip
439 direction, ranging from east-dipping in the east to NNE-dipping in the north and WNW-dipping in
440 the west, which result into a c. 15–20 kilometers wide, north- to NNE-plunging dome-
441 shaped/convex-upwards geometry (black lines in ~~Figure 3~~Figure 3e–f). This portion of the thrust
442 system is interpreted to be folded into a major NNE- to north-plunging upright fold, whose 3D
443 geometry was accurately constrained due to good seismic coverage in this area (~~Figure 1~~Figure
444 4c).

445 Small-scale structures within the Kongsfjorden–Cowanodden fault zone also show
446 asymmetric folds and internal seismic units terminating upwards with convex-upwards reflections
447 (yellow lines in ~~Figure 3~~Figure 3e–f) suggesting top-SSW nappe thrusting in the northern portion
448 of the thrust system. However, on E–W cross sections, seismic data reveal a set of west-verging
449 folds in the east and a more chaotic pattern of symmetrical, dominantly upright folds in the west
450 (yellow lines in ~~Figure 3~~Figure 3e) and below a major, high-angle, east-dipping disruption surface
451 (thick red line in ~~Figure 3~~Figure 3e) that crosscuts the Kongsfjorden–Cowanodden fault zone.

452 Shallow brittle faults

453 The high-angle, east-dipping disruption surface (thick red line in ~~Figure 3~~Figure 3e) is
454 associated with minor subvertical to steeply east-dipping disruption surfaces (thin red lines in
455 ~~Figure 3~~Figure 3e). This feature shows a major reverse, top-west offset (> 0.5 second TWT) of
456 seismic units and reflections at depth > 0.75 second (TWT; e.g., black lines in ~~Figure 3~~Figure 3e),
457 and minor reverse offset (< 0.1 second TWT) and upwards-convex curving of adjacent reflections
458 at depth < 0.75 second (TWT; white line and yellow lines within blue and units in ~~Figure 3~~Figure
459 3e). Since the major disruption coincides with the location of the Agardhbukta Fault (Piepjohn et
460 al., 2019; see ~~Figure 1~~Figure 4 for location) and shows a steep inclination near the surface similar
461 to that of the Agardhbukta Fault, it is interpreted as the subsurface expression of this fault. The
462 Agardhbukta Fault offsets the Kongsfjorden–Cowanodden fault zone in a reverse fashion (>0.5
463 second TWT; black lines in ~~Figure 3~~Figure 3e), and terminates upwards within and slightly offsets

Formatted: Font: 12 pt, Not Bold

Formatted: Font: 12 pt, Not Bold, Not Italic

Formatted: Font: 12 pt, Not Bold

Formatted: Font: 12 pt, Not Bold, Not Italic

Formatted: Font: 12 pt, Not Bold

Formatted: Font: 12 pt, Not Bold, Not Italic

Formatted: Font: 12 pt, Not Bold

Formatted: Font: 12 pt, Not Bold, Not Italic

Formatted: Font: 12 pt, Not Bold

Formatted: Font: 12 pt, Not Bold, Not Italic

Formatted: Font: 12 pt, Not Bold

Formatted: Font: 12 pt, Not Bold, Not Italic

Formatted: Font: 12 pt, Not Bold

Formatted: Font: 12 pt, Not Bold, Not Italic

Formatted: Font: 12 pt, Not Bold

Formatted: Font: 12 pt, Not Bold, Not Italic

Formatted: Font: 12 pt, Not Bold

Formatted: Font: 12 pt, Not Bold, Not Italic

Formatted: Font: 12 pt, Not Bold

Formatted: Font: 12 pt, Not Bold, Not Italic

Formatted: Font: 12 pt, Not Bold

Formatted: Font: 12 pt, Not Bold, Not Italic

Formatted: Font: 12 pt, Not Bold

Formatted: Font: 12 pt, Not Bold, Not Italic

Formatted: Font: 12 pt, Not Bold

Formatted: Font: 12 pt, Not Bold, Not Italic

464 upper Paleozoic–Mesozoic sedimentary rocks (blue and black units and associated yellow lines in
465 Figure 3Figure 3e), which were correlated to onshore outcrops in eastern Spitsbergen (Andresen et
466 al., 1992; Haremo and Andresen, 1992; Dallmann, 2015). As a result, these rocks are folded into a
467 N–S-trending, open, upright fold around the fault tip, both of which suggest top-west movements
468 along the fault (Figure 3Figure 3e).

469 Pre-Pennsylvanian dykes

470 In the hanging wall and on the eastern flank of the folded Kongsfjorden–Cowanodden fault
471 zone in Nordmannsfunna, high- to low-amplitude, gently east-dipping seismic reflections, which
472 possibly represent sedimentary strata (light orange unit in Figure 3Figure 3e), are crosscut but not
473 offset by moderately west-dipping, high-amplitude planar reflections (blue lines in Figure 3Figure
474 3e). In NNE–SSW-trending cross-sections, these high-amplitude, cross-cutting seismic reflections
475 appear sub-horizontal (blue lines in Figure 3Figure 3f). These crosscutting, west-dipping
476 reflections are mildly folded in places and either terminate upwards within the suggested, gently
477 east-dipping, sedimentary strata (light orange unit in Figure 3Figure 3e) or are truncated by the
478 base-Pennsylvanian unconformity (white line in Figure 3Figure 3e). Downwards within the
479 Kongsfjorden–Cowanodden fault zone (black lines in Figure 3Figure 3e), these inclined reflections
480 can be vaguely traced as a series of discontinuous, subtle features (see blue lines in Figure 3Figure
481 3e). In the footwall of the Kongsfjorden–Cowanodden fault zone, the inclined reflections become
482 more prominent again, still do not offset background reflections, and extend to depths of 3–3.5
483 seconds (TWT; blue lines in Figure 3Figure 3e). The high amplitude of these planar west-dipping
484 reflections, the absence of offset across them, and their discontinuous geometries across the
485 Agardhbukta Fault and the Kongsfjorden–Cowanodden fault zone suggest that they may represent
486 dykes (see Phillips et al., 2018). Because they appear truncated by the Base-Pennsylvanian
487 unconformity, we suggest such dykes were emplaced prior to development of this unconformity.
488 The Kongsfjorden–Cowanodden fault zone is folded into a broad, 15–20 kilometers wide anticline,
489 and offset > 0.5 second (TWT) by the Agardhbukta Fault, whereas the west-dipping dykes (blue
490 lines in Figure 3Figure 3e) and the gently east-dipping sedimentary strata they intrude (light orange
491 unit in Figure 3Figure 3e) are only mildly folded and show no offset across the Agardhbukta Fault
492 (Figure 3Figure 3e). These differences in deformation suggest that the latter were deformed during
493 a mild episode of late contraction but not by the same early episode of intense contraction that
494 resulted in macrofolding of the Kongsfjorden–Cowanodden fault zone.

Formatted: Font: 12 pt, Not Bold

Formatted: Font: 12 pt, Not Bold, Not Italic

Formatted: Font: 12 pt, Not Bold

Formatted: Font: 12 pt, Not Bold, Not Italic

Formatted: Font: 12 pt, Not Bold

Formatted: Font: 12 pt, Not Bold, Not Italic

Formatted: Font: 12 pt, Not Bold

Formatted: Font: 12 pt, Not Bold, Not Italic

Formatted: Font: 12 pt, Not Bold

Formatted: Font: 12 pt, Not Bold, Not Italic

Formatted: Font: 12 pt, Not Bold

Formatted: Font: 12 pt, Not Bold, Not Italic

Formatted: Font: 12 pt, Not Bold

Formatted: Font: 12 pt, Not Bold, Not Italic

Formatted: Font: 12 pt, Not Bold

Formatted: Font: 12 pt, Not Bold, Not Italic

Formatted: Font: 12 pt, Not Bold

Formatted: Font: 12 pt, Not Bold, Not Italic

Formatted: Font: 12 pt, Not Bold

Formatted: Font: 12 pt, Not Bold, Not Italic

Formatted: Font: 12 pt, Not Bold

Formatted: Font: 12 pt, Not Bold, Not Italic

Formatted: Font: 12 pt, Not Bold

Formatted: Font: 12 pt, Not Bold, Not Italic

Formatted: Font: 12 pt, Not Bold

Formatted: Font: 12 pt, Not Bold, Not Italic

495 Cretaceous dykes and sills

496 Near or at the surface, thin, kilometer-wide, lenticular packages of gently dipping,
497 moderate–high-amplitude seismic reflections (black units in [Figure 3Figure 3e–f](#)) correlate with
498 surface outcrops of Cretaceous sills of the Diabasodden Suite in eastern Spitsbergen (Senger et al.,
499 2013; Dallmann, 2015). In places, these sills are associated with areas showing high-frequency
500 disruptions of underlying sub-horizontal seismic reflections (dotted black lines in [Figure 3Figure](#)
501 [3f](#)) correlated with onshore occurrences of Pennsylvanian–Mesozoic sedimentary strata (Andresen
502 et al., 1992; Haremo and Andresen, 1992; Dallmann, 2015). We interpret these areas of high-
503 frequency disruption in otherwise relatively undisturbed and only mildly deformed Pennsylvanian–
504 Mesozoic sedimentary strata as zones with occurrences of Cretaceous feeder dykes. Alternatively,
505 disruption may be related to scattering and attenuation of seismic energy caused on the sills.

506

507 *Stappen High (northwestern Norwegian Barents Sea north of Bjørnøya)*

508 On the Stappen High between Bjørnøya and Spitsbergen ([Figure 1Figure 1c](#)), seismic
509 reflections at depth of 2–6 seconds (TWT) are dominated by moderate- to high-amplitude
510 reflections with limited (< five kilometers) lateral continuity showing asymmetric, dominantly
511 SSW-leaning curving geometries with a few hundreds of meters to a few kilometers width (yellow
512 lines within pink unit in [Figure 3Figure 3c](#)), i.e., analogous to those in folded Precambrian
513 basement rocks farther north ([Figure 3Figure 3a](#) and [Figure 4Figure 4a](#)). These reflections are
514 truncated by gently to moderately NNE- (and subsidiary SSW-) dipping disruption surfaces (black
515 lines within pink and purple units in [Figure 3Figure 3c](#)), some of which connect upwards with
516 shallow (0–2 seconds TWT), NNE-dipping, high-angle listric disruptions near Bjørnøya in the
517 south (red lines in [Figure 3Figure 3c](#)). Notably, major seismic reflections near the upwards
518 termination of deep, moderately–gently NNE-dipping disruption surfaces display characteristic
519 gently curving-upwards geometries (yellow lines within pink and purple units in [Figure 3Figure](#)
520 [3c](#)) and overlying seismic onlaps (white half arrows in [Figure 3Figure 3c](#)) similar to those observed
521 just south of major NNE-dipping thrust systems in Storfjorden and the northeastern Norwegian
522 Barents Sea ([Figure 3Figure 3a](#) and supplement S2).

523 We interpret deep (2–6 seconds TWT), curving, discontinuous seismic reflections ((yellow
524 lines within pink and purple units in [Figure 3Figure 3c](#)) as folded Precambrian–lower Paleozoic
525 basement rocks, and dominantly NNE-dipping disruption surfaces (black lines within pink and

Formatted: Font: 12 pt, Not Bold

Formatted: Font: 12 pt, Not Bold, Not Italic

Formatted: Font: 12 pt, Not Bold

Formatted: Font: 12 pt, Not Bold, Not Italic

Formatted: Font: 12 pt, Not Bold

Formatted: Font: 12 pt, Not Bold, Not Italic

Formatted: Font: 12 pt, Not Bold

Formatted: Font: 12 pt, Not Bold, Not Italic

Formatted: Font: 12 pt, Not Bold

Formatted: Font: 12 pt, Not Bold, Not Italic

Formatted: Font: 12 pt, Not Bold

Formatted: Font: 12 pt, Not Bold, Not Italic

Formatted: Font: 12 pt, Not Bold

Formatted: Font: 12 pt, Not Bold, Not Italic

Formatted: Font: 12 pt, Not Bold

Formatted: Font: 12 pt, Not Bold, Not Italic

Formatted: Font: 12 pt, Not Bold

Formatted: Font: 12 pt, Not Bold, Not Italic

Formatted: Font: 12 pt, Not Bold

Formatted: Font: 12 pt, Not Bold, Not Italic

Formatted: Font: 12 pt, Not Bold

Formatted: Font: 12 pt, Not Bold, Not Italic

Formatted: Font: 12 pt, Not Bold

Formatted: Font: 12 pt, Not Bold, Not Italic

526 purple units in [Figure 3](#) as brittle–ductile thrust possibly partly mylonitic, though with
527 less intense deformation than the major NNE-dipping thrust systems observed farther north in
528 Storfjorden and the northeastern Norwegian Barents Sea, like the Kongsfjorden–Cowanodden fault
529 zone. These brittle–ductile thrusts can be traced eastwards on seismic data on the Stappen High
530 and into the Sørkapp Basin ([Figure 1](#)).

531 Based on their geometries and on gentle folding of the seafloor reflection (yellow lines
532 within green unit in [Figure 3](#)), shallow, NNE-dipping, high-angle listric disruptions are
533 interpreted as mildly inverted normal faults overprinting deep NNE-dipping thrusts. Based on
534 previous fieldwork on Bjørnøya (Worsley et al., 2001), on seismic mapping in the area (Lasabuda
535 et al., 2018), and on well tie to Hopen and Edgeøya, relatively continuous (> five kilometers)
536 shallow (0–2 seconds TWT), gently curved–undulating seismic reflections overlying folded
537 Precambrian–lower Paleozoic basement rocks are interpreted as mildly folded upper Paleozoic–
538 Mesozoic (–Cenozoic?) sedimentary strata (orange and green units in [Figure 3](#)).

540 *Potential field data and regional gravimetric and magnetic anomalies*

541 *NNE-dipping thrusts*

542 In the northern Barents Sea, Storfjorden and central–eastern Spitsbergen, the seismic
543 occurrences of the Kongsfjorden–Cowanodden, Bellsundbanken and Kinnhøgda–
544 Daudbjørnpynten fault zones coincide with gradual, step-like, southwards increases in gravimetry
545 and, in places, with high magnetic anomalies in cross-section ([Figure 3](#) a–b and d–f).
546 Similar southwards gradual and step-like increases in the Bouguer and magnetic anomalies
547 correlate with major thrusts north of Bjørnøya ([Figure 3](#) c; see [Figure 1](#) for
548 location of Bjørnøya). These patterns suggest that the footwall of the thrust systems consists of
549 relatively denser rock units, which is supported by seismic interpretation showing thickening of
550 metamorphosed and folded Precambrian basement rock units (pink unit in [Figure 3](#) a and
551 c–d) in the footwall of the thrusts further support this claim.

552 In map-view gravimetric and magnetic data, the three thrust systems in Storfjorden (black
553 lines in [Figure 3](#) a) coincide with three high, WNW–ESE-trending, continuous, gently
554 undulating (and, in place, merging/splaying) gravimetric and discontinuous magnetic anomalies
555 (dashed yellow lines in [Figure 5](#) a–c) that are separated from each other by areas showing
556 relatively low gravimetric and magnetic anomalies (e.g., see green to blue areas in [Figure 5](#)).

Formatted: Font: 12 pt, Not Bold

Formatted: Font: 12 pt, Not Bold, Not Italic

Formatted: Font: 12 pt, Not Bold

Formatted: Font: 12 pt, Not Bold, Not Italic

Formatted: Font: 12 pt, Not Bold

Formatted: Font: 12 pt, Not Bold, Not Italic

Formatted: Font: 12 pt, Not Bold

Formatted: Font: 12 pt, Not Bold, Not Italic

Formatted: Font: 12 pt, Not Bold

Formatted: Font: 12 pt, Not Bold, Not Italic

Formatted: Font: 12 pt, Not Bold

Formatted: Font: 12 pt, Not Bold, Not Italic

Formatted: Font: 12 pt, Not Bold

Formatted: Font: 12 pt, Not Bold, Not Italic

Formatted: Font: 12 pt, Not Bold, Not Italic

Formatted: Font: 12 pt, Not Bold

Formatted: Font: 12 pt, Not Bold, Not Italic

Formatted: Font: 12 pt, Not Bold

Formatted: Font: 12 pt, Not Bold, Not Italic

Formatted: Font: 12 pt, Not Bold

Formatted: Font: 12 pt, Not Bold, Not Italic

557 5a). Some of these anomalies extend from central Spitsbergen to Storfjorden and the northern
558 Barents Sea (below the Ora and Olga basins) as curving, E–W- and NW–SE-trending, 50–100
559 kilometers wide anomalies (dashed yellow lines in [Figure 5Figure 5a–c](#)). Analogously, thrust
560 systems north of Bjørnøya ([Figure 3Figure 3c](#)) and north of the Ora and Olga basins (supplement
561 S2b) correlate with comparable WNW–ESE-trending, curving magnetic and gravimetric anomalies
562 (dashed yellow lines in [Figure 5Figure 5a–c](#)). The WNW–ESE-trending anomalies appear clearer
563 by using a slope-direction shader [for gravimetric data](#), which accentuates the contrast between each
564 trend of anomalies (green and red areas in [Figure 5Figure 5b](#)).

565 Most of the recognized, regional WNW–ESE-trending magnetic and gravimetric anomalies
566 (dashed yellow lines in [Figure 5Figure 5a–c](#)) can be traced into the Russian Barents Sea where they
567 are linear and are crosscut by major N–S- to NNW–SSE-trending anomalies (dashed black and
568 white lines in [Figure 5Figure 5a–c](#)). Subtle WNW–ESE-trending magnetic and gravimetric
569 anomalies further extend onshore northwestern Russia (e.g., Kanin Peninsula and southern Novaya
570 Zemlya) where they correlate with major Timanian thrusts and folds, some of which are suspected
571 to extend thousands of kilometers between northwestern Russia and the Varanger Peninsula in
572 northern Norway (e.g., Trollfjorden–Komagelva Fault Zone and Central Timan Fault; Siedlecka,
573 1975; Siedlecka and Roberts, 1995; Olovyanishnikov et al., 2000; Kostyuchenko et al., 2006). In
574 addition, two of the southernmost WNW–ESE-trending gravimetric and magnetic anomalies
575 coincide with the location of well known, crustal-scale, SSW-verging Timanian thrust faults, the
576 Trollfjorden–Komagelva Fault Zone and the Central Timan Fault. Thus, based on their overall
577 WNW–ESE trend, patterns of alternating highs and lows both for gravimetric and magnetic
578 anomalies (see [Figure 5Figure 5a](#)), location at the boundary of oppositely dipping slopes (see slope-
579 direction shader map in [Figure 5Figure 5b](#)), and extensive field studies and seismic and well data
580 in northwestern Russia (e.g., Kanin Peninsula and Timan Range; Siedlecka and Roberts, 1995;
581 Olovyanishnikov et al., 2000; Kostyuchenko et al., 2006) and northern Norway (e.g., Varanger
582 Peninsula; Siedlecka, 1975), WNW–ESE-trending anomalies are interpreted as a combination of
583 basement-seated Timanian macrofolds and top-SSW reverse faults ([Figure 5Figure 5a–c](#)).

585 *N–S-trending folds*

586 Large N–S-trending open folds (e.g., black and yellow lines in [Figure 3Figure 3b](#)) coincide
587 with N–S- to NNE–SSW-trending, 20–100 kilometers wide, arcuate gravimetric and magnetic

Formatted: Font: 12 pt, Not Bold

Formatted: Font: 12 pt, Not Bold, Not Italic

Formatted: Font: 12 pt, Not Bold

Formatted: Font: 12 pt, Not Bold, Not Italic

Formatted: Font: 12 pt, Not Bold

Formatted: Font: 12 pt, Not Bold, Not Italic

Formatted: Font: 12 pt, Not Bold

Formatted: Font: 12 pt, Not Bold, Not Italic

Formatted: Font: 12 pt, Not Bold

Formatted: Font: 12 pt, Not Bold, Not Italic

Formatted: Font: 12 pt, Not Bold

Formatted: Font: 12 pt, Not Bold, Not Italic

Formatted: Font: 12 pt, Not Bold

Formatted: Font: 12 pt, Not Bold, Not Italic

Formatted: Font: 12 pt, Not Bold

Formatted: Font: 12 pt, Not Bold, Not Italic

Formatted: Font: 12 pt, Not Bold

Formatted: Font: 12 pt, Not Bold, Not Italic

Formatted: Font: 12 pt, Not Bold

Formatted: Font: 12 pt, Not Bold, Not Italic

Formatted: Font: 12 pt, Not Bold

Formatted: Font: 12 pt, Not Bold, Not Italic

Formatted: Font: 12 pt, Not Bold

Formatted: Font: 12 pt, Not Bold, Not Italic

Formatted: Font: 12 pt, Not Bold

Formatted: Font: 12 pt, Not Bold, Not Italic

Formatted: Font: 12 pt, Not Bold

Formatted: Font: 12 pt, Not Bold, Not Italic

Formatted: Font: 12 pt, Not Bold

Formatted: Font: 12 pt, Not Bold, Not Italic

Formatted: Font: 12 pt, Not Bold

Formatted: Font: 12 pt, Not Bold, Not Italic

588 anomalies (dashed white and black lines in [Figure 5Figure 5a-c](#)), which are highly oblique to
589 WNW–ESE-trending gravimetric and magnetic anomalies and thrust systems (dashed yellow lines
590 in [Figure 5Figure 5a-c](#)). Notably, major N–S- to NNE–SSW-trending synclines in [Figure 3Figure](#)
591 [3b](#) (marked as red lines over a white line in [Figure 5Figure 5a](#) and [c](#) and as pink lines over a red
592 line in [Figure 5Figure 5b](#)) coincides with similarly trending gravimetric and magnetic anomalies
593 (dashed black lines in [Figure 5Figure 5a](#) and [c](#) and dashed white lines in [Figure 5Figure 5b](#)). On
594 the slope-direction shader map [of gravimetric data](#), these N–S- to NNE–SSW-trending anomalies
595 are localized along the boundary between areas with eastwards- (ca. 90–100°; blue areas in [Figure](#)
596 [5Figure 5b](#)) and westwards-facing slopes (ca. 270–280°; white areas in [Figure 5Figure 5b](#)).

597 Notably where the main thrusts are preserved, major N–S-trending synforms (see 50–60
598 kilometers wide U-shaped depression formed by the Kinnhøgda–Daudbjørnpynten fault zone, i.e.,
599 black lines, in [Figure 3Figure 3b](#)) coincide with gravimetric and magnetic highs (white and black
600 dashed lines in [Figure 5Figure 5a-c](#)), whereas major antiforms where major NNE-dipping thrusts
601 are partly eroded (e.g., c. 100 kilometers wide areas where the Kinnhøgda–Daudbjørnpynten fault
602 zone is absent in [Figure 3Figure 3b](#)) coincide with gravimetric and magnetic lows (the lows are
603 parallel to white and black dashed lines symbolizing magnetic and gravimetric highs in [Figure](#)
604 [5Figure 5a-c](#)). The correlation of the interpreted NNE-dipping thrust systems with gravimetric
605 highs suggests that the thrusts consist of relatively denser rocks. This supports the inferred
606 mylonitic component of the thrusts because mylonites are relatively denser due to the formation of
607 high-density minerals with increasing deformation (e.g., Arbaret and Burg, 2003; Colombu et al.,
608 2015).

609 In the northwestern part of the Barents Sea (i.e., area covered by seismic data presented in
610 [Figure 3Figure 3](#)), N–S- to NNE–SSW-trending gravimetric and magnetic anomalies (white and
611 black dashed lines in [Figure 5Figure 5a-c](#)) are typically 20–50 kilometers wide and correlate with
612 similarly trending Caledonian folds and thrusts onshore Nordaustlandet (e.g., Rijpdalen Anticline;
613 Johansson et al., 2004; 2005; Dumais and Brønner, 2020) and northeastern Spitsbergen (e.g.,
614 Atomfjella Antiform; Gee et al., 1994; Witt-Nilsson et al., 1998), whose width is comparable to
615 that of the anomalies. In the south, N–S- to NNE–SSW-trending gravimetric and magnetic
616 anomalies merge together and swing into a NE–SW trend onshore–nearshore the Kola Peninsula
617 and northern Norway. These anomalies mimic the attitude of Caledonian thrusts and folds in the
618 southern Norwegian Barents Sea (Gernigon and Brønner, 2012; Gernigon et al., 2014) and onshore

Formatted: Font: 12 pt, Not Bold

Formatted: Font: 12 pt, Not Bold, Not Italic

Formatted: Font: 12 pt, Not Bold

Formatted: Font: 12 pt, Not Bold, Not Italic

Formatted: Font: 12 pt, Not Bold

Formatted: Font: 12 pt, Not Bold, Not Italic

Formatted: Font: 12 pt, Not Bold

Formatted: Font: 12 pt, Not Bold, Not Italic

Formatted: Font: 12 pt, Not Bold

Formatted: Font: 12 pt, Not Bold, Not Italic

Formatted: Font: 12 pt, Not Bold

Formatted: Font: 12 pt, Not Bold, Not Italic

Formatted: Font: 12 pt, Not Bold

Formatted: Font: 12 pt, Not Bold, Not Italic

Formatted: Font: 12 pt, Not Bold

Formatted: Font: 12 pt, Not Bold, Not Italic

Formatted: Font: 12 pt, Not Bold

Formatted: Font: 12 pt, Not Bold, Not Italic

Formatted: Font: 12 pt, Not Bold

Formatted: Font: 12 pt, Not Bold, Not Italic

Formatted: Font: 12 pt, Not Bold

Formatted: Font: 12 pt, Not Bold, Not Italic

Formatted: Font: 12 pt, Not Bold

Formatted: Font: 12 pt, Not Bold, Not Italic

Formatted: Font: 12 pt, Not Bold

Formatted: Font: 12 pt, Not Bold, Not Italic

Formatted: Font: 12 pt, Not Bold

Formatted: Font: 12 pt, Not Bold, Not Italic

Formatted: Font: 12 pt, Not Bold

Formatted: Font: 12 pt, Not Bold, Not Italic

619 northern Norway (Sturt et al., 1978; Townsend, 1987; Roberts and Williams, 2013). In the east, N-
620 S- to NNE-SSW-trending anomalies broaden to up to 150 kilometers in the Russian Barents Sea
621 (Figure 5a-c).

622 In places, the intersections of high, WNW-ESE- and N-S- to NNE-SSW-trending
623 gravimetric and magnetic anomalies generate relatively higher, oval-shaped anomalies (e.g., dotted
624 white lines in Figure 5a and c). Notable examples are found in the Ora and Olga basins
625 and east and south of these basins (see dotted white lines in Figure 5a and c).

627 Discussion

628 In the discussion, we consider the lateral extent of the interpreted NNE-dipping thrust
629 systems, their possible timing of formation, and potential episodes of reactivation and overprinting.
630 Then we briefly discuss the implications of these thrust systems for plate tectonics reconstructions
631 in the Arctic.

632 *Extent of NNE-dipping thrust systems*

634 Four major NNE-dipping systems of mylonitic thrusts and shear zones (Steiløya-Krylen,
635 Kongsfjorden-Cowanodden, Bellsundbanken, Kinnhøgda-Daudbjørnpynten fault zones) were
636 identified at depths > 1-2 seconds (TWT) in central-eastern Spitsbergen, Storfjorden and the
637 northeastern Barents Sea, and several systems with less developed ductile fabrics between
638 Spitsbergen and Bjørnøya on the Stappen High (Figure 3a-f).

639 The Kongsfjorden-Cowanodden fault zone is relatively easy to trace and correlate in
640 Sassenfjorden, Sassendalen, Nordmannsfonna, Storfjorden and the northeastern Barents Sea (east
641 of Edgeøya) because (i) the seismic data in the these areas have a high resolution and good
642 coverage, (ii) internal seismic reflections are characterized by high amplitudes (e.g., brittle-ductile
643 thrusts and mylonitic shear zones), (iii) kinematic indicators within the thrust system consistently
644 show dominantly top-SSW sense of shear with SSW-verging fold structures (Figure 3a
645 and d-f, and supplement S2), (iv) the geometry and kinematics indicators along shallow brittle
646 overprints are regionally consistent (listric, down-NNE, brittle normal faults; Figure 3a
647 and d-f), and (v) this thrust consistently coincides with increase in gravimetric and magnetic
648 anomaly in cross-section (Figure 3a and d) and with analogously trending gravimetric and
649 magnetic anomalies in central-eastern Spitsbergen and the northern Barents Sea (Figure 5a-c).

Formatted: Font: 12 pt, Not Bold

Formatted: Font: 12 pt, Not Bold, Not Italic

Formatted: Font: 12 pt, Not Bold

Formatted: Font: 12 pt, Not Bold, Not Italic

Formatted: Font: 12 pt, Not Bold

Formatted: Font: 12 pt, Not Bold, Not Italic

Formatted: Font: 12 pt, Not Bold

Formatted: Font: 12 pt, Not Bold, Not Italic

Formatted: Font: 12 pt, Not Bold

Formatted: Font: 12 pt, Not Bold, Not Italic

Formatted: Font: 12 pt, Not Bold

Formatted: Font: 12 pt, Not Bold, Not Italic

Formatted: Font: 12 pt, Not Bold

Formatted: Font: 12 pt, Not Bold, Not Italic

Formatted: Font: 12 pt, Not Bold

Formatted: Font: 12 pt, Not Bold, Not Italic

650 ~~5a–b~~). This thrust system was previously identified below the Ora Basin by Klitzke et al. (2019),
651 though interpreted as potential Timanian grain instead of a discrete structure. The proposed
652 correlation based on seismic, and cross-section and map-view gravimetric and magnetic data
653 suggests a lateral extent of c. 550–600 kilometers along strike for the Kongsfjorden–Cowanodden
654 fault zone. However, the regional magnetic and gravimetric anomalies associated with this thrust
655 in the Norwegian Barents Sea and Svalbard extend potentially farther east as a series of WNW–
656 ESE-trending anomalies to the mainland of Russia (~~Figure 5~~~~Figure 5a–c~~). Notably, these anomalies
657 correlate with the southern edge of Novaya Zemlya (~~Figure 5~~~~Figure 5a–c~~) and, more specifically,
658 with WNW–ESE-striking fault segments of the Baidaratsky fault zone (~~Figure 1~~~~Figure 1a~~; Lopatin
659 et al., 2001; Korago et al., 2004), a major thrust fault that bounds a major basement high in the
660 central Russian Barents Sea, the Ludlov Saddle (Johansen et al., 1992; Drachev et al., 2010). Thus,
661 it is possible that the Kongsfjorden–Cowanodden fault zone also extends farther east, possibly
662 merging with the Baidaratsky fault zone, i.e., with a minimum extent of 1700–1800 kilometers
663 (~~Figure 5~~~~Figure 5a–c~~).

664 The overall NNE-dipping and folded (into NNE-plunging folds) geometry of the
665 Kongsfjorden–Cowanodden fault zone (~~Figure 3~~~~Figure 3e–f~~ and Klitzke et al., 2019, their figures
666 3–5) may explain the alternating NW–SE- and E–W-trending geometry of the gravimetric and
667 magnetic anomalies correlating with this thrust system (~~Figure 5~~~~Figure 5a–b~~). E–W- and NW–SE-
668 trending segments of these anomalies may represent respectively the western and eastern limbs of
669 open, gently NNE-plunging macro-anticlines in the northern Norwegian Barents Sea. ~~This is~~
670 ~~supported by~~ ~~T~~he relatively higher, oval-shaped gravimetric and magnetic anomalies at the
671 intersection of WNW–ESE- and N–S- to NNE–SSW-trending magnetic and gravimetric highs,
672 which are interpreted as the interaction of two sub-orthogonal fold trends further support this claim
673 (~~Figure 5~~~~Figure 5a~~ and c).

674 Interpretation of seismic sections (~~Figure 3~~~~Figure 3e–f~~ and supplement S2) and regional
675 magnetic and gravimetric data (~~Figure 5~~~~Figure 5a–c~~) in central–eastern Spitsbergen show that
676 NNE-dipping, top-SSW Kongsfjorden–Cowanodden and Bellsundbanken fault zones likely extend
677 westwards into central (and possibly northwestern) Spitsbergen (e.g., Sassendalen, Sassenfjorden,
678 Tempelfjorden, and Billefjorden; see ~~Figure 1~~~~Figure 1c~~ for locations). This is further supported by
679 recent field, bathymetric and seismic mapping in central Spitsbergen showing that (inverted)
680 Devonian–Carboniferous NNE-dipping brittle normal faults in Billefjorden and Sassenfjorden–

Formatted: Font: 12 pt, Not Bold

Formatted: Font: 12 pt, Not Bold, Not Italic

Formatted: Font: 12 pt, Not Bold

Formatted: Font: 12 pt, Not Bold, Not Italic

Formatted: Font: 12 pt, Not Bold

Formatted: Font: 12 pt, Not Bold, Not Italic

Formatted: Font: 12 pt, Not Bold

Formatted: Font: 12 pt, Not Bold, Not Italic

Formatted: Font: 12 pt, Not Bold

Formatted: Font: 12 pt, Not Bold, Not Italic

Formatted: Font: 12 pt, Not Bold

Formatted: Font: 12 pt, Not Bold, Not Italic

Formatted: Font: 12 pt, Not Bold

Formatted: Font: 12 pt, Not Bold, Not Italic

Formatted: Font: 12 pt, Not Bold

Formatted: Font: 12 pt, Not Bold, Not Italic

Formatted: Font: 12 pt, Not Bold

Formatted: Font: 12 pt, Not Bold, Not Italic

Formatted: Font: 12 pt, Not Bold

Formatted: Font: 12 pt, Not Bold, Not Italic

681 Tempelfjorden merge with kilometer-scale, NNE-dipping, Precambrian basement fabrics and shear
682 zones at depth (Koehl, 2020a; Koehl et al., 2021 in review). Other examples of WNW–ESE-
683 trending fabrics include faults within Precambrian basement and Carboniferous sedimentary rocks
684 in northeastern Spitsbergen (Witt-Nilsson et al., 1998; Koehl and Muñoz-Barrera, 2018), and
685 within Devonian sedimentary rocks in northern and northwestern Spitsbergen (Friend et al., 1997;
686 McCann, 2000; Dallmann and Piepjohn, 2020). These suggest a repeated and regional influence of
687 WNW–ESE-trending thrust systems and associated basement fabrics in Spitsbergen.

688 Analogously to the Kongsfjorden–Cowanodden fault zone, the Bellsundbanken and
689 Kinnhøgda–Daudbjørnpynten fault zones (Figure 3Figure 3a) geometries and kinematics on
690 seismic data, and their coinciding with parallel gravimetric and magnetic anomalies in map view
691 and with magnetic and gravimetric highs in cross-section suggest that they extend from Storfjorden
692 to the island of Hopen (Figure 1Figure 1c, Figure 3Figure 3a, Figure 5Figure 5a–c, and supplement
693 S2). Notably, a 50–100 kilometers wide, NNE–SSW-trending gravimetric and associated magnetic
694 anomaly interpreted as Caledonian grain in Nordaustlandet (Rijpdalen Anticline; Dumais and
695 Brønner, 2020) bends across the trace of these two thrust systems (Figure 5Figure 5a–c). Farther
696 east, the Bellsundbanken and Kinnhøgda–Daudbjørnpynten fault zones parallel gravimetric and
697 magnetic, alternating E–W- and NW–SE-trending anomalies that follow the trends and map-view
698 shapes of the Ora and Olga basins in the northeastern Norwegian Barents Sea (Anell et al., 2016;
699 see Figure 1Figure 1b–c for location). This suggests that these two thrust systems extend into the
700 northeastern Norwegian Barents Sea and, potentially, into the Russian Barents Sea, and affected
701 the development of Paleozoic sedimentary basins. This is also the case of the Steiløya–Krylen fault
702 zone (supplement S2b), which coincides with mild, discontinuous, WNW–ESE-trending
703 gravimetric and magnetic anomalies that extend well into the Russian Barents Sea and, possibly,
704 across Novaya Zemlya (Figure 5Figure 5a–c).

705 In southwestern Spitsbergen, field mapping revealed the presence of a major, subvertical,
706 kilometer-thick, WNW–ESE-striking mylonitic shear zone metamorphosed under amphibolite
707 facies conditions, the Vimsodden–Kosibapasset Shear Zone (Majka et al., 2008, 2012; Mazur et
708 al., 2009; see Figure 1Figure 1c for location). This major sinistral shear zone aligns along a WNW–
709 ESE-trending axis with the Kinnhøgda–Daudbjørnpynten fault zone in the northwestern
710 Norwegian Barents Sea (Figure 3Figure 3a), and shows a folded geometry in map view that is
711 comparable to that of major NNE-dipping thrust systems in the northern Norwegian Barents Sea

Formatted: Font: 12 pt, Not Bold

Formatted: Font: 12 pt, Not Bold, Not Italic

Formatted: Font: 12 pt, Not Bold

Formatted: Font: 12 pt, Not Bold, Not Italic

Formatted: Font: 12 pt, Not Bold

Formatted: Font: 12 pt, Not Bold, Not Italic

Formatted: Font: 12 pt, Not Bold

Formatted: Font: 12 pt, Not Bold, Not Italic

Formatted: Font: 12 pt, Not Bold

Formatted: Font: 12 pt, Not Bold, Not Italic

Formatted: Font: 12 pt, Not Bold

Formatted: Font: 12 pt, Not Bold, Not Italic

Formatted: Font: 12 pt, Not Bold

Formatted: Font: 12 pt, Not Bold, Not Italic

Formatted: Font: 12 pt, Not Bold

Formatted: Font: 12 pt, Not Bold, Not Italic

Formatted: Font: 12 pt, Not Bold

Formatted: Font: 12 pt, Not Bold, Not Italic

712 (Figure 3a and e-f, Figure 5a-c, and supplement S2; Klitzke et al., 2019). In
713 addition, the Vimsodden–Kosibapasset Shear Zone juxtaposes relatively old Proterozoic basement
714 rocks in the north against relatively young rocks in the south, thus suggesting a similar
715 configuration and kinematics as along the Kinnhøgda–Daubjørnpynnten fault zone in Storfjorden
716 and the northeastern Norwegian Barents Sea. Moreover, von Gosen and Piepjohn (2001) and Bergh
717 and Grogan (2003) reported that Devonian–Mississippian sedimentary successions and Cenozoic
718 fold structures (e.g., Hyrnefjellet Anticline) are offset sinistrally by a few kilometers in Hornsund.
719 Thus, we propose that the Vimsodden–Kosibapasset Shear Zone extends into Hornsund and
720 represents the westwards continuation of the Kinnhøgda–Daubjørnpynnten fault zone. This
721 suggests a minimum extent of 400–450 kilometers for this thrust system (Figure 1b-c and
722 Figure 5a-c).

724 **Timing of formation of major NNE-dipping thrust systems and N–S-trending folds**

725 *NNE-dipping thrust systems*

726 The several-kilometer thickness and hundreds–thousands of kilometers along-strike extent
727 of NNE-dipping thrust systems in central–eastern Spitsbergen, Storfjorden, and the northwestern
728 and northeastern Norwegian Barents Sea suggest that they formed during a major contractional
729 tectonic event. The overall WNW–ESE trend and the consistent north-northeastwards dip and top-
730 SSW sense of shear along the newly evidenced deep thrust systems preclude formation during the
731 Grenvillian, Caledonian, and Ellesmerian orogenies, and the Eurekan tectonic event. These tectonic
732 events all involved dominantly E–W-oriented contraction and resulted in the formation of overall
733 N–S- to NNE–SSW-trending fabrics, structures and deformation belts in Svalbard (i.e., sub-
734 orthogonal to the newly identified thrust systems) such as the Atomfjella Antiform (Gee et al.,
735 1994; Witt-Nilsson et al., 1998), the Vestfonna and Rijpdalen anticlines (Johansson et al., 2004;
736 2005; Dumais and Brønner, 2020), the Dickson Land and Germaniahavøya fold-thrust zones
737 (McCann, 2000; Piepjohn, 2000; Dallmann and Piepjohn, 2020), and the West Spitsbergen Fold-
738 and-Thrust Belt and related early Cenozoic structures in eastern Spitsbergen (Andresen et al., 1992;
739 Haremo and Andresen, 1992; Dallmann et al., 1993), and NE–SW- to NNE–SSW-striking thrusts
740 and folds in northern Norway (Sturt et al., 1978; Townsend, 1987; Roberts and Williams, 2013)
741 and the southwestern Barents Sea (Gernigon et al., 2014).

Formatted: Font: 12 pt, Not Bold

Formatted: Font: 12 pt, Not Bold, Not Italic

Formatted: Font: 12 pt, Not Bold

Formatted: Font: 12 pt, Not Bold, Not Italic

Formatted: Font: 12 pt, Not Bold

Formatted: Font: 12 pt, Not Bold, Not Italic

Formatted: Font: 12 pt, Not Bold

Formatted: Font: 12 pt, Not Bold, Not Italic

742 A possible cause for the formation of the observed NNE-dipping thrust systems is the late
743 Neoproterozoic Timanian Orogeny, which is well known onshore northwestern Russia (e.g., Kanin
744 Peninsula, Timan Range and central Timan; Siedlecka and Roberts, 1995; Olovyanishnikov et al.,
745 2000; Kostyuchenko et al., 2006) and northeastern Norway (Varanger Peninsula; Siedlecka and
746 Siedlecki, 1967; Siedlecka, 1975; Roberts and Olovyanishnikov, 2004), and traces of which were
747 recently found in southwestern Spitsbergen (Majka et al., 2008, 2012, 2014) and northern
748 Greenland (Rosa et al., 2016; Estrada et al., 2018). The overall transport direction during this
749 orogeny was directed towards the south-southwest and most thrust systems show NNE-dipping
750 geometries (Olovyanishnikov et al., 2000; Kostyuchenko et al., 2006), e.g., the Timanian thrust
751 front on the Varanger Peninsula in northeastern Norway (Trollfjorden–Komagelva Fault Zone;
752 Siedlecka and Siedlecki, 1967; Siedlecka, 1975). In addition, the size of Timanian thrust systems
753 in the Timan Range (e.g., Central Timan Fault) is comparable (≥ 3 –4 seconds TWT; Kostyuchenko
754 et al., 2006 their figure 17) to that of thrust systems in the northern Norwegian Barents Sea and
755 Svalbard (Figure 3a and c–d).

756 Thus, based on their overall WNW–ESE strike (Figure 1b–c), their vergence to the
757 south-southwest (Figure 3a, c–d and f), their coincidence with gravimetric and magnetic
758 highs (Figure 5a–c), their upward truncation by a major unconformity consistently
759 throughout the study area (see top-Precambrian unconformity in Figure 3a–d), and the
760 correlation of these NNE-dipping thrusts (via gravimetric and magnetic anomalies) to similarly
761 striking and verging structures of comparable size (i.e., several seconds TWT thick) onshore–
762 nearshore northwestern Russia and northern Norway (Siedlecka, 1975; Siedlecka and Roberts,
763 1995; Olovyanishnikov et al., 2000; Roberts and Siedlecka, 2002; Gee and Pease, 2004;
764 Kostyuchenko et al., 2006), NNE-dipping thrusts in the northern Norwegian Barents Sea,
765 Storfjorden, and central–eastern Spitsbergen are interpreted as the western continuation of
766 Timanian thrusts.

767 Timanian grain was recently identified in the northeastern Norwegian Barents Sea through
768 interpretation of new seismic, magnetic and gravimetric datasets shown in Figure 5a–c
769 (Klitzke et al., 2019). The alignment, coincident location, and matching geometries (e.g., curving
770 E–W to NW–SE strike/trend and kilometer-wide NNE–SSW-trending anticline) between Timanian
771 grain and structures mapped by Klitzke et al. (2019) and the major, NNE-dipping, top-SSW thrust
772 systems described in central–eastern Spitsbergen, Storfjorden and the Norwegian Barents Sea

Formatted: Font: 12 pt, Not Bold

Formatted: Font: 12 pt, Not Bold, Not Italic

Formatted: Font: 12 pt, Not Bold

Formatted: Font: 12 pt, Not Bold, Not Italic

Formatted: Font: 12 pt, Not Bold

Formatted: Font: 12 pt, Not Bold, Not Italic

Formatted: Font: 12 pt, Not Bold

Formatted: Font: 12 pt, Not Bold, Not Italic

Formatted: Font: 12 pt, Not Bold

Formatted: Font: 12 pt, Not Bold, Not Italic

Formatted: Font: 12 pt, Not Bold

Formatted: Font: 12 pt, Not Bold, Not Italic

773 (Figure 3a–f and supplement S2) further support a Timanian origin for the latter. Further
774 evidence of relic Timanian structural grain as far as the Loppa High and Bjørnøya Basin are
775 documented by previous magnetic studies and modelling (Marello et al., 2010). Moreover, seismic
776 mapping suggests that Timanian thrust systems extend well into central Spitsbergen (Figure
777 3e–f and supplement S2c–d; Koehl, 2020a; Koehl et al., 2021 in review), and regional
778 gravimetric and magnetic anomaly maps suggest that Timanian thrust systems might extend farther
779 west to (north-) western Spitsbergen (Figure 5a–c).

780 Probable reasons as to why these major (hundreds–thousands of kilometers long) thrust
781 systems were not identified before during fieldwork in Svalbard are their burial to high depth (>
782 1–2 seconds TWT in the study area, i.e., several kilometers below the surface; Figure 3a–
783 f), and their strong overprinting by younger tectonic events like the Caledonian Orogeny in areas
784 where they are exposed (e.g., Vimsodden–Kosibapasset Shear Zone in southwestern Spitsbergen;
785 Faehnrich et al., 2020). Possible areas of interest for future studies include the western and
786 northwestern parts of Spitsbergen where Caledonian and Eureka E–W contraction contributed to
787 uplift and exhume deep basement rocks, and where Timanian rocks potentially crop out (e.g.,
788 Peucat et al., 1989).

790 *N–S-trending folds*

791 N–S-trending upright folds involve the NNE-dipping thrust systems (Figure 3b and
792 e) and correlate (via gravimetric and magnetic anomalies) with major Caledonian folds in
793 northeastern Spitsbergen and Nordaustlandet, like the Atomfjella Antiform (Gee et al., 1994; Witt-
794 Nilsson et al., 1998) and Rijpdalen Anticline (Johansson et al., 2004; 2005; Dumais and Brønner,
795 2020), with Caledonian grain in the southern Norwegian Barents Sea (Gernigon and Brønner, 2012;
796 Gernigon et al., 2014), and with major NE–SW-trending Caledonian folds onshore northern
797 Norway (Sturt et al., 1978; Townsend, 1987; Roberts and Williams, 2013). In addition, the width
798 of the NE–SW- to N–S-trending gravimetric and magnetic anomalies associated with these folds
799 increases up to 150 kilometers eastwards, i.e., away from the Caledonian collision zone (Figure
800 5a–c; Corfu et al., 2014; Gasser, 2014). Thus, N–S-trending folds in the northern
801 Norwegian Barents Sea are interpreted as Caledonian regional folds in Precambrian–lower
802 Paleozoic rocks. The relatively broader geometry of Caledonian folds away from the Caledonian
803 collision zone (e.g., in the Russian Barents Sea) is inferred to be related to gentler fold geometries

Formatted: Font: 12 pt, Not Bold

Formatted: Font: 12 pt, Not Bold, Not Italic

Formatted: Font: 12 pt, Not Bold

Formatted: Font: 12 pt, Not Bold, Not Italic

Formatted: Font: 12 pt, Not Bold

Formatted: Font: 12 pt, Not Bold, Not Italic

Formatted: Font: 12 pt, Not Bold

Formatted: Font: 12 pt, Not Bold, Not Italic

Formatted: Font: 12 pt, Not Bold

Formatted: Font: 12 pt, Not Bold, Not Italic

Formatted: Font: 12 pt, Not Bold

Formatted: Font: 12 pt, Not Bold, Not Italic

804 due to decreasing deformation intensity in this direction. This is further supported by relatively low
805 grade Caledonian metamorphism in Franz Josef Land (Knudsen et al., 2019; see [Figure 1](#)
806 [4a–b](#) for location). By contrast, the presence of tighter Caledonian folds near the collision zone in
807 the northern Norwegian Barents Sea (e.g., [Figure 3](#)
808 [Figure 3b](#) and e, and Atomfjella Antiform and Rijpdalen Anticline onshore; Gee et al., 1994; Witt-Nilsson et al., 1998; Johansson et al., 2004,
809 2005; Dumais and Brønner, 2020) is associated with much narrower (20–50 kilometers wide)
810 gravimetric and magnetic anomalies ([Figure 5](#)
811 [Figure 5a–c](#)). Note that the Atomfjella Antiform and Rijpdalen Anticline can be directly correlated with 20–50 kilometers wide, N–S-trending high
812 gravimetric and magnetic anomalies ([Figure 5](#)
813 [Figure 5a–c](#)). Noteworthy, some of the NNE–SSW-trending folds and anomalies in the northernmost Norwegian Barents Sea may reflect a
814 combination of Caledonian and superimposed early Cenozoic Eureka folding (e.g., Kairanov et
815 al., 2018).

816 The interference of WNW–ESE- and N–S- to NNE–SSW-trending gravimetric highs,
817 which are correlated to Timanian and Caledonian folds respectively, produces oval-shaped
818 gravimetric and magnetic highs ([Figure 5](#)
819 [Figure 5a](#)). These relatively higher, oval-shaped gravimetric anomalies are interpreted to correspond to dome-shaped folds resulting from the
820 interaction of Timanian and Caledonian folds involving refolding of WNW–ESE-trending
821 Timanian folds during E–W Caledonian contraction. [This interpretation is supported by field](#)
822 [studies on the Varanger Peninsula in northern Norway and by seismic studies of Timanian thrusts](#)
823 [off northern Norway where the interaction of Timanian and Caledonian folds produced dome-](#)
824 [shaped fold structures \(Ramsay, 1962\), e.g., like the Ragnarokk Anticline \(Siedlecka and Siedlecki,](#)
825 [1971; Koehl, in prep.\) also support this interpretation.](#) Furthermore, Barrère et al. (2011) suggested
826 that basins and faults in the southern Norwegian Barents Sea are controlled by the interaction of
827 Caledonian and Timanian structural grain, and Marello et al. (2010) argued that elbow-shaped
828 magnetic anomalies reflect the interaction of Caledonian and Timanian structural grains in the
829 Barents Sea, potentially as far west as the Loppa High and the Bjørnøya Basin.

830

831 *Phanerozoic reactivation and overprinting of Timanian thrust systems*

832 *Caledonian reactivation and overprint*

833 The geometry of the Kongsfjorden–Cowanodden and Kinnhøgda–Daudbjørnpynten fault
834 zones in Nordmannsfonna ([Figure 3](#)
835 [Figure 3e](#)) and the northeastern Norwegian Barents Sea ([Figure](#)

Formatted: Font: 12 pt, Not Bold

Formatted: Font: 12 pt, Not Bold, Not Italic

Formatted: Font: 12 pt, Not Bold

Formatted: Font: 12 pt, Not Bold, Not Italic

Formatted: Font: 12 pt, Not Bold

Formatted: Font: 12 pt, Not Bold, Not Italic

Formatted: Font: 12 pt, Not Bold

Formatted: Font: 12 pt, Not Bold, Not Italic

Formatted: Font: 12 pt, Not Bold

Formatted: Font: 12 pt, Not Bold, Not Italic

Formatted: Font: 12 pt, Not Bold

Formatted: Font: 12 pt, Not Bold, Not Italic

Formatted: Font: 12 pt, Not Bold

835 [3Figure 3b](#); Klitzke et al., 2019), where they are folded into broad NNE-plunging upright anticlines
836 and synclines suggests that these thrust systems were deformed after they accommodated top-SSW
837 Timanian thrusting ([Figure 6Figure 6a](#) and [Figure 7Figure 7a](#)). In addition, subsidiary top-west
838 kinematics (west-verging folds and top-west minor thrusts) suggest that these thrust systems were
839 partly reactivated–overprinted during an episode of intense E–W contraction ([Figure 6Figure 6b](#)
840 and [Figure 7Figure 7b](#)). However, west-dipping dykes crosscutting and gently east-dipping
841 sedimentary strata overlying the eastern part of the folded Kongsfjorden–Cowanodden fault zone
842 are only mildly folded, and upper Paleozoic sedimentary strata lie flat over folded and partly eroded
843 Precambrian–lower Paleozoic rocks and the Kinnhøgda–Daudbjørnpynten fault zone, thus
844 suggesting that these sedimentary strata and dykes were not involved in this episode of E–W
845 contraction ([Figure 3Figure 3e](#)).

846 A notable episode of E–W contraction in Svalbard is the Caledonian Orogeny in the early–
847 mid Paleozoic, which resulted in the formation of west-verging thrusts and N–S-trending folds of
848 comparable size (c. 15–25 kilometers wide) to those affecting the Kongsfjorden–Cowanodden and
849 Kinnhøgda–Daudbjørnpynten fault zones in Nordmannsfunna and the northern Norwegian Barents
850 Sea ([Figure 3Figure 3b](#) and [e](#); Klitzke et al., 2019, their figures 3–5), such as the Atomfjella
851 Antiform in northeastern Spitsbergen (Gee et al., 1994; Witt-Nilsson et al., 1998; Lyberis and
852 Manby, 1999) and the Rijpdalen Anticline in Nordaustlandet ([Figure 1Figure 1b](#)). Since the NNE-
853 plunging anticline in Nordmannsfunna does not affect overlying Pennsylvanian–Mesozoic
854 sedimentary strata ([Figure 3Figure 3e](#)), we propose that they formed during Caledonian contraction
855 ([Figure 7Figure 7b](#)). This is supported by the involvement of the top-Precambrian unconformity
856 and underlying NNE-dipping thrusts in N–S- to NNE-SSW-trending folds, and by the truncation
857 of these folds by the top-Silurian unconformity, which is overlapped by mildly deformed to flat-lying
858 upper Paleozoic strata ([Figure 3Figure 3b](#) and [Figure 4Figure 4f](#)). Furthermore, structures with
859 geometries comparable to NNE-plunging folds in the northern Barents Sea and Svalbard were
860 observed in northern Norway. An example is the Ragnarokk Anticline, a dome-shaped fold
861 structure along the Timanian front thrust on the Varanger Peninsula, which results from the re-
862 folding of Timanian thrusts and folds into a NE–SW-trending Caledonian trend (Siedlecka and
863 Siedlecki, 1971).

864 Further support of a Caledonian origin for upright NNE-plunging folds in eastern
865 Spitsbergen, Storfjorden and the northern Norwegian Barents Sea is that these folds are relatively

Formatted: Font: 12 pt, Not Bold, Not Italic

Formatted: Font: 12 pt, Not Bold

Formatted: Font: 12 pt, Not Bold, Not Italic

Formatted: Font: 12 pt, Not Bold

Formatted: Font: 12 pt, Not Bold, Not Italic

Formatted: Font: 12 pt, Not Bold

Formatted: Font: 12 pt, Not Bold, Not Italic

Formatted: Font: 12 pt, Not Bold

Formatted: Font: 12 pt, Not Bold, Not Italic

Formatted: Font: 12 pt, Not Bold

Formatted: Font: 12 pt, Not Bold, Not Italic

Formatted: Font: 12 pt, Not Bold

Formatted: Font: 12 pt, Not Bold, Not Italic

Formatted: Font: 12 pt, Not Bold

Formatted: Font: 12 pt, Not Bold, Not Italic

Formatted: Font: 12 pt, Not Bold

Formatted: Font: 12 pt, Not Bold, Not Italic

Formatted: Font: 12 pt, Not Bold

Formatted: Font: 12 pt, Not Bold, Not Italic

Formatted: Font: 12 pt, Not Bold

Formatted: Font: 12 pt, Not Bold, Not Italic

Formatted: Font: 12 pt, Not Bold

Formatted: Font: 12 pt, Not Bold, Not Italic

866 tight in the west, in Nordmannsfonna and the northwestern Barents Sea (Figure 3b and e),
867 whereas they show gradually gentler and more open geometries in the east, i.e., away from the
868 Caledonian collision zone (Figure 3b). This is also shown by the gradual eastwards
869 broadening of regional gravimetric and magnetic anomalies correlated with Caledonian folds
870 suggesting gentler fold geometries related to decreasing (Caledonian) deformation intensity in this
871 direction (Figure 5a-c). This contrasts with the homogeneous intensity of deformation
872 along NNE-dipping thrusts on seismic data and with the homogeneous width of related
873 gravimetric-magnetic anomalies from west to east in Svalbard and the Barents Sea (Figure 3
874 3a-f and Figure 5a-c and supplement S2).

875 In Nordmannsfonna, the Caledonian origin of the major 15–20 kilometers wide anticline,
876 and the truncation of overlying, gently east-dipping, mildly folded sedimentary strata and
877 crosscutting west-dipping dykes by the base-Pennsylvanian unconformity suggest that these
878 sedimentary strata and dykes are Devonian (–Mississippian?) in age (Figure 6c-d). This is
879 supported by the presence of thick Devonian–Mississippian collapse deposits in adjacent areas of
880 central–northern Spitsbergen (Cutbill et al., 1976; Murascov and Mokin, 1979; Aakvik, 1981;
881 Gjølberg, 1983; Manby and Lyberis, 1992; Friend et al., 1997), and by Middle Devonian to
882 Mississippian ages (395–327 Ma) for dykes in central–northern Spitsbergen (Evdokimov et al.,
883 2006), northern Norway (Lippard and Prestvik, 1997; Guise and Roberts, 2002), and northwestern
884 Russia (Roberts and Onstott, 1995).

885 The occurrence of a > 0.5 second (TWT) reverse offset of the folded Kongsfjorden–
886 Cowanodden fault zone and the lack of offset of the Devonian (–Mississippian?) dykes across the
887 Agardhbukta Fault indicate that the latter fault formed as a top-west thrust during the Caledonian
888 Orogeny. At depth, the Agardhbukta Fault merges with the eastern flank of the folded
889 Kongsfjorden–Cowanodden fault zone. This, together with the presence of minor, high-angle, top-
890 west brittle thrusts within the Kongsfjorden–Cowanodden fault zone (Figure 3e), indicates
891 that the Agardhbukta Fault reactivated and/or overprinted the eastern portion of the Kongsfjorden–
892 Cowanodden fault zone in Nordmannsfonna during Caledonian contraction (Figure 6b and
893 Figure 7b). Depth conversion using seismic velocities from Gernigon et al. (2018) suggest
894 that the Agardhbukta Fault offset the Kongsfjorden–Cowanodden fault zone by ca. 2.4–2.5
895 kilometers top-west during Caledonian contraction (Figure 3e and supplement S3g). These
896 kinematics are consistent with field observation in eastern Spitsbergen by Piepjohn et al. (2019,

Formatted: Font: 12 pt, Not Bold

Formatted: Font: 12 pt, Not Bold, Not Italic

Formatted: Font: 12 pt, Not Bold

Formatted: Font: 12 pt, Not Bold, Not Italic

Formatted: Font: 12 pt, Not Bold

Formatted: Font: 12 pt, Not Bold, Not Italic

Formatted: Font: 12 pt, Not Bold

Formatted: Font: 12 pt, Not Bold, Not Italic

Formatted: Font: 12 pt, Not Bold

Formatted: Font: 12 pt, Not Bold, Not Italic

Formatted: Font: 12 pt, Not Bold

Formatted: Font: 12 pt, Not Bold, Not Italic

Formatted: Font: 12 pt, Not Bold

Formatted: Font: 12 pt, Not Bold, Not Italic

Formatted: Font: 12 pt, Not Bold

Formatted: Font: 12 pt, Not Bold, Not Italic

Formatted: Font: 12 pt, Not Bold

Formatted: Font: 12 pt, Not Bold, Not Italic

Formatted: Font: 12 pt, Not Bold

Formatted: Font: 12 pt, Not Bold, Not Italic

897 their figure 17b). However, Piepjohn et al. (2019) also suggested a significant component of
898 Mesozoic–Cenozoic, down-east normal movement, which was not identified in Nordmannsfonna.
899 This suggests either along strike variation in the movement history of the Agardhbukta Fault, either
900 that the fault mapped on seismic data in Nordmannsfonna does not correspond to the Agardhbukta
901 Fault of Piepjohn et al. (2019).

902 Considering the presence of crustal-scale, NNE-dipping, hundreds (to thousands?) of
903 kilometers long (Timanian) thrust systems extending from the Barents Sea (and possibly from
904 onshore Russia) to central–eastern and southern Spitsbergen and the northwestern Norwegian
905 Barents Sea (Figure 5a–c) prior to the onset of E–W-oriented Caledonian contraction, it is
906 probable that such large structures would have (at least partially) been reactivated and/or
907 overprinted during subsequent tectonic events if suitably oriented. Under E–W contraction, WNW–
908 ESE-striking, dominantly NNE-dipping Timanian faults would be oriented at c. 30° to the direction
909 of principal stress and, therefore, be suitable (according to Anderson’s stress model) to
910 reactivate/be overprinted with sinistral strike-slip movements. Such kinematics were recorded
911 along the Vimsodden–Kosibapasset Shear Zone in Wedel Jarlsberg Land (Mazur et al., 2009) and
912 within Hornsund (von Gosen and Piepjohn, 2001).

913 However, recent ⁴⁰Ar–³⁹Ar geochronological determinations on muscovite within this
914 structure suggest that this structure formed during the Caledonian Orogeny (Faehnrich et al. 2020).
915 Nonetheless, the same authors also obtained Timanian ages (600–540 Ma) for (initial) movements
916 along minor shear zones nearby and parallel to the Vimsodden–Kosibapasset Shear Zone. Since
917 this large shear zone must have represented a major preexisting zone of weakness when Caledonian
918 contraction initiated, it is highly probable that it was preferentially chosen to reactivate instead of
919 minor shear zones. Thus, the Caledonian ages obtained along the Vimsodden–Kosibapasset Shear
920 Zone most likely reflect complete resetting of the geochronometer along the shear zone due to large
921 amounts of Caledonian reactivation–overprinting, while minor nearby shear zones preserved traces
922 of initial Timanian deformation. This is also supported by observations in northern Norway
923 suggesting that Timanian thrusts (e.g., Trollfjorden–Komagelva Fault Zone) were reactivated as
924 major strike-slip faults during the Caledonian Orogeny (Roberts, 1972; Herrevold et al., 2009; Rice
925 2014). This interpretation reconciles the strong differences in dipping angle and depth between the
926 Kinnhøgda–Daudbjørnpynten fault zone and the Vimsodden–Kosibapasset Shear Zone. The
927 former was located away from the Caledonian collision zone and essentially retained its initial,

Formatted: Font: 12 pt, Not Bold

Formatted: Font: 12 pt, Not Bold, Not Italic

928 moderately NNE-dipping Timanian geometry and was deeply buried during the Phanerozoic,
929 whereas the latter was intensely deformed, pushed into a sub-vertical position, and uplifted and
930 exhumed to the surface because it was located near or within the Caledonian collision zone.

931

932 *Devonian–Carboniferous normal overprint–reactivation*

933 In Nordmannsfunna, the wedge shape of Devonian (–Mississippian?) sedimentary strata in
934 the hanging wall of the Kongsfjorden–Cowanodden fault zone suggest that the eastern portion of
935 this thrust was reactivated as a gently–moderately dipping extensional detachment (~~Figure 6~~
936 ~~6c~~) and, thus, that Devonian (–Mississippian?) strata in this area represent analogs to collapse
937 deposits in northern Spitsbergen. ~~This is supported by the~~ intrusion of west-dipping Devonian (–
938 Mississippian?) dykes orthogonal to the eastern portion of the thrust system, i.e., orthogonal to
939 extensional movements along the inverted east-dipping portion of the thrust (~~Figure 3~~
940 ~~Figure 6d~~) also supports this interpretation. Similar relationships were inferred in
941 northwestern Spitsbergen, where Devonian collapse sediments were deposited along a N–S-
942 trending Precambrian basement ridge bounded by a gently dipping, extensional mylonitic
943 detachment (Braathen et al., 2018).

944 In Sassenfjorden, Storfjorden and the northeastern Norwegian Barents Sea, listric brittle
945 normal faults showing down-NNE offsets and syn-tectonic thickening within Devonian–
946 Carboniferous (–Permian?) sedimentary strata merge at depth with the uppermost part of NNE-
947 dipping Timanian thrust systems like the Kongsfjorden–Cowanodden fault zone (~~Figure 3~~
948 ~~3a and d and supplement S2c~~). This indicates that Timanian thrust systems were used as preexisting
949 zones of weakness during late–post-orogenic collapse of the Caledonides in the Devonian–
950 Carboniferous (~~Figure 6~~
951 ~~Figure 6c–e and Figure 7~~
952 ~~Figure 7c~~).

951 The presence of the Kongsfjorden–Cowanodden fault zone in Storfjorden and below
952 Edgeøya also explains the strong differences between the Paleozoic sedimentary successions
953 penetrated by the Plurdalen-1 and Raddendalen-1 exploration wells (Bro and Shvarts, 1983;
954 Harland and Kelly, 1997). Notably, the Plurdalen-1 well penetrated (at least) ca. 1600 meters thick
955 Devonian–Mississippian sedimentary rocks in the direct hanging wall of the Kongsfjorden–
956 Cowanodden fault zone and related listric brittle overprints (~~Figure 3~~
957 ~~Figure 3a~~), whereas the interpretation of Bro and Shvarts (1983) suggests that the Raddendalen-1 well encountered thin (90–
958 290 meters thick) Mississippian strata overlying (> 2 kilometers) thick lower Paleozoic

Formatted: Font: 12 pt, Not Bold

Formatted: Font: 12 pt, Not Bold, Not Italic

Formatted: Font: 12 pt, Not Bold

Formatted: Font: 12 pt, Not Bold, Not Italic

Formatted: Font: 12 pt, Not Bold

Formatted: Font: 12 pt, Not Bold, Not Italic

Formatted: Font: 12 pt, Not Bold

Formatted: Font: 12 pt, Not Bold, Not Italic

Formatted: Font: 12 pt, Not Bold

Formatted: Font: 12 pt, Not Bold, Not Italic

Formatted: Font: 12 pt, Not Bold

Formatted: Font: 12 pt, Not Bold, Not Italic

Formatted: Font: 12 pt, Not Bold

Formatted: Font: 12 pt, Not Bold, Not Italic

959 sedimentary rocks ca. 30 kilometers farther northeast, i.e., away from the Kongsfjorden–
960 Cowanodden fault zone and related overprints. The presence of thick Devonian sedimentary strata
961 in the direct hanging wall of listric overprints of the Kongsfjorden–Cowanodden fault zone further
962 supports late–post-Caledonian extensional reactivation–overprinting of NNE-dipping Timanian
963 thrusts.

964 In central Spitsbergen, recently identified Early Devonian–Mississippian normal faults
965 formed along and overprinted–reactivated major NNE-dipping ductile (mylonitic) shear zones and
966 fabrics in Billefjorden (Koehl et al., 2021 in review) and Sassenfjorden–Tempelfjorden (Koehl,
967 2020a). These show sizes, geometries and kinematics comparable to those of the Kongsfjorden–
968 Cowanodden fault zone, and are, therefore, interpreted as the western continuation of this thrust
969 system. The Devonian–Carboniferous extensional reactivation–overprinting of the Kongsfjorden–
970 Cowanodden fault zone in central Spitsbergen explains the southward provenance of northwards
971 prograding sedimentary rocks of the uppermost Silurian–Lower Devonian Siktefjellet and Red Bay
972 groups and Wood Bay Formation and the enigmatic WNW–ESE trend of the southern boundary of
973 the Devonian Graben in central–northern Spitsbergen (Gee and Moody-Stuart, 1966; Friend et al.,
974 1966; Friend and Moody-Stuart, 1972; Murascov and Mokin, 1979; Friend et al., 1997; McCann,
975 2000; Dallmann and Piepjohn, 2020; Koehl et al., 2021 in review).

976

977 *Mild Triassic overprint*

978 The Kongsfjorden–Cowanodden fault zone and associated overprints align with WNW–
979 ESE- to NW–SE-striking normal faults onshore southern and southwestern Edgeøya in
980 Kvalpynten, Negerpynten, and Øhmanfjellet (Osmundsen et al., 2014; Ogata et al., 2018). These
981 faults display both listric and steep planar geometries in cross-section and bound thickened syn-
982 sedimentary growth strata in lowermost Upper Triassic sedimentary rocks of the Tschermakfjellet
983 and De Geerdalen formations (Ogata et al., 2018; Smyrak-Sikora et al., 2020). The Norwegian
984 Barents Sea and Svalbard are believed to have remained tectonically quiet throughout the Triassic
985 apart from minor deep-rooted normal faulting in the northwestern Norwegian Barents Sea (Anell
986 et al., 2013) and Uralides-related contraction in the (south-) east (Müller et al., 2019). Hence, we
987 propose that the progradation and accumulation of thick sedimentary deposits of the Triassic deltaic
988 systems above the southeastward continuation of the Kongsfjorden–Cowanodden fault zone may
989 have triggered minor tectonic adjustments resulting in the development of a system of small half-

990 grabens over the thrust system. Alternatively or complementary, the deposition of thick Triassic
991 deltaic systems may have locally accelerated compaction of sedimentary strata underlying the
992 Tschermakjellet Formation in south- and southwest-Edgeøya, e.g., of the potential pre-Triassic
993 syn-tectonic growth strata along the Kongsfjorden–Cowanodden fault zone, and, thus, facilitated
994 the development of minor half-grabens within the Triassic succession along this thrust system.

995

996 *Eurekan reactivation–overprint*

997 In eastern Spitsbergen, the Agardhbukta Fault segment of the Lomfjorden Fault Zone
998 truncates the Kongsfjorden–Cowanodden fault zone with a major, > 0.5 second (TWT) top-west
999 reverse offset (Figure 3e). The Agardhbukta fault also mildly folds Pennsylvanian–
1000 Mesozoic sedimentary rocks and Cretaceous sills into a gentle upright (fault-propagation) fold with
1001 no major offset (Figure 6f–g), which is supported by onshore field observations in eastern
1002 and northeastern Spitsbergen (Piepjohn et al., 2019). Mild folding of Mesozoic sedimentary rocks
1003 and of Cretaceous intrusions indicates that the Agardhbukta Fault was most likely mildly
1004 reactivated as a top-west thrust during the early Cenozoic Eurekan tectonic event (Figure 6
1005 g and Figure 7d).

1006 Seismic data show that high-angle listric Devonian–Carboniferous normal faults were
1007 mildly reactivated as reverse faults that propagated upwards and gently folded adjacent upper
1008 Paleozoic–Mesozoic (–Cenozoic?) sedimentary strata in the northwestern Norwegian Barents Sea,
1009 Storfjorden and central–eastern Spitsbergen (Figure 3a–c and supplement S2), but not in
1010 the northeastern Norwegian Barents Sea (Figure 3d). Since normal faults were not inverted
1011 in the east, it is probable that inversion of these faults in central–eastern Spitsbergen, Storfjorden
1012 and the northwestern Norwegian Barents Sea first occurred during the Eurekan tectonic event in
1013 the early Cenozoic, when Greenland collided with western Spitsbergen (Figure 7d). This
1014 is also supported by the gently folded character of Devonian–Mesozoic (–Cenozoic?) sedimentary
1015 successions in the west (Figure 3a and c), whereas these successions are essentially flat-
1016 lying (i.e., undeformed) in the east (Figure 3b and d). Nevertheless, folding of the seafloor
1017 reflection in Storfjorden and the northwestern Norwegian Barents Sea suggests ongoing
1018 contractional deformation along several of these faults in the northwestern Norwegian Barents Sea
1019 and Storfjorden (Figure 3a–c).

Formatted: Font: 12 pt, Not Bold

Formatted: Font: 12 pt, Not Bold, Not Italic

Formatted: Font: 12 pt, Not Bold

Formatted: Font: 12 pt, Not Bold, Not Italic

Formatted: Font: 12 pt, Not Bold

Formatted: Font: 12 pt, Not Bold, Not Italic

Formatted: Font: 12 pt, Not Bold

Formatted: Font: 12 pt, Not Bold, Not Italic

Formatted: Font: 12 pt, Not Bold

Formatted: Font: 12 pt, Not Bold, Not Italic

Formatted: Font: 12 pt, Not Bold

Formatted: Font: 12 pt, Not Bold, Not Italic

Formatted: Font: 12 pt, Not Bold

Formatted: Font: 12 pt, Not Bold, Not Italic

Formatted: Font: 12 pt, Not Bold

Formatted: Font: 12 pt, Not Bold, Not Italic

Formatted: Font: 12 pt, Not Bold

Formatted: Font: 12 pt, Not Bold, Not Italic

Formatted: Font: 12 pt, Not Bold

Formatted: Font: 12 pt, Not Bold, Not Italic

1020 Major, top-SSW mylonitic shear zones in Sassenfjorden–Tempelfjorden and Billefjorden
1021 display early Cenozoic overprints including top-SSW duplexes in uppermost Devonian–
1022 Mississippian coals of the Billefjorden Group acting as a partial décollement along a major
1023 basement-seated listric brittle fault (Koehl, 2020a; supplement S2) and NNE-dipping brittle faults
1024 offsetting the east-dipping Billefjorden Fault Zone by hundreds of meters to several kilometers left-
1025 laterally (Koehl et al., 2021 in review). Thus, the correlation of the Kongsfjorden–Cowanodden
1026 fault zone with these top-SSW mylonitic shear zones in Sassenfjorden–Tempelfjorden and
1027 Billefjorden (see [Figure 1c](#) for location) supports reactivation–overprinting of major NNE-
1028 dipping Timanian thrust systems as top-SSW, sinistral-reverse, oblique-slip thrusts in the early
1029 Cenozoic Eurekan tectonic event. Such correlation explains the NW–SE trend and the location of
1030 the northeastern boundary of the Central Tertiary Basin, which terminates just southwest of
1031 Sassenfjorden and Sassendalen in central Spitsbergen ([Figure 1b–c](#)). It also explains the
1032 dominance of NW–SE- to WNW–ESE-striking faults within Cenozoic deposits of the Central
1033 Tertiary Basin (Livshits, 1965a), and the northwestwards provenance (Petersen et al., 2016) and
1034 northwards thinning of sediments deposited in the basin (Livshits, 1965b), which were probably
1035 sourced from uplifted areas in the hanging wall of the reactivated–overprinted thrust.

1036 Noteworthy, Livshits (1965a) argued that the Central Tertiary Basin was bounded to the
1037 north by a major WNW–ESE-striking fault extending from Kongsfjorden to southern Billefjorden–
1038 Sassenjorden where the NNE-dipping Kongsfjorden–Cowanodden fault zone was mapped (present
1039 study; supplement S2). This indicates that the Kongsfjorden–Cowanodden fault zone might extend
1040 west of Billefjorden and Sassenfjorden, potentially until Kongsfjorden (see [Figure 1c](#) for
1041 location). Should it be the case, the Kongsfjorden–Cowanodden fault zone would coincide with a
1042 major terrane boundary in Svalbard, which was speculated to correspond to one or more regional
1043 WNW–ESE- to N–S-striking faults in earlier works, e.g., Kongsvegen Fault and Lapsdalen Thrust
1044 (Harland and Horsfield, 1974), Kongsvegen Fault Zone and/or Central–West Fault Zone (Harland
1045 and Wright, 1979), and Kongsfjorden–Hansbreen Fault Zone (Harland et al., 1993). The presence
1046 of a major, (inherited Timanian) NNE-dipping, basement-seated fault zone in this area would
1047 explain the observed strong differences between Precambrian basement rocks in Svalbard’s
1048 northwestern and southwestern terranes.

1049 In southern Spitsbergen, von Gosen and Piepjohn (2001) and Bergh and Grogan (2003)
1050 suggested the presence of a WNW–ESE-striking, sinistral-reverse strike-slip fault in Hornsund

Formatted: Font: 12 pt, Not Bold

Formatted: Font: 12 pt, Not Bold, Not Italic

Formatted: Font: 12 pt, Not Bold

Formatted: Font: 12 pt, Not Bold, Not Italic

Formatted: Font: 12 pt, Not Bold

Formatted: Font: 12 pt, Not Bold, Not Italic

1051 based on a one-kilometer left-lateral offset of Devonian–Carboniferous sedimentary successions
1052 and of the early Cenozoic Hyrnefjellet Anticline across the fjord. This fault is part of the
1053 Kinnhøgda–Daudbjørnpynten fault zone and was most likely reactivated–overprinted during
1054 Eureka contraction–transpression in the early Cenozoic.

1055

1056 *Present day tectonism*

1057 Seismic data show that the seafloor reflection is folded and/or offset in a reverse fashion by
1058 high-angle brittle faults merging at depth with interpreted Timanian thrust systems in Storfjorden
1059 and just north of Bjørnøya in the northwestern Norwegian Barents (~~Figure 3~~Figure 3a and c, and
1060 ~~Figure 4~~Figure 4h). This indicates that some of the Timanian thrust systems are still active at
1061 present and are reactivated/overprinted by reverse faults (~~Figure 7~~Figure 7e). A potential
1062 explanation for ongoing reactivation–overprinting is transfer of extensional tectonic stress in the
1063 Fram Strait as ridge–push tectonism through Spitsbergen and Storfjorden.

1064

1065 *Implication for plate tectonics reconstructions of the Barents Sea and Svalbard in the late* 1066 *Neoproterozoic–Paleozoic*

1067 The presence of hundreds to thousands of kilometers long Timanian faults throughout the
1068 northern Norwegian Barents Sea and central and southwestern (and possibly northwestern?)
1069 Spitsbergen indicates that the northwestern, northeastern and southwestern basement terranes of
1070 the Svalbard Archipelago were most likely already accreted together and attached to the Barents
1071 Sea, northern Norway and northwestern Russia in the late Neoproterozoic (ca. 600 Ma). Svalbard’s
1072 three terranes were previously thought to have been juxtaposed during the Caledonian and
1073 Ellesmerian orogenies through hundreds–thousands of kilometers of displacement along presumed
1074 thousands of kilometers long N–S-striking strike-slip faults like the Billefjorden Fault Zone
1075 (Harland, 1969; Harland et al. 1992, Labrousse et al., 2008; ~~Figure 2~~Figure 2). The presence of
1076 laterally continuous (undisrupted), hundreds–thousands of kilometers long, Timanian thrust
1077 systems from southwestern and central Spitsbergen to the northern Norwegian and Russian Barents
1078 Sea clearly shows that this is not possible (~~Figure 8~~Figure 8).

1079 The continuous character of these thrust systems from potentially as far as onshore
1080 northwestern Russia through the Barents Sea and Svalbard precludes any major strike-slip
1081 displacement along N–S-striking faults such as the Billefjorden Fault Zone and Lomfjorden Fault

Formatted: Font: 12 pt, Not Bold

Formatted: Font: 12 pt, Not Bold, Not Italic

Formatted: Font: 12 pt, Not Bold

Formatted: Font: 12 pt, Not Bold, Not Italic

Formatted: Font: 12 pt, Not Bold

Formatted: Font: 12 pt, Not Bold, Not Italic

Formatted: Font: 12 pt, Not Bold

Formatted: Font: 12 pt, Not Bold, Not Italic

Field Code Changed

Formatted: Font: (Default) Times New Roman

Formatted: Font: Not Bold, Not Italic

1082 Zone (as proposed by Harland et al., 1974, 1992; Labrousse et al., 2008: [Figure 2](#)) and any hard-
1083 linked connection between these faults in Svalbard and analogous, NE–SW-striking faults in
1084 Scotland in the Phanerozoic (as proposed by Harland, 1969). Instead, the present work suggests
1085 that the crust constituting the Barents Sea and the northeastern and southwestern basement terranes
1086 of Svalbard should be included as part of Baltica in future Arctic plate tectonics reconstructions for
1087 the late Neoproterozoic–Paleozoic period (i.e., until ca. 600 Ma; [Figure 8](#)). It also suggests that the
1088 Caledonian suture zone, previously inferred to lie east of Svalbard in the Barents Sea (e.g., Gee
1089 and Teben’kov, 2004; Breivik et al., 2005; Barrère et al., 2011; Knudsen et al., 2019) may be
1090 located west of the presently described Timanian thrust systems, i.e., probably west of or in western
1091 Spitsbergen where Caledonian blueschist and eclogite metamorphism ~~w~~has been recorded in
1092 Precambrian basement rocks (Horsfield, 1972; Dallmeyer et al., 1990a; Ohta et al., 1995;
1093 Kosminska et al., 2014).

Formatted: Font: 12 pt, Not Bold

Formatted: Font: 12 pt, Not Bold, Not Italic

Formatted: Font: (Default) Times New Roman

Formatted: Font: Not Bold, Not Italic

1094

1095 Conclusions

- 1096 1) Seismic data in the northern Norwegian Barents Sea and Svalbard reveal the existence of
1097 several systems of hundreds–thousands of kilometers long, several kilometers thick, top-
1098 SSW ~~Timanian~~ thrusts comprised of brittle–ductile thrusts, mylonitic shear zones and
1099 associated SSW-verging folds that appear to extend from onshore northwestern Russia to
1100 the northern Norwegian Barents Sea and to central and southwestern Spitsbergen. A notable
1101 structure is the Kongsfjorden–Cowanodden fault zone in Svalbard and the Norwegian
1102 Barents Sea, which likely merges with the Baidaratsky fault zone in the Russian Barents
1103 Sea and southern Novaya Zemlya. [We interpret these thrust systems as being related to the](#)
1104 [Neoproterozoic Timanian Orogeny.](#)
- 1105 2) In the east (away from the Caledonian collision zone), these Timanian thrusts systems were
1106 folded into NNE-plunging folds, offset, and reactivated as and/or overprinted by top-west,
1107 oblique-slip sinistral-reverse, brittle–ductile thrusts during subsequent Caledonian (e.g.,
1108 Agardhbukta Fault segment of the Lomfjorden Fault Zone) and, possibly, during Eurekan
1109 contraction, and are deeply buried. By contrast, in the west (near or within the Caledonian
1110 collision zone), Timanian thrusts were intensely deformed, pushed into sub-vertical
1111 positions, extensively overprinted, and exhumed to the surface.

- 1112 3) In eastern Spitsbergen, a major NNE-dipping Timanian thrust system, the Kongsfjorden–
1113 Cowanodden fault zone, is crosscut by a swarm of Devonian (–Mississippian?) dykes that
1114 intruded contemporaneous sedimentary strata deposited during extensional reactivation of
1115 the eastern portion of the thrust system as a low-angle extensional detachment during late–
1116 post-Caledonian collapse.
- 1117 4) Timanian thrust systems were overprinted by NNE-dipping, brittle normal faults in the late
1118 Paleozoic during the collapse of the Caledonides and/or subsequent rifting in the Devonian–
1119 Carboniferous.
- 1120 5) Timanian thrust systems and associated Caledonian and Devonian–Carboniferous brittle
1121 overprints (e.g., Agardhbukta Fault) in the northwestern Norwegian Barents Sea and
1122 Svalbard were mildly reactivated during the early Cenozoic Eurekan tectonic event, which
1123 resulted in minor folding and minor reverse offsets of Devonian–Mesozoic sedimentary
1124 strata and intrusions. Timanian thrusts and related overprints in the northeastern Norwegian
1125 Barents Sea were not reactivated during the Eurekan tectonic event.
- 1126 6) The presence of hundreds–thousands of kilometers long Timanian thrust systems may
1127 suggests that the Barents Sea and Svalbard’s three basement terranes were already attached
1128 to northern Norway and northwestern Russia in the late Neoproterozoic (ca. 600 Ma). If
1129 correct, a Timanian origin for these structures would, precludes any major strike-slip
1130 movements along major N–S-striking faults like the Billefjorden and Lomfjorden fault
1131 zones in the Phanerozoic, and suggests-imply that the Caledonian suture zone is located
1132 west of or in western Spitsbergen.

1133

1134 **Acknowledgements**

1135 The present study was supported by the Research Council of Norway, the Tromsø Research
1136 Foundation, and six industry partners through the Research Centre for Arctic Petroleum
1137 Exploration (ARCEX; grant number 228107), the SEAMSTRESS project (grant number 287865),
1138 and the Centre for Earth Evolution and Dynamics (CEED; grant number 223272). We thank the
1139 Norwegian Petroleum Directorate and the Federal Institute for Geosciences and Natural Resources
1140 (BGR) for granting access and allowing publication of seismic, magnetic and gravimetric data in
1141 Svalbard and the Norwegian Barents Sea. Prof. Steffen Bergh, Dr. Winfried Dallmann, Prof. Jiri
1142 Konopasek, Assoc. Prof. Mélanie Forien, Dr. Kate Waghorn (UiT The Arctic University of Norway

1143 in Tromsø), Dr. Peter Klitzke (Federal Institute for Geosciences and Natural Resources –
1144 Germany), Anna Dichiarante (Norway Seismic Array), Rune Matningsdal (Norwegian Petroleum
1145 Directorate), and Prof. Carmen Gaina (Centre for Earth Evolution and Dynamics, University of
1146 Oslo) are thanked for fruitful discussion.

1147

1148 **Data availability**

1149 For high-resolution versions of the figures and supplements, the reader is referred to the
1150 Open Access data repository DataverseNO (doi.org/10.18710/CE8RQH). ~~The complete seismic~~
1151 ~~study is also available from the corresponding author upon request.~~

1152

1153 **References**

- 1154 Aakvik, R.: Fاسies analyse av Undre Karbonske kullførende sedimenter, Billefjorden, Spitsbergen,
1155 Ph.D. Thesis, University of Bergen, Bergen, Norway, 219 pp., 1981.
- 1156 Andresen, A., Haremo, P., Swensson, E. and Bergh, S. G.: Structural geology around the southern
1157 termination of the Lomfjorden Fault Complex, Agardhdalen, east Spitsbergen, Norsk Geol.
1158 Tidsskr., 72, 83–91, 1992.
- 1159 Anell, I., Braathen, A., Olaussen, S. and Osmundsen, P. T.: Evidence of faulting contradicts a
1160 quiescent northern Barents Shelf during the Triassic, First Break, 31, 67–76, 2013.
- 1161 Anell, I. M., Braathen, A. and Olaussen, S.: Regional constraints of the Sørkapp Basin: A
1162 Carboniferous relic or a Cretaceous depression, Mar. Petrol. Geol., 54, 123–138, 2014.
- 1163 Anell, I. M., Faleide, J. I. and Braathen, A.: Regional tectono-sedimentary development of the
1164 highs and basins of the northwestern Barents Shelf, Norsk Geologisk Tidsskrift, 96, 1, 27–
1165 41, 2016.
- 1166 Arbaret, L. and Burg, J.-P.: Complex flow in lowest crustal, anastomosing mylonites: Strain
1167 gradients in a Kohistan gabbro, northern Pakistan, J. Geophys. Res., 108, 2467, 2003.
- 1168 Barrère, C., Ebbing, J. and Gernigon, L.: Offshore prolongation of Caledonian structures and
1169 basement characterization in the western Barents Sea from geophysical modelling,
1170 Tectonophys., 470, 71–88, 2009.
- 1171 Barrère, C., Ebbing, J. and Gernigon, L.: 3-D density and magnetic crustal characterization of the
1172 southwestern Barents Shelf: implications for the offshore prolongation of the Norwegian
1173 Caledonides, Geophys. J. Int., 184, 1147–1166, 2011.

- 1174 Boyer, S. E. and Elliott, D.: Thrust Systems, AAPG Bulletin, 66, 9, 1196–1230, 1982.
- 1175 Braathen, A., Bælum, K., Maher Jr., H. D. and Buckley, S. J.: Growth of extensional faults and
1176 folds during deposition of an evaporite-dominated half-graben basin; the Carboniferous
1177 Billefjorden Trough, Svalbard, Norsk Geol. Tidsskr., 91, 137–160, 2011.
- 1178 Braathen, A., Osmundsen, P. T., Maher, H. and Ganerød, M.: The Keisarhjelmen detachment
1179 records Silurian–Devonian extensional collapse in Northern Svalbard, Terra Nova, 30, 34–
1180 39, 2018.
- 1181 Breivik, A. J., Mjelde, R., Grogan, P., Shimamura, H., Murai, Y. and Nishimura, Y.: Caledonide
1182 development offshore–onshore Svalbard based on ocean bottom seismometer, conventional
1183 seismic, and potential field data, Tectonophys., 401, 79–117, 2005.
- 1184 Bro, E. G. and Shvarts, V. H.: Processing results from drill hole Raddedalen-1, Edge Island,
1185 Spitzbergen Archipelago, All-Russian Research Institute for Geology and Mineral
1186 Resources of the World Ocean, St. Petersburg, Pangaea, Report 5750, 1983.
- 1187 Cawood, P. A., McCausland, P. J. A. and Dunning, G. R.: Opening Iapetus: Constraints from the
1188 Laurentian margin in Newfoundland, GSA Bull., 113, 4, 443–453, 2001.
- 1189 Chalmers, J. A. and Pulvertaft, T. C. R.: Development of the continental margins of the Labrador
1190 Sea: a review, in: Non-Volcanic Rifting of Continental Margins: A Comparison of
1191 Evidence from Land and Sea, edited by: Wilson, R. C. L., Taylor, R. B. and Froitzheim,
1192 N., Geol. Soc. London, Spec. Publi., 187, 77–105, 2001.
- 1193 Cocks, L. R. M. and Torsvik, T. H.: Baltica from the late Precambrian to mid-Palaeozoic times:
1194 The gain and loss of a terrane’s identity, Earth-Sci. Rev., 72, 39–66, 2005.
- 1195 Colombu, S., Cruciani, G., Fancello, D., Franceschelli, M. and Musumeci, G.: Petrophysical
1196 properties of a granite-protomylonite-ultramylonite sequence: insight from the Monte
1197 Grighini shear zone, central Sardinia, Italy, Eur. J. Mineral, 27, 471–486, 2015.
- 1198 Corfu, F., Andersen, T. B. and Gasser, D.: The Scandinavian Caledonides: main features,
1199 conceptual advances and critical questions, in: New Perspectives on the Caledonides of
1200 Scandinavia and Related Areas, edited by: Corfu, F., Gasser, D. and Chew, D. M., Geol.
1201 Soc., London, Spec. Publi., 390, 9–43, 2014.
- 1202 Cutbill, J. L. and Challinor, A.: Revision of the Stratigraphical Scheme for the Carboniferous and
1203 Permian of Spitsbergen and Bjørnøya, Geol. Mag., 102, 418–439, 1965.

- 1204 Cutbill, J. L., Henderson, W. G. and Wright, N. J. R.: The Billefjorden Group (Early Carboniferous)
1205 of central Spitsbergen, Norsk Polarinst. Skr., 164, 57–89, 1976.
- 1206 Dallmann, W. K.: Geoscience Atlas of Svalbard, Norsk Polarinstitut, Tromsø, Norway,
1207 Rapportserie nr. 148, 2015.
- 1208 Dallmann, W. K. and Krasil'scikov, A. A.: Geological map of Svalbard 1:50,000, sheet D20G
1209 Bjørnøya, Norsk Polarinst. Temakart, 27, 1996.
- 1210 Dallmann, W. K. and Piepjohn, K.: The structure of the Old Red Sandstone and the Svalbardian
1211 Orogenic Event (Ellesmerian Orogeny) in Svalbard, Norg. Geol. Unders. B., Spec. Publi.,
1212 15, 106 pp., 2020.
- 1213 Dallmeyer, R. D., Peucat, J. J., Hirajima, T. and Ohta, Y.: Tectonothermal chronology within a
1214 blueschist–eclogite complex, west-central Spitsbergen, Svalbard: Evidence from $^{40}\text{Ar}/^{39}\text{Ar}$
1215 and Rb–Sr mineral ages, Lithos, 24, 291–304, 1990a.
- 1216 Dallmeyer, R. D., Peucat, J. J. and Ohta, Y.: Tectonothermal evolution of contrasting metamorphic
1217 complexes in northwest Spitsbergen (Biskayerhalvøya): Evidence from $^{40}\text{Ar}/^{39}\text{Ar}$ and Rb–
1218 Sr mineral ages, GSA Bull., 102, 653–663, 1990b.
- 1219 Dewey, J. F. and Strachan, R. A.: Changing Silurian–Devonian relative plate motion in the
1220 Caledonides: sinistral transpression to sinistral transtension, J. Geol. Soc., London, 160,
1221 219–229, 2003.
- 1222 Drachev, S. S.: Fold belts and sedimentary basins of the Eurasian Arctic, Arktos, 2:21, 2016.
- 1223 Drachev, S. S., Malyshev, N. A. and Nikishin, A. M.: Tectonic history and petroleum geology of
1224 the Russian Arctic Shelves: an overview, Petrol. Geol. Conf. series, 7, 591–619, 2010.
- 1225 Dumais, M.-A. and Brönnner, M.: Revisiting Austfonna, Svalbard, with potential field methods – a
1226 new characterization of the bed topography and its physical properties, The Cryosphere,
1227 14, 183–197, 2020.
- 1228 Eldholm, O. and Ewing, J.: Marine Geophysical Survey in the Southwestern Barents Sea, J.
1229 Geophys. Res., 76, 17, 3832–3841, 1971.
- 1230 Engen, Ø., Faleide, J. I. and Dyreng, T. K.: Opening of the Fram Strait gateway: A review of plate
1231 tectonic constraints, Tectonophysics, 450, 51–69, 2008.
- 1232 Estrada, S., Tessensohn, F. and Sonntag, B.-L.: A Timanian island-arc fragment in North
1233 Greenland: The Midtkap igneous suite, J. Geodyn., 118, 140–153, 2018.

- 1234 Faehnrich, K., Majka, J., Schneider, D., Mazur, S., Manecki, M., Ziemniak, G., Wala, V. T. and
1235 Strauss, J. V.: Geochronological constraints on Caledonian strike-slip displacement in
1236 Svalbard, with implications for the evolution of the Arctic, *Terra Nova*, 2020, 32, 290–299.
- 1237 Fortey, R. A. and Bruton, D. L.: Lower Ordovician trilobites of the Kirtonryggen Formation,
1238 Spitsbergen, *ossils and Strata*, 59, Wiley Blackwell, 120 pp., 2013.
- 1239 Fountain, D. M., Hurich, C. A. and Smithson, S. B.: Seismic relectivity of mylonite zones in the
1240 crust, *Geology*, 12, 195–198, 1984.
- 1241 Friend, P. F. and Moody-Stuart, M.: Sedimentation of the Wood Bay Formation (Devonian) of
1242 Spitsbergen: Regional analysis of a late orogenic basin, *Norsk Polarinst. Skr.*, 157, 80 pp.,
1243 1972.
- 1244 Friend, P. F., Heintz, N. and Moody-Stuart, M.: New unit terms for the Devonian of Spitsbergen
1245 and a new stratigraphical scheme for the Wood Bay Formation, *Polarinst. Årbok*, 1965, 59–
1246 64, 1966.
- 1247 Friend, P. F., Harland, W. B., Rogers, D. A., Snape, I. and Thornley, R. S.: Late Silurian and Early
1248 Devonian stratigraphy and probable strike-slip tectonics in northwestern Spitsbergen, *Geol.*
1249 *Mag.*, 134, 4, 459–479, 1997.
- 1250 Gasser, D.: The Caledonides of Greenland, Svalbard and other Arctic areas: status of research and
1251 open questions, in: *New Perspectives on the Caledonides of Scandinavia and Related Areas*,
1252 edited by: Corfu, F., Gasser, D. and Chew, D. M., *Geol. Soc., London, Spec. Publi.*, 390,
1253 93–129, 2014.
- 1254 Gee, D. G. and Moody-Stuart, M.: The base of the Old Red Sandstone in central north Haakon VII
1255 Land, Vestspitsbergen, *Polarinst. Årbok*, 1964, 57–68, 1966.
- 1256 Gee, D. G. and Pease, V.: The Neoproterozoic Timanide Orogen of eastern Baltica: introduction,
1257 in: *The Neoproterozoic Timanide Orogen of eastern Baltica*, edited by: Gee, D. G. and
1258 Pease, V., *Geol. Soc. London, Mem.*, 30, 1–3, 2004.
- 1259 Gee, D. G. and Teben'kov, A. M.: Svalbard: a fragment of the Laurentian margin, in: *The*
1260 *Neoproterozoic Timanide Orogen of eastern Baltica*, edited by: Gee, D. G. and Pease, V.,
1261 *Geol. Soc. London, Mem.*, 30, 191–206, 2004.
- 1262 Gee, D. G., Björklund, L. and Stølen, L.-K.: Early Proterozoic basement in Ny Friesland–
1263 implications for the Caledonian tectonics of Svalbard, *Tectonophys.*, 231, 171–182, 1994.

- 1264 Gee, D. G., Fossen, H., Henriksen, N. and Higgins, A. K.: From the Early Paleozoic Platforms of
1265 Baltica and Laurentia to the Caledonide Orogen of Scandinavia and Greenland, Episodes,
1266 31, 1, 44–51, 2008.
- 1267 Gernigon, L. and Brönnner, M.: Late Palaeozoic architecture and evolution of the southwestern
1268 Barents Sea: insights from a new generation of aeromagnetic data, J. Geol. Soc., London,
1269 169, 449–459, 2012.
- 1270 Gernigon, L., Brönnner, M., Roberts, D., Olesen, O., Nasuti, A. and Yamasaki, T.: Crustal and basin
1271 evolution of the southwestern Barents Sea: From Caledonian orogeny to continental
1272 breakup, Tectonics, 33, 347–373, 2014.
- 1273 Gernigon, L., Brönnner, M., Dumais, M.-A., Gradmann, S., Grønlie, A., Nasuti, A. and Roberts, D.:
1274 Basement inheritance and salt structures in the SE Barents Sea: Insights from new potential
1275 field data, J. Geodyn., 119, 82–106, 2018.
- 1276 Griffin, W. L., Nikolic, N., O'Reilly, S. Y. and Pearson, N. J.: Coupling, decoupling and
1277 metasomatism: Evolution of crust–mantle relationships beneath NW Spitsbergen, Lithos,
1278 149, 115–135, 2012.
- 1279 Gudlaugsson, S. T., Faleide, J. I., Johansen, S. E. and Breivik, A. J.: Late Palaeozoic structural
1280 development of the South-western Barents Sea. Mar. Petrol. Geol., 15, 73–102, 1998.
- 1281 Haremo, P. and Andresen, A.: Tertiary décollements thrusting and inversion structures along
1282 Billefjorden and Lomfjorden Fault Zones, East Central Spitsbergen, in: Structural and
1283 Tectonic Modelling and its Application to Petroleum Geology, edited by: Larsen, R. M.,
1284 Brekke, H., Larsen, B. T. and Talleraas, E., Norwegian Petroleum Society (NPF) Special
1285 Publications, 1, 481–494, 1992.
- 1286 Harland, W. B.: Contribution of Spitsbergen to understanding of tectonic evolution of North
1287 Atlantic region, AAPG Memoirs, 12, 817–851, 1969.
- 1288 Harland, W. B. and Horsfield, W. T.: West Spitsbergen Orogen, in: Mesozoic–Cenozoic Orogenic
1289 Belts, data for Orogenic Studies, J. Geol. Soc. London, Spec. Publi., 4, 747–755, 1974.
- 1290 Harland, W. B. and Kelly, S. R. A.: Eastern Svalbard Platform, in: Geology of Svalbard, edited by:
1291 Harland, W. B., Geol. Soc. London, Mem., 17, 521 pp., 1997.
- 1292 Harland, W. B. and Wright, N. J. R.: Alternative hypothesis for the pre-Carboniferous evolution of
1293 Svalbard, Norsk Polarinst. Skr., 167, 89–117, 1979.

- 1294 Harland, W. B., Cutbill, L. J., Friend, P. F., Gobbett, D. J., Holliday, D. W., Maton, P. I., Parker,
1295 J. R. and Wallis, R. H.: The Billefjorden Fault Zone, Spitsbergen – the long history of a
1296 major tectonic lineament, *Norsk Polarinst. Skr.*, 161, 1–72, 1974.
- 1297 Harland, W. B., Scott, R. A., Auckland, K. A. and Snape, I.: The Ny Friesland Orogen, Spitsbergen,
1298 *Geol. Mag.*, 129, 6, 679–708, 1992.
- 1299 Harland, W. B., Hambrey, M. J. and Waddams, P.: Vendian geology of Svalbard, *Norsk Polarinst.*
1300 *Skri.*, 193, 152 pp., 1993.
- 1301 Hassaan, M., Faleide, J. I., Gabrielsen, R. H. and Tsikalas, F.: Carboniferous graben structures,
1302 evaporite accumulations and tectonic inversion in the southeastern Norwegian Barents Sea,
1303 *Mar. Petrol. Geol.*, 112, 104038, 2020a.
- 1304 Hassaan, M., Faleide, J. I., Gabrielsen, R. H. and Tsikalas, F.: Architecture of the evaporite
1305 accumulation and salt structures dynamics in Tiddlybanken Basin, southeastern Norwegian
1306 Barents Sea, *Basin Res.*, 33, 91–117, 2020b.
- 1307 Herrevold, T., Gabrielsen, R. H. and Roberts, D.: Structural geology of the southeastern part of the
1308 Trollfjorden-Komagelva Fault Zone, Varanger Peninsula, Finnmark, North Norway,
1309 *Norwegian Journal of Geology*, 89, 305-325, 2009.
- 1310 Horsfield, W. T.: Glauconite schists of Caledonian age from Spitsbergen, *Geol. Mag.*, 109, 1,
1311 29–36, 1972.
- 1312 Hurich, C. A., Smithson, S. B., Fountain, D. M. and Humphreys, M. C.: Seismic evidence of
1313 mylonite reflectivity and deep structure in the Kettle dome metamorphic core complex,
1314 Washington, *Geology*, 13, 577–580, 1985.
- 1315 Jakobsson, M., Mayer, L., Coackley, B., Dowdeswell, J. A., Forbes, S., Fridman, B., Hodnesdal,
1316 H., Noormets, R., Pedersen, R., Rebesco, M., Schenke, H. W., Zarayskaya, Y., Accettella,
1317 D., Armstrong, A., Anderson, R. M., Bienhoff, P., Camerlenghi, A., Church, I., Edwards,
1318 M., Gardner, J. V., Hall, J. K., Hell, B., Hestvik, O., Kristoffersen, Y., Marcussen, C.,
1319 Mohammad, R., Mosher, D., Nghiem, S. V., Pedrosa, M. T., Travaglini, P. G., and
1320 Weatherall, P.: The International Bathymetric Chart of the Arctic Ocean (IBCAO) Version
1321 3.0, *Geophys. Res. Lett.*, 39, L12609, <https://doi.org/10.1029/2012GL052219>, 2012.
- 1322 Johansen, S. E., Ostist, B. K., Birkeland, Ø., Fedorovsky, Y. F., Martirosjan, V. N., Bruun
1323 Christensen, O., Cheredeev, S. I., Ignatenko, E. A. and Margulis, L. S.: Hydrocarbon
1324 potential in the Barents Sea region: play distribution and potential, in: *Arctic Geology and*

1325 Petroleum Potential, edited by: Vorren, T. O., Bergsager, E., Dahl-Stamnes, Ø. A., Holter,
1326 E., Johansen, B., Lie, E. and Lund, T. B., NPF Spec. Publi., 2, 273–320, Elsevier,
1327 Amsterdam, 1992.

1328 Johansson, Å., Larionov, A. N., Gee, D. G., Ohta, Y., Tebenkov, A. M. and Sandelin, S.:
1329 Grenvillian and Caledonian tectono-magmatic activity in northeasternmost Svalbard, in:
1330 The Neoproterozoic Timanide Orogen of Eastern Baltica, edited by: Gee, D. G. and Pease,
1331 V., Geol. Soc. London Memoirs, 30, 207–232, 2004.

1332 Johansson, Å., Gee, D. G., Larionov, A. N., Ohta, Y. and Tebenkov, A. M.: Grenvillian and
1333 Caledonian evolution of eastern Svalbard – a tale of two orogenies, Terra Nova, 17, 317–
1334 325, 2005.

1335 Kairanov, B., Escalona, A., Mordascova, A., Sliwinska, K. and Suslova, A.: Early Cretaceous
1336 tectonostratigraphy evolution of the north central Barents Sea, J. Geodyn., 119, 183–198,
1337 2018.

1338 Klitzke, P., Franke, D., Ehrhardt, A., Lutz, R., Reinhardt, L., Heyde, I. and Faleide, J. I.: The
1339 Palaeozoic Evolution of the Olga Basin Region, Northern Barents Sea: A Link to the
1340 Timanian Orogeny, Geochem., Geophy., Geosy., 20, 614–629, 2019.

1341 Knudsen, C., Gee, D. G., Sherlock, S. C. and Yu, L.: Caledonian metamorphism of metasediments
1342 from Franz Josef Land, GFF, 141, 295–307, 2019.

1343 Koehl, J.-B. P.: Early Cenozoic Eurekan strain partitioning and decoupling in central Spitsbergen,
1344 Svalbard, Solid Earth, 12, 1025–1049, 2020a.

1345 Koehl, J.-B. P.: Impact of Timanian thrusts on the Phanerozoic tectonic history of Svalbard,
1346 Keynote lecture, EGU General Assembly, May 3rd–8th 2020, Vienna, Austria, 2020b.

1347 Koehl, J.-B. P. and Muñoz-Barrera, J. M.: From widespread Mississippian to localized
1348 Pennsylvanian extension in central Spitsbergen, Svalbard, Solid Earth, 9, 1535–1558, 2018.

1349 Koehl, J.-B. P., Bergh, S. G., Henningsen, T. and Faleide, J. I.: Middle to Late Devonian–
1350 Carboniferous collapse basins on the Finnmark Platform and in the southwesternmost
1351 Nordkapp basin, SW Barents Sea, Solid Earth, 9, 341–372, 2018.

1352 Koehl, J.-B. P., Bergh, S. G., Osmundsen, P. T., Redfield, T., Indrevær, K., Lea, H. and Bergø, E.:
1353 Late Devonian–Carboniferous faulting and controlling structures and fabrics in NW
1354 Finnmark, Norw. J. Geol., 99, 3, 1–40, 2019.

- 1355 Koehl, J.-B. P., Allaart, L. and Noormets, R.: Devonian–Carboniferous collapse and segmentation
1356 of the Billefjorden Trough, and Eureka inversion–overprint and strain partitioning and
1357 decoupling along inherited WNW–ESE-striking faults, in review, 2021.
- 1358 Korago, E. A., Kovaleva, G. N., Lopatin, B. G. and Orgo, V. V.: The Precambrian rocks of Novaya
1359 Zemlya, in: *The Neoproterozoic Timanide Orogen of Eastern Baltica*, edited by: Gee, D.
1360 G. and Pease, V., *Geol. Soc. London, Mem.*, 30, 135–143, 2004.
- 1361 Kosminska, K., Majka, J., Mazur, S., Krumbholz, M., Klonowska, I., Manecki, M., Czerny, J. and
1362 Dwornik, M.: Blueschist facies metamorphism in Nordenskiöld Land of west-central
1363 Svalbard, *Terra Nova*, 26, 377–386, 2014.
- 1364 Kostyuchenko, A., Sapozhnikov, R., Egorkin, A., Gee, D. G., Berzin, R. and Solodilov, L.: Crustal
1365 structure and tectonic model of northeastern Baltica, based on deep seismic and potential
1366 field data, in: *European Lithosphere Dynamics*, edited by: Gee, D. G. and Stephenson, R.
1367 A., *Geol. Soc. London Mem.*, 32, 521–539, 2006.
- 1368 Labrousse, L., Elvevold, S., Lepvrier, C. and Agard, P.: Structural analysis of high-pressure
1369 metamorphic rocks of Svalbard: Reconstructing the early stages of the Caledonian orogeny,
1370 *Tectonics*, 27, 22 pp., 2008.
- 1371 Lamar, D. L. and Douglass, D. N.: Geology of an area astride the Billefjorden Fault Zone, Northern
1372 Dicksonland, Spitsbergen, Svalbard, *Polarist. Skr.*, 197, 46 pp., 1995.
- 1373 Lamar, D. L., Reed, W. E. and Douglass, D. N.: Billefjorden fault zone, Spitsbergen: Is it part of a
1374 major Late Devonian transform?, *GSA*, 97, 1083–1088, 1986.
- 1375 Larssen, G. B., Elvebakk, G., Henriksen, L. B., Kristensen, S.-E., Nilsson, I., Samuelsberg, T. J.,
1376 Svånå, T. A., Stemmerik, L. and Worsley, D.: Upper Palaeozoic lithostratigraphy of the
1377 Southern part of the Norwegian Barents Sea, *Norges geol. unders. Bull.*, 444, 45 pp., 2005.
- 1378 Lasabuda, A., Laberg, J. S., Knutsen, S.-M. and Safronova, P.: Cenozoic tectonostratigraphy and
1379 pre-glacial erosion: A mass-balance study of the northwestern Barents Sea margin,
1380 *Norwegian Arctic, J. Geodyn.*, 119, 149–166, 2018.
- 1381 Lippard, S. J. and Prestvik, T.: Carboniferous dolerite dykes on Magerøy: new age determination
1382 and tectonic significance, *Norsk Geologisk Tidsskrift*, 77, 159–163, 1997.
- 1383 Livshits, Yu. Ya.: Tectonics of Central Vestspitsbergen, in: *Geology of Spitsbergen*, edited by:
1384 Sokolov, V. N., National Lending Library of Science and Technology, Boston Spa.,
1385 Yorkshire, UK, 59–75, 1965a.

- 1386 Livshits, Yu. Ya.: Paleogene deposits of Nordenskiöld Land, Vestspitsbergen, in: *Geology of*
1387 *Spitsbergen*, edited by: Sokolov, V. N., National Lending Library of Science and
1388 *Technology*, Boston Spa., Yorkshire, UK, 193–215, 1965b.
- 1389 Lopatin, B. G., Pavlov, L. G., Orgo, V. V. and Shkarubo, S. I.: *Tectonic Structure of Novaya*
1390 *Zemlya*, *Polarforschung*, 69, 131–135, 2001.
- 1391 Lorenz, H., Männik, P., Gee, D. and Proskurnin, V.: *Geology of the Severnaya Zemlya Archipelago*
1392 *and the North Kara Terrane in the Russian high Arctic*, *Int. J. Earth Sci.*, 97, 519–547, 2008.
- 1393 Lowell, J. D.: *Spitsbergen tertiary Orogenic Belt and the Spitsbergen Fracture Zone*, *GSA Bull.*,
1394 83, 3091–3102, 1972.
- 1395 Lyberis, N. and Manby, G.: *Continental collision and lateral escape deformation in the lower and*
1396 *upper crust: An example from Caledonide Svalbard*, *Tectonics*, 18, 1, 40–63, 1999.
- 1397 Majka, J. and Kosminska, K.: *Magmatic and metamorphic events recorded within the Southwestern*
1398 *Basement Province of Svalbard*, *Arktos*, 3:5, 2017.
- 1399 Majka, J., Mazur, S., Manecki, M., Czerny, J. and Holm, D. K.: *Late Neoproterozoic amphibolite-*
1400 *facies metamorphism of a pre-Caledonian basement block in southwest Wedel Jarlsberg*
1401 *Land, Spitsbergen: new evidence from U–Th–Pb dating of monazite*, *Geol. Mag.*, 145, 6,
1402 822–830, 2008.
- 1403 Majka, J., Larionov, A. N., Gee, D. G., Czerny, J. and Prsek, J.: *Neoproterozoic pegmatite from*
1404 *Skoddefjellet, Wedel Jarlsberg Land, Spitsbergen: Additional evidence for c. 640 Ma*
1405 *tectonothermal event in the Caledonides of Svalbard*, *Polish Polar Res.*, 33, 1–17, 2012.
- 1406 Majka, J., De’eri-Shlevin, Y., Gee, D. G., Czerny, J., Frei, D. and Ladenberger, A.: *Torellian (c.*
1407 *640 Ma) metamorphic overprint of Tonian (c. 950 Ma) basement in the Caledonides of*
1408 *southwestern Svalbard*, *Geol. Mag.*, 151, 4, 732–748, 2014.
- 1409 Manby, G. M. and Lyberis, N.: *Tectonic evolution of the Devonian Basin of northern Spitsbergen*,
1410 *Norsk Geol. Tidsskr.*, 72, 7–19, 1992.
- 1411 Manby, G. M., Lyberis, N., Chorowicz, J. and Thiedig, F.: *Post-Caledonian tectonics along the*
1412 *Billefjorden fault zone, Svalbard, and implications for the Arctic region*, *Geol. Soc. Am.*
1413 *Bul.*, 105, 201–216, 1994.
- 1414 Manecki, M., Holm, D. K., Czerny, J. and Lux, D.: *Thermochronological evidence for late*
1415 *Proterozoic (Vendian) cooling in southwest Wedel Jarlsberg Land, Spitsbergen*, *Geological*
1416 *Magazine*, 135, 63–9, 1998.

- 1417 Marelló, L., Ebbing, J. and Gernigon, L.: Magnetic basement study in the Barents Sea from
1418 inversion and forward modelling, *Tectonophys.*, 493, 153–171, 2010.
- 1419 Marelló, L., Ebbing, J. and Gernigon, L.: Basement inhomogeneities and crustal setting in the
1420 Barents Sea from a combined 3D gravity and magnetic model, *Geophys. J. Int.*, 193, 2,
1421 557–584, 2013.
- 1422 Mazur, S., Czerny, J., Majka, J., Manecki, M., Holm, D., Smyrak, A. and Wypych, A.: A strike-
1423 slip terrane boundary in Wedel Jarlsberg Land, Svalbard, and its bearing on correlations of
1424 SW Spitsbergen with the Pearya terrane and Timanide belt, *J. Geol. Soc. London*, 166, 529–
1425 544, 2009.
- 1426 McCann, A. J.: Deformation of the Old Red Sandstone of NW Spitsbergen; links to the Ellesmerian
1427 and Caledonian orogenies, in: *New Perspectives on the Old Red Sandstone*, edited by:
1428 Friends, P. F. and Williams, B. P. J., *Geol. Soc. London*, 180, 567–584, 2000.
- 1429 Merdith, A. S., Williams, S. E., Collins, A. S., Tetley, M. G., Mulder, J. A., Blades, M. L., Young,
1430 A., Armistead, S. E., Cannon, J., Zahirovic, S. and Müller, R. D.: Extending full-plate
1431 tectonic models into deep time: Linking the Neoproterozoic and the Phanerozoic, *Earth-
1432 Sci. Rev.*, 214, 103477, 2021.
- 1433 Müller, R., Klausen, T. G., Faleide, J. I., Olaussen, S., Eide, C. H. and Suslova, A.: Linking regional
1434 unconformities in the Barents Sea to compression-induced forebulge uplift at the Triassic-
1435 Jurassic transition, *Tectonophys.*, 765, 35–51, 2019.
- 1436 Murascov, L. G. and Mokin, Ju. I.: Stratigraphic subdivision of the Devonian deposits of
1437 Spitsbergen, *Polarinst. Skr.*, 167, 249–261, 1979.
- 1438 Nasuti, A., Roberts, D. and Gernigon, L.: Multiphase mafic dykes in the Caledonides of northern
1439 Finnmark revealed by a new high-resolution aeromagnetic dataset, *Norwegian Journal of
1440 Geology*, 95, 251–263, 2015.
- 1441 Norton, M. G., McClay, K. R. and Way, N. A.: Tectonic evolution of Devonian basins in northern
1442 Scotland and southern Norway, *Norsk Geol. Tidsskr.*, 67, 323–338, 1987.
- 1443 Oakey, G. N. and Chalmers, J. A.: A new model for the Paleogene motion of Greenland relative to
1444 North America: Plate reconstructions of the Davis Strait and Nares Strait regions between
1445 Canada and Greenland, *J. of Geophys. Res.*, 117, B10401, 2012.
- 1446 Ogata, K., Mulrooney, M. J., Braathen, A., Maher, H., Osmundsen, P. T., Anell, I., Smyrak-Sikora,
1447 A. A. and Balsamo, F.: Architecture, deformation style and petrophysical properties of

- 1448 growth fault systems: the Late Triassic deltaic succession of southern Edgeøya (East
1449 Svalbard), *Basin Res.*, 30, 5, 1042–1073, 2018.
- 1450 Ohta, Y., Dallmeyer, R. D. and Peucat, J. J.: Caledonian terranes in Svalbard, *GSA Spec. Paper*,
1451 230, 1–15, 1989.
- 1452 Ohta, Y., Krasil'scikov, A. A., Lepvrier, C. and Teben'kov, A. M.: Northern continuation of
1453 Caledonian high-pressure metamorphic rocks in central-western Spitsbergen, *Polar Res.*,
1454 14, 3, 303–315, 1995.
- 1455 Olovyanishnikov, V. G., Roberts, D. and Siedlecka, A.: Tectonics and Sedimentation of the
1456 Meso- to Neoproterozoic Timan-Varanger Belt along the Northeastern Margin of Baltica,
1457 *Polarforschung*, 68, 267–274, 2000.
- 1458 Osmundsen, P-T., Braathen, A., Rød, R. S. and Hynne, I. B.: Styles of normal faulting and fault-
1459 controlled sedimentation in the Triassic deposits of Eastern Svalbard, *Norwegian Petroleum*
1460 *directorates Bulletin*, 10, 61–79, 2014.
- 1461 Petersen, T. G., Thomsen, T. B., Olaussen, S. and Stemmerik, L.: Provenance shifts in an evolving
1462 Eurekan foreland basin: the Tertiary Central Basin, Spitsbergen, *J. Geol. Soc., London*, 173,
1463 634–648, 2016.
- 1464 Peucat, J.-J., Ohta, Y., Gee, D. G. and Bernard-Griffiths, J.: U-Pb, Sr and Nd evidence for
1465 Grenvillian and latest Proterozoic tectonothermal activity in the Spitsbergen Caledonides,
1466 *Arctic Ocean, Lithos*, 22, 275–285, 1989.
- 1467 Phillips, T., Jackson, C. A-L., Bell, R. E., Duffy, O. B. and Fossen, H.: Reactivation of
1468 intrabasement structures during rifting: A case study from offshore southern Norway,
1469 *Journal of Structural Geology*, 91, 54–73, 2016.
- 1470 Piepjohn, K.: The Svalbardian–Ellesmerian deformation of the Old Red Sandstone and the pre-
1471 Devonian basement in NW Spitsbergen (Svalbard), in: *New Perspectives on the Old Red*
1472 *Sandstone*, edited by: Friend, P. F. and Williams, B. P. J., *Geol. Soc. London Spec. Publi.*,
1473 180, 585–601, 2000.
- 1474 Piepjohn, K.: von Gosen, W., Läufer, A., McClelland, W. C. and Estrada, S.: Ellesmerian and
1475 Eurekan fault tectonics at the northern margin of Ellesmere Island (Canadian High Arctic),
1476 *Z. Dt. Ges. Geowiss.*, 164, 1, 81–105, 2013.
- 1477 Piepjohn, K., Dallmann, W. K. and Elvevold, S.: The Lomfjorden Fault Zone in eastern Spitsbergen
1478 (Svalbard), in: *Circum-Arctic Structural Events: Tectonic Evolution of the Arctic Margins*

1479 and Trans-Arctic Links with Adjacent Orogens, edited by: Piepjohn, K., Strauss, J. V.,
1480 Reinhardt, L. and McClelland, W. C., GSA Spec. Paper, 541, 95–130, 2019.

1481 Ramsay, J. G.: Interference Patterns Produced by the Superposition of Folds of Similar Type, J.
1482 Geol., 70, 4, 466–481, 1962.

1483 Rice, A. H. N.: Restoration of the External Caledonides, Finnmark, North Norway, in: New
1484 Perspectives on the Caledonides of Scandinavia and Related Areas, Corfu, F., Gasser, D.
1485 and Chew, D. M. (eds), Geological Society, London, Special Publications, 390, 271-299,
1486 2014.

1487 Roberts, D.: Tectonic Deformation in the Barents Sea Region of Varanger Peninsula, Finnmark,
1488 Norges geol. unders., 282, 1–39, 1972.

1489 Roberts, D. and Olovyanishshnikov, V.: Structural and tectonic development of the Timanide
1490 orogeny, in: The Neoproterozoic Timanide Orogen of Eastern Baltica, edited by: Gee, D.
1491 G. and Pease, V., Geol. Soc. London, Mem., 30, 47–57, 2004.

1492 Roberts, D. and Siedlecka, A.: Timanian orogenic deformation along the northeastern margin of
1493 Baltica, Northwest Russia and Northeast Norway, and Avalonian-Cadomian connections,
1494 Tectonophysics, 352, 1r69-184, 2002.

1495 Roberts, D. and Williams, G. D.: Berggrunnskart Kjøllefjord 2236 IV, M 1:50.000, foreløpig
1496 utgave, Norges geol. unders., 2013.

1497 Roberts, D., Mitchell, J. G. and Andersen, T. B.: A post-Caledonian dyke from Magerøy North
1498 Norway: age and geochemistry, Norwegian Journal of Geology, 71, 289-294, 1991.

1499 Rosa, D., Majka, J., Thrane, K. and Guarnieri, P.: Evidence for Timanian-age basement rocks in
1500 North Greenland as documented through U–Pb zircon dating of igneous xenoliths from the
1501 Midtkap volcanic centers, Precambrian Res., 275, 394–405, 2016.

1502 Schiffer, C., Doré, A. G., Foulger, G. R., Franke, D., Geoffroy, L., Gernigon, L., Holdsworth, B.,
1503 Kuszniir, N., Lundin, E., McCaffrey, K., Peace, A. L., Petersen, K. D., Phillips, T. B.,
1504 Stephenson, R., Stoker, M. S. and Welford, J. K.: Structural inheritance in the North
1505 Atlantic, Earth-Science Reviews, 206, 102975, 2020.

1506 Senger, K., Roy, S., Braathen, A., Buckley, S., Bælum, K., Gernigon, L., Mjelde, R., Noormets,
1507 R., Ogata, K., Olausson, S., Planke, S., Ruud, B. O. and Tveranger, J.: Geometries of
1508 doleritic intrusions in central Spitsbergen, Svalbard: an integrated study of an onshore-

1509 offshore magmatic province with applications to CO₂ sequestration, *Norw. J. Geol.*, 93,
1510 143–166, 2013.

1511 Siedlecka, A.: Late Precambrian Stratigraphy and Structure of the North-Eastern Margin of the
1512 Fennoscandian Shield (East Finnmark – Timan Region), *Nor. geol. unders.*, 316, 313-348,
1513 1975.

1514 Siedlecka, A. and Roberts, D.: Report from a visit to the Komi Branch of the Russian Academy of
1515 Sciences in Syktyvkar, Russia, and from fieldwork in the central Timans, August 1995,
1516 *Norges geol. unders. report*, 95.149, 32 pp., 1995.

1517 Siedlecka, A. and Siedlecki, S.: Some new aspects of the geology of Varanger peninsula (Northern
1518 Norway), *Nor. geol. unders.*, 247, 288-306, 1967.

1519 Siedlecka, A. and Siedlecki, S.: Late Precambrian sedimentary rocks of the Tanafjord–
1520 Varangerfjord region of Varanger Peninsula, Northern Norway, in: *The Caledonian
1521 Geology of Northern Norway*, edited by: Roberts, D. and Gustavson, M., *Norges geol.
1522 unders.*, 269, 246–294, 1971.

1523 Smyrak-Sikora, A., Osmundsen, P. T., Braathen, A., Ogata, K., Anell, I., Mulrooney, M. J. and
1524 Zuchuat, V: Architecture of growth basins in a tidally influenced, prodelta to delta-front
1525 setting: The Triassic succession of Kvalpynten, East Svalbard, *Basin Research*, 32, 5, 959–
1526 988, 2020.

1527 Stouge, S., Christiansen, J. L. and Holmer, L. E.: Lower Palaeozoic stratigraphy of
1528 Murchisonfjorden and Sparreneset, Nordaustlandet, Svalbard, *Geografiska Annaler: Series
1529 A, Physical Geography*, 93, 209–226, 2011.

1530 Sturt, B. A., Pringle, I. R. and Ramsay, D. M.: The Finnmarkian phase of the Caledonian Orogeny,
1531 *J. Geol., Soc., London*, 135, 597–610, 1978.

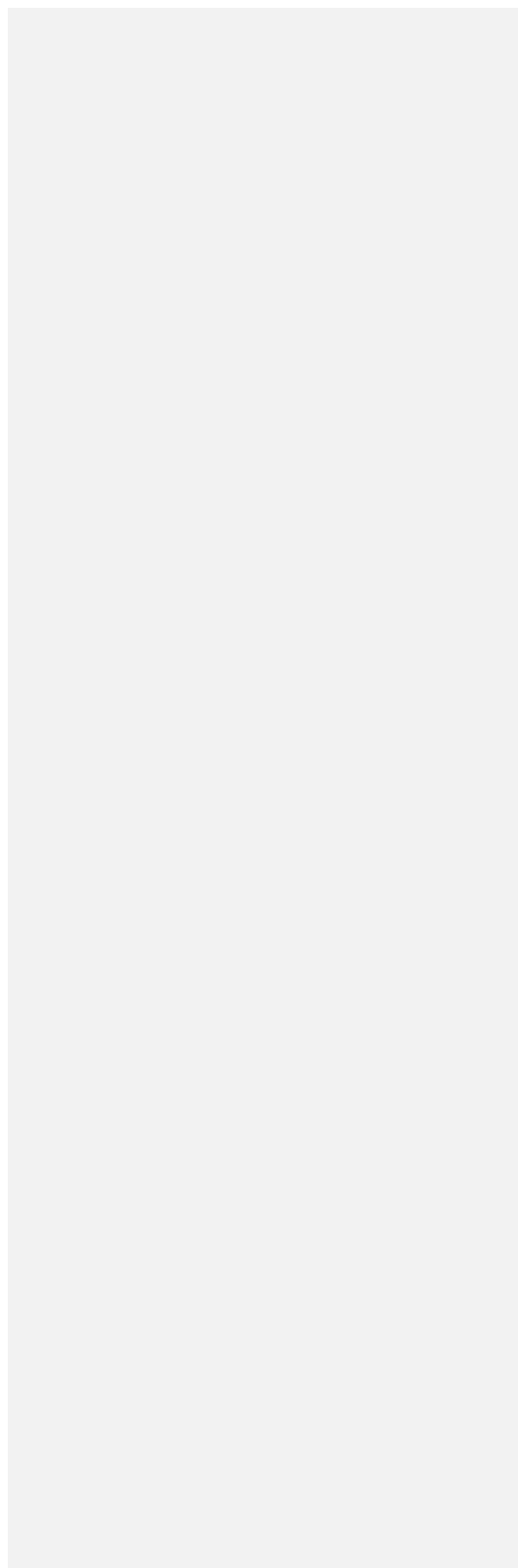
1532 Thiede, J., Pfirman, S., Schenke, H.-W. and Reil, W.: Bathymetry of Molloy Deep: Fram Strait
1533 Between Svalbard and Greenland, *Mar. Geophys. Res.*, 12, 197–214, 1990.

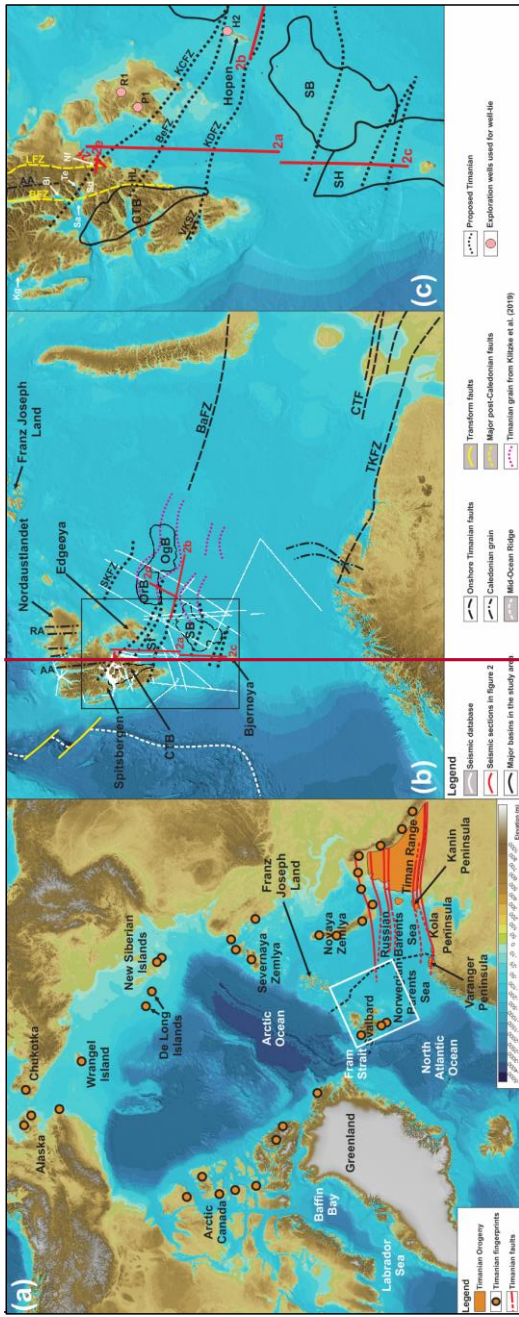
1534 Tonstad, S. A.: The Late Paleozoic development of the Ottar basin from seismic 3D interpretation,
1535 *Master's Thesis*, University of Tromsø, Tromsø, Norway, 135 pp., 2018.

1536 Torsvik, T. H. and Trench, A.: The Ordovician history of the Iapetus Ocean in Britain: new
1537 palaeomagnetic constraints, *J. Geol. Soc., London*, 148, 423–425, 1991.

1538 Torsvik, T. H., Burke, K., Steinberger, B., Webb, S. J. and Ashwal, L. D.: Diamond sampled by
1539 plumes from the core–mantle boundary, *Nature Lett.*, 466, 352–355, 2010.

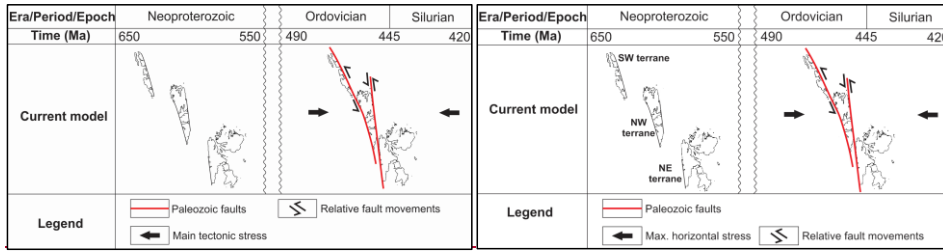
- 1540 Townsend, C.: Thrust transport directions and thrust sheet restoration in the Caledonides of
1541 Finnmark, North Norway, *J. Structural Geol.*, 9, 3, 345–352, 1987.
- 1542 Vernikovsky, V. A., Metelkin, D. V., Vernikovskaya, A. E., Matushkin, N. Yu., Lobkovsky, L. I.
1543 and Shipilov, E. V.: Early evolution stage of the arctic margins (Neoproterozoic-Paleozoic)
1544 and plate reconstructions, ICAM VI Proceedings, May 2011, Fairbanks, Alaska, USA, 265–
1545 285, 2011.
- 1546 Von Gosen, W. and Piepjohn, K.: Polyphase Deformation in the Eastern Hornsund Area, *Geol. Jb.*,
1547 B91, 291–312, 2001.
- 1548 Witt-Nilsson, P., Gee, D. G. and Hellman, F. J.: Tectonostratigraphy of the Caledonian Atomfjella
1549 Antiform of northern Ny Friesland, Svalbard, *Norsk Geol. Tidsskr.*, 78, 67–80, 1998.
- 1550 Worsley, D., Agdestein, T., Gjelberg, J. G., Kirkemo, K., Mørk, A., Nilsson, I., Olausson, S., Steel,
1551 R. J. and Stemmerik, L.: The geological evolution of Bjørnøya, Arctic Norway:
1552 implications for the Barents Shelf, *Norsk Geol. Tidsskr.*, 81, 195–234, 2001.
- 1553 Ziegler, P. A.: Evolution of the Arctic–North Atlantic and the Western Tethys, *AAPG Mem.* 43,
1554 1988.
- 1555



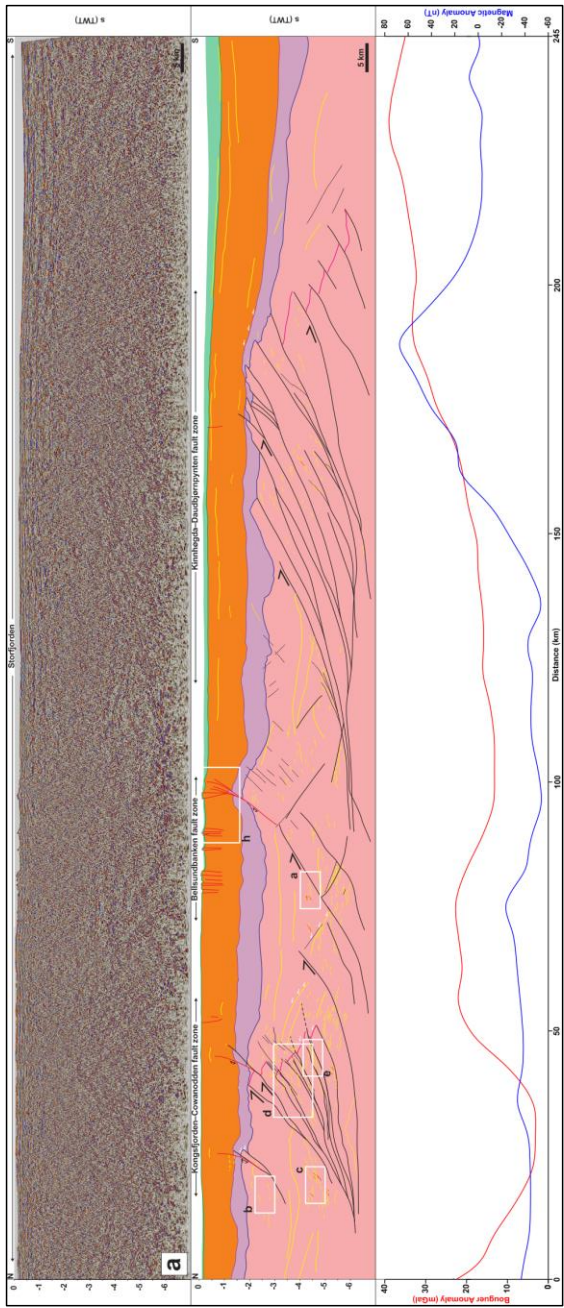


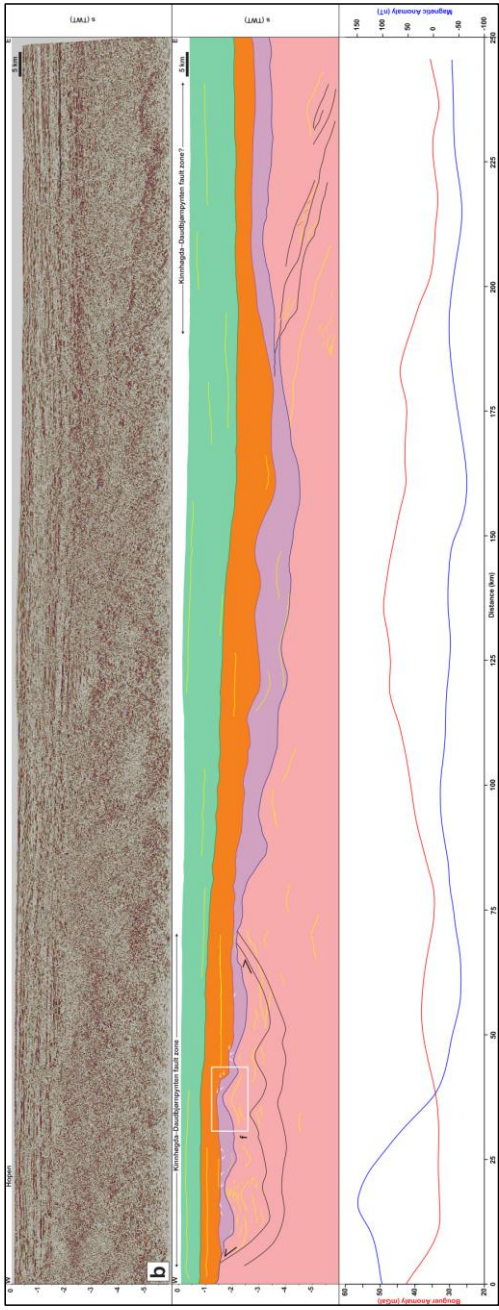
1559 Figure 1: (a) Overview map showing the Timanian belt in Russia and Norway, and occurrences of Timanian fingerprints
1560 throughout the Arctic; (b) Regional map of Svalbard and the Barents Sea the main geological elements and the seismic
1561 database used in the present study. The location of (b) is shown as a white frame in (a); (c) Zoom in the northern Norwegian
1562 Barents Sea and Svalbard showing the main faults and basins in the study area, and the proposed Timanian structures. The
1563 location of (c) is shown as a black frame in (b). The location of the Raddedalen-1 well is from Smyrak-Sikora et al. (2020).
1564 Topography and bathymetry are from Jakobsson et al. (2012). Abbreviations: AA: Atomfjella Antiform; BaFZ: Baidaratsky
1565 fault zone; BeFZ: Bellsundbanken fault zone; BFZ: Billefjorden Fault Zone; Bi: Billefjorden; CTB: Central Tertiary Basin;
1566 HL: Heer Land; **Hs: Hornsund**; H2: Hopen-2; KCFZ: Kongsfjorden–Cowanodden fault zone; KDFZ: Kinnhøgda–
1567 Daudbjørnpynten fault zone; Kg: Kongsfjorden; LFZ: Lomfjorden Fault Zone; Nf: Nordmannsfonna; OgB: Olga Basin;
1568 OrB: Ora Basin; P1: Plurdalen-1; RA: Rijpdalen Anticline; R1: Raddedalen-1; Sa: Sassenfjorden; SB: Sørkapp Basin; Sf:
1569 Storfjorden; SH: Stappen High; SKFZ: Steiløya–Krylen fault zone; Te: Tempelfjorden; TKFZ: Trollfjorden–Komagelva
1570 Fault Zone; VKSZ: Vimsodden–Kosibapasset Shear Zone.

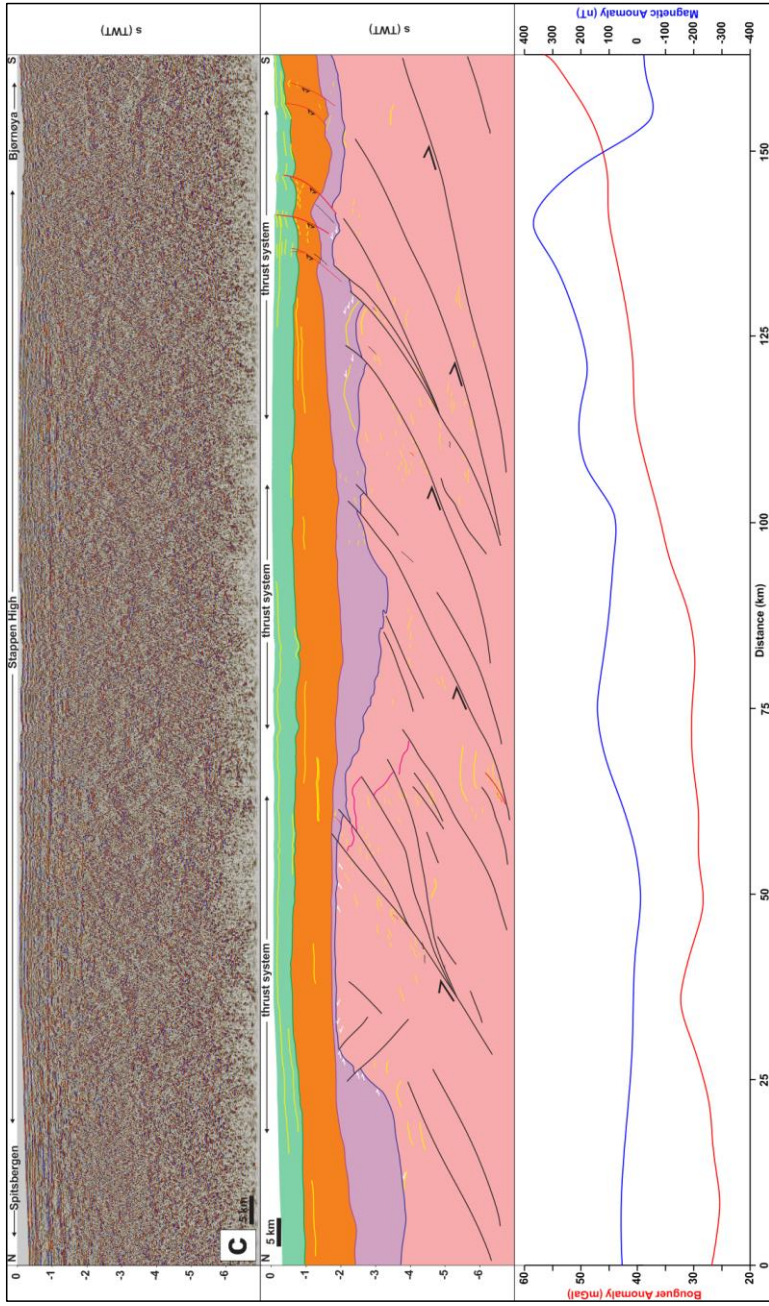
1571

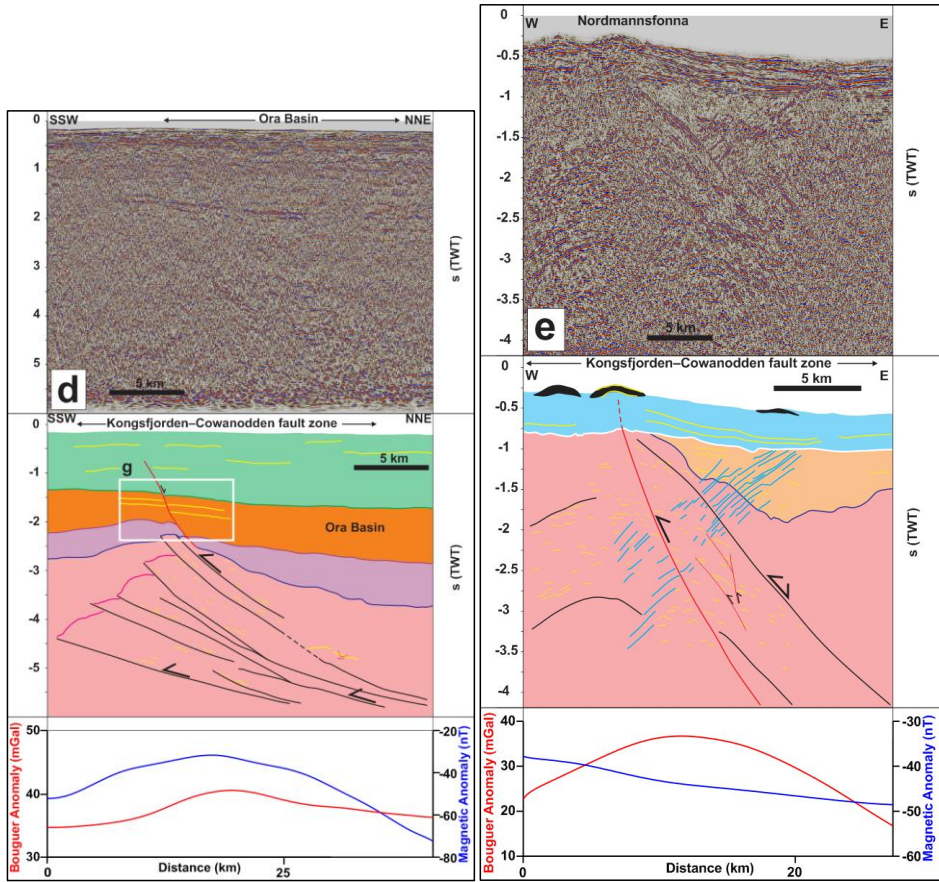


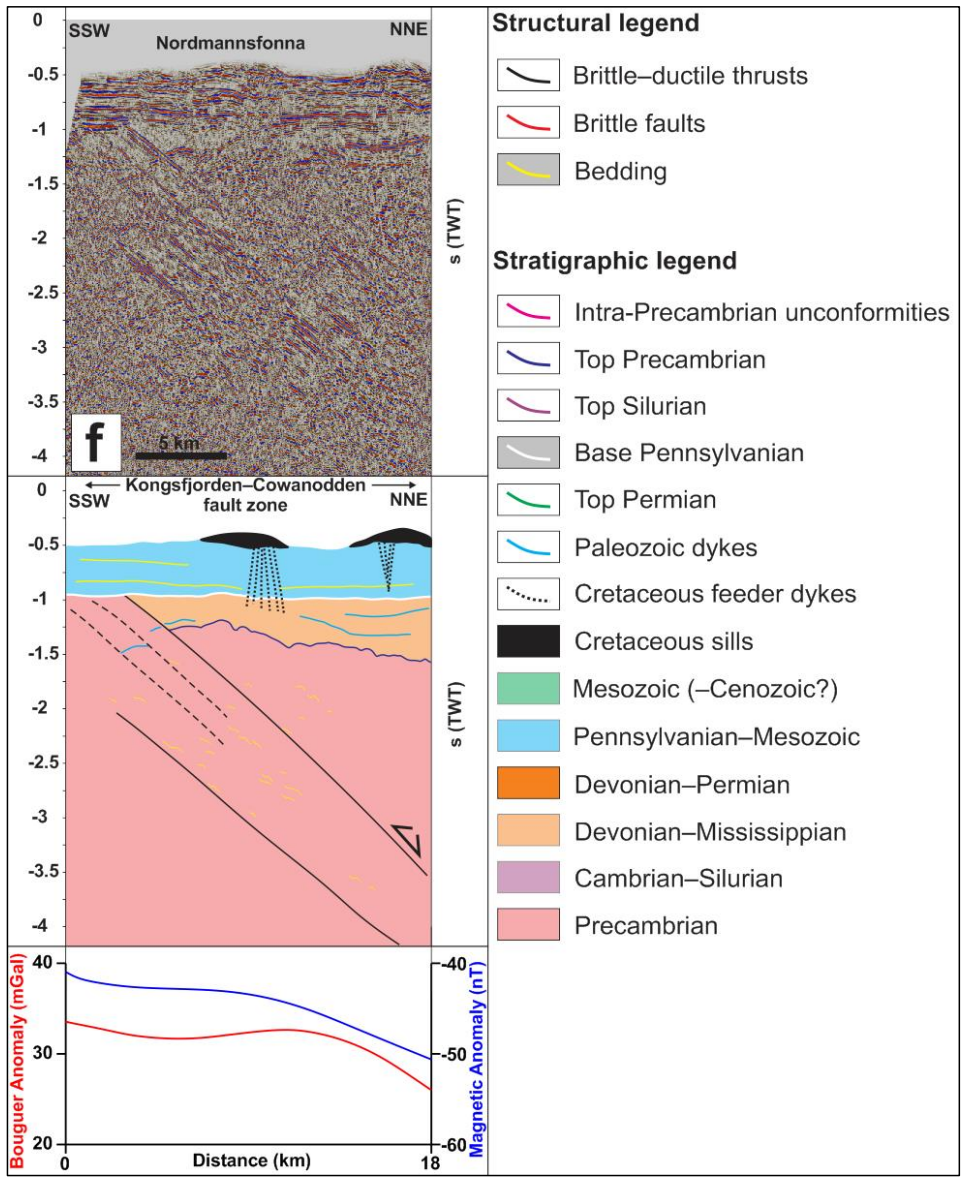
1572 **Figure 2: Paleogeographic reconstruction of the Svalbard Archipelago in the latest Neoproterozoic during the Timanian**
1573 **Orogeny and in the early–mid Paleozoic during the Caledonian Orogeny according to previous models (e.g., Harland, 1969;**
1574 **Labrousse et al., 2008).**







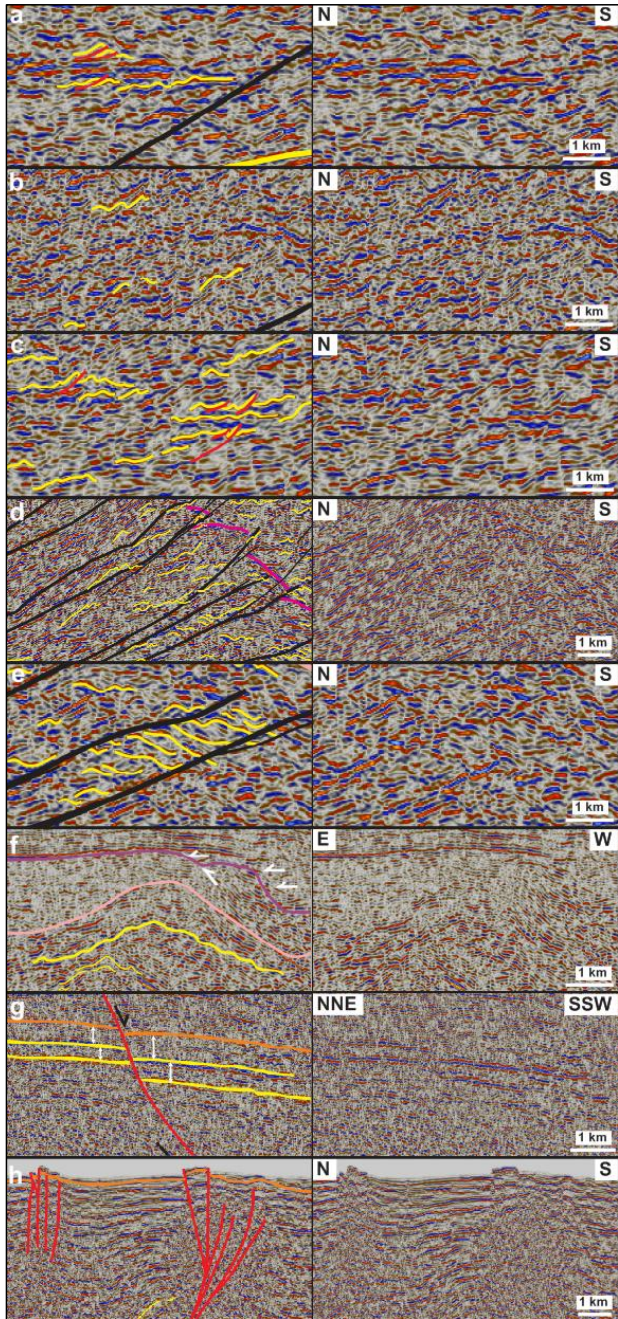




1579
 1580 Figure 3: Interpreted seismic profiles and associated potential field data (a) in Storfjorden, (b) south of Hopen, (c) on the
 1581 Stappen High in the northwestern Norwegian Barents Sea between Spitsbergen and Bjørnøya, (d) on the southern flank of
 1582 the Ora Basin in the northeastern Norwegian Barents Sea, and (e and f) in Nordmannsonna in eastern Spitsbergen. The
 1583 seismic profiles show top-SSW Timanian thrusts that were reactivated and overprinted during subsequent tectonic events
 1584 such as Caledonian contraction, Devonian–Carboniferous late–post Caledonian collapse and rifting, Eurekan contraction,
 1585 and present-day contraction. Profiles (e) and (f) also show Paleozoic and Cretaceous intrusions. The white frames show the

1586 location of zoomed-in portions of the profiles displayed in [Figure 4](#). Potential field data below the seismic profiles
1587 include Bouguer anomaly (red lines) and magnetic anomaly (blue lines). The potential field data show consistently high
1588 gravimetric anomalies and partial correlation with high magnetism towards the footwall of each major thrust systems (i.e.,
1589 towards thickened portions of the crust).

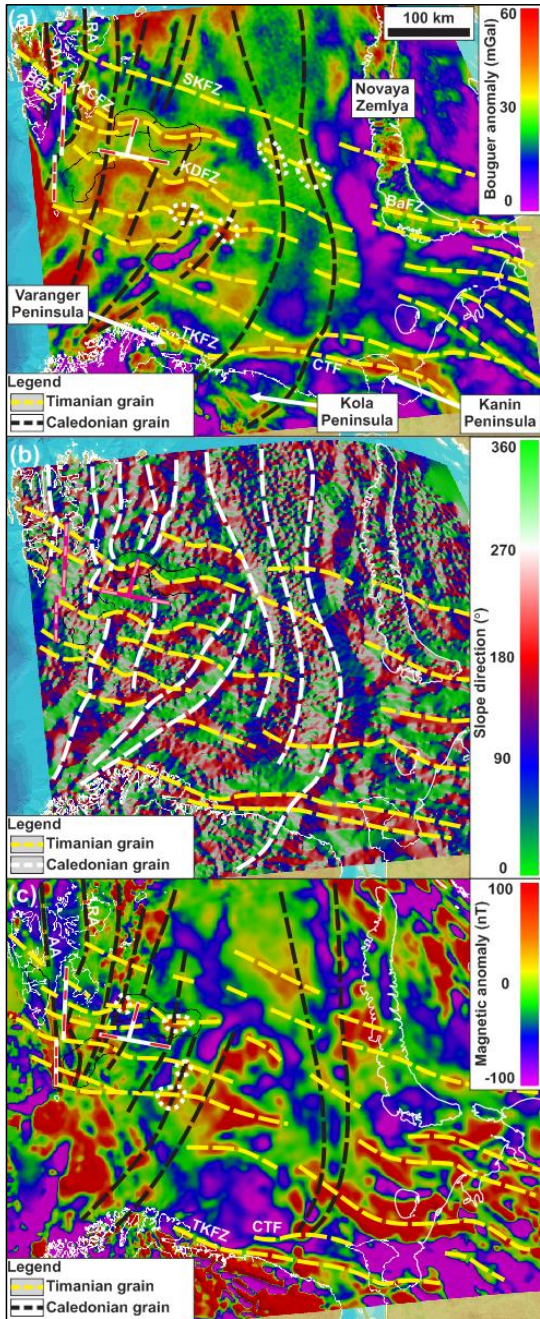
1590



1591

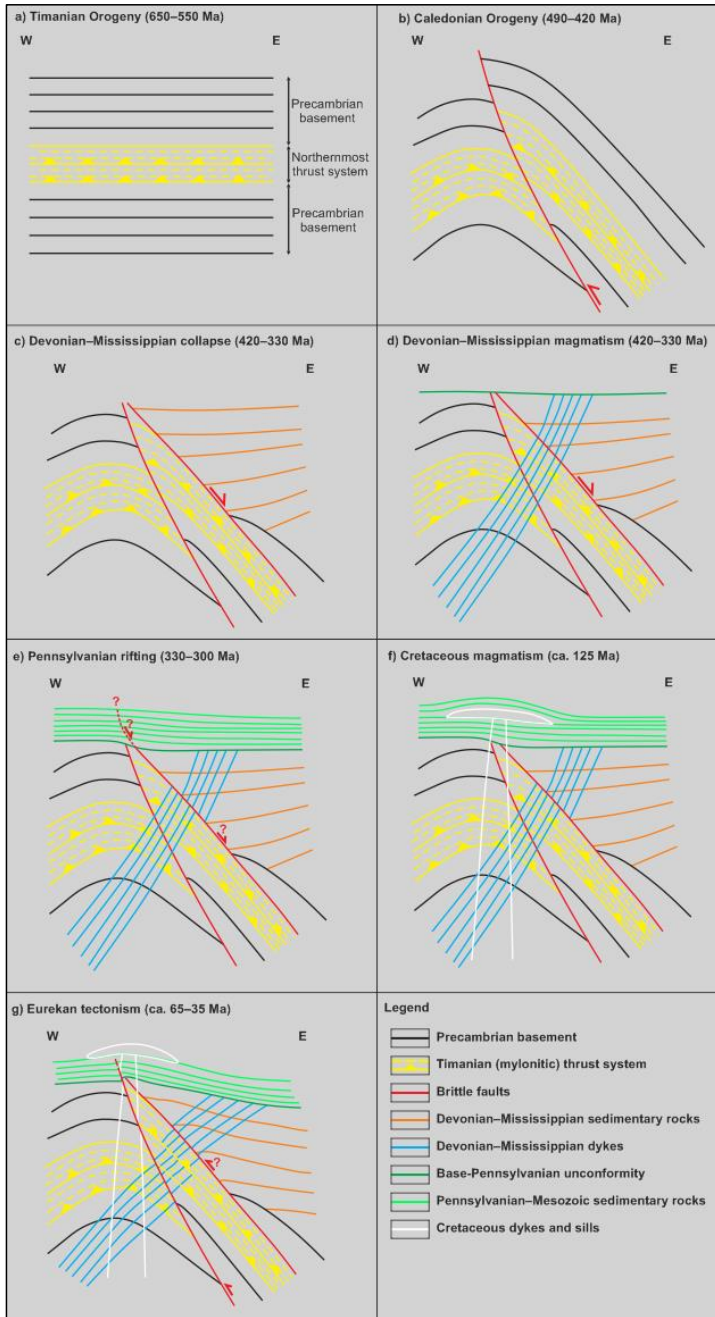
1592 Figure 4: Zooms in seismic profiles shown in [Figure 3](#) showing (a) upright fold structures, (b) SSW-verging folds
1593 and (c) top-SSW minor thrusts in Precambrian–lower Paleozoic (meta-) sedimentary basement rocks, (d) SSW-verging folds
1594 and NNE-dipping mylonitic shear zones within a major thrust that offsets major basement unconformities (fuchsia lines)
1595 top-SSW, (e) duplex structures within a major top-SSW thrust, (f) a N-S- to NNE–SSW-trending, 5–15 kilometers wide,
1596 symmetrical, upright macro-fold and associated, kilometer- to hundreds of meter-scale, parasitic macro- to meso-folds, (g)
1597 syn-tectonic thickening in Devonian–Carboniferous (–Permian?) sedimentary strata offset down-NNE by a normal fault
1598 that merges with a thick mylonitic shear zone at depth, and (h) recent–ongoing reverse offsets of the seafloor reflection by
1599 multiple, inverted, NNE-dipping normal faults in Storfjorden. See [Figure 3](#) for location of each zoom and for legend.

1600



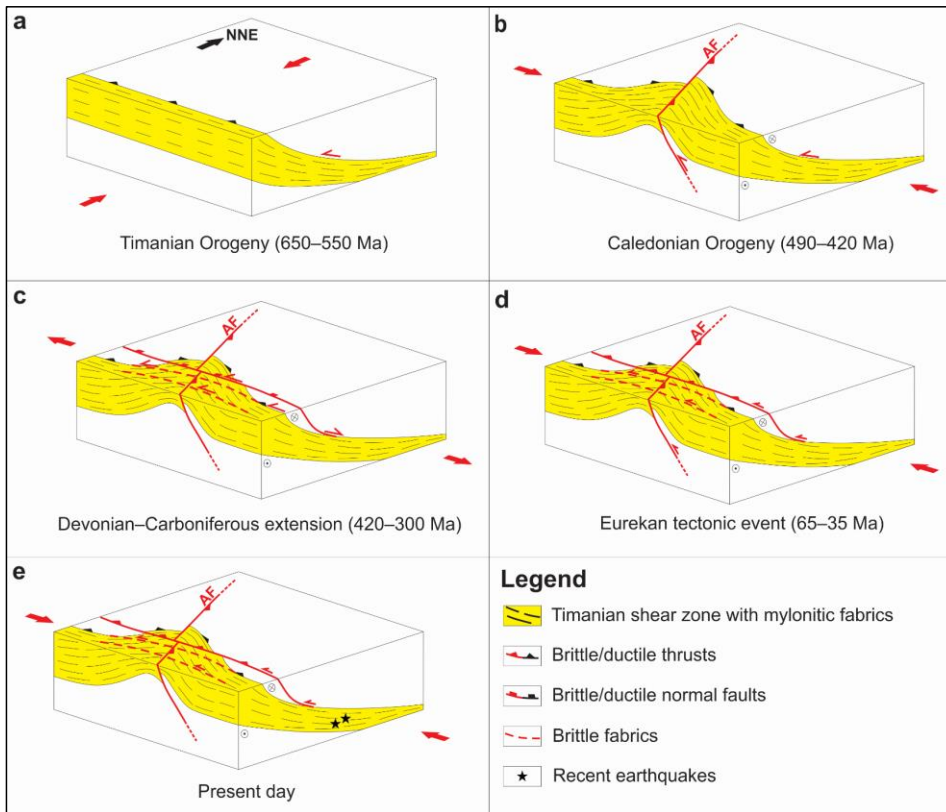
1602 Figure 5: Gravimetric (a and b) and magnetic (c) anomaly maps over the Barents Sea and adjacent onshore areas in Russia
1603 (see location as a dashed white frame in Figure 1b), Norway and Svalbard showing E–W- to NW–SE-trending anomalies
1604 (dashed yellow lines) that correlate with the proposed NNE-dipping Timanian thrust systems in Svalbard and the northern
1605 Norwegian Barents Sea. Note the high obliquity of E–W- to NW–SE-trending Timanian grain with NE–SW- to N–S-trending
1606 Caledonian grain (dashed black/white lines). Note that dashed lines in (a) and (c) denote high gravimetric and magnetic
1607 anomalies. Also notice the oval-shaped high gravimetric and magnetic anomalies (dotted white lines) at the intersection of
1608 WNW–ESE- and N–S- to NNE–SSW-trending anomalies in (a) and (c) resulting from the interaction of the two (Timanian
1609 and Caledonian) thrust and fold trends. The location of seismic profiles presented in Figure 3a–d are shown as thick
1610 white lines in (a) and (c) and as fuchsia lines in (b). Within these thick white and fuchsia lines, the location and extent of
1611 thrust systems evidenced on seismic data (Figure 3) is shown in white in (a) and (c) and in pink in (b). For the E–
1612 W-trending seismic profile shown in Figure 3b, this implies that the red and pink lines represent N–S-trending
1613 synclines. Abbreviations: AA: Atomfjella Antiform; BaFZ: Baidaratsky fault zone; BeFZ: Bellsundbanken fault zone; CTF:
1614 Central Timan Fault; KCFZ: Kongsfjorden–Cowanodden fault zone; KDFZ: Kinnhøgda–Daudbjørnpynten fault zone;
1615 RA: Rijpdalen Anticline; SKFZ: Steiløya–Krylen fault zone; TKFZ: Trollfjorden–Komagelva Fault Zone.

1616



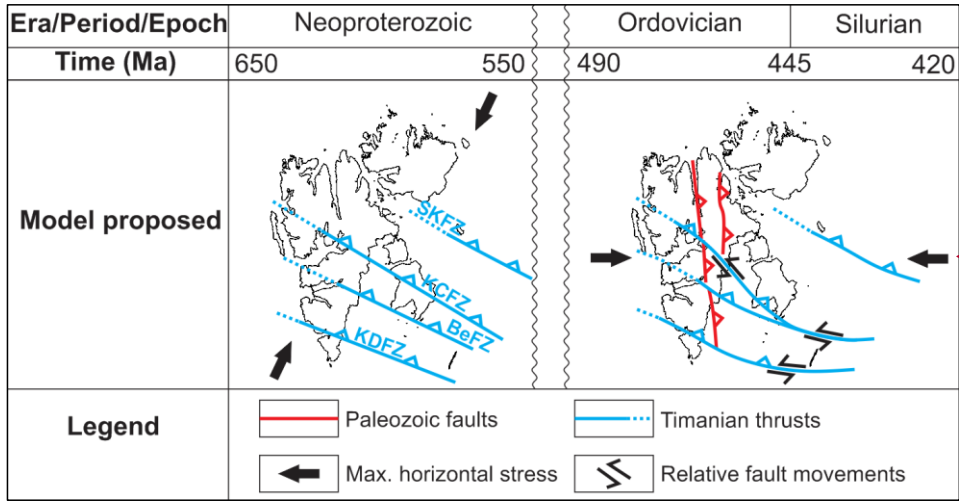
1618 Figure 6: Sketches showing a possible reconstruction of the tectonic history of the E–W seismic profile in Nordmannsfonna
1619 shown in [Figure 3](#) ~~Figure 3e~~. (a) Formation of a NNE-dipping, mylonitic thrust system (Kongsfjorden–Cowanodden fault
1620 zone) within Precambrian basement rocks during the Timanian Orogeny in the latest Neoproterozoic. The NNE-dipping
1621 Kongsfjorden–Cowanodden fault zone appears near horizontal on the E–W transect; (b) Top-west thrusting along the east-
1622 dipping Agardhbukta Fault and folding of the Kongsfjorden–Cowanodden fault zone into a broad, moderately NNE-
1623 plunging anticline during the Caledonian Orogeny; (c) Inversion of the Kongsfjorden–Cowanodden fault zone along the
1624 eastern flank of the Caledonian anticline and deposition of thickened, gently west-dipping, syn-tectonic, Devonian (–
1625 Mississippian?) sedimentary strata during post-Caledonian collapse-related extension; (d) Intrusion of Precambrian
1626 basement and Devonian (–Mississippian?) sedimentary rocks by steeply west-dipping dykes in the Devonian–Mississippian;
1627 (e) Regional erosion in the mid-Carboniferous (latest Mississippian) and deposition of Pennsylvanian sedimentary strata,
1628 possibly along a high-angle brittle splay of the inverted portion of the Kongsfjorden–Cowanodden fault zone during rift-
1629 related extension; (f) Deposition of Mesozoic sedimentary strata and intrusion of Cretaceous dolerite dykes and sills; (g)
1630 Erosion of Pennsylvanian–Mesozoic strata and reactivation of the Kongsfjorden–Cowanodden fault zone and Agardhbukta
1631 Fault with minor reverse movements in the early Cenozoic during the Eurekan tectonic event as shown by mild folding and
1632 offset of overlying post-Caledonian sedimentary strata, dykes and Base-Pennsylvanian unconformity. Also note the back-
1633 tilting (i.e., clockwise rotation) of Devonian–Mississippian dykes in the hanging wall of the Agardhbukta Fault and of the
1634 Kongsfjorden–Cowanodden fault zone.

1635



1636
 1637 **Figure 7: Tectonic evolution of Timanian thrust systems in eastern Spitsbergen, Storfjorden and the northwestern**
 1638 **Norwegian Barents Sea including (a) top-SSW thrusting during the Timanian Orogeny, (b) reactivation as oblique-slip**
 1639 **sinistral-reverse thrusts and offset by top-west brittle thrust overprints (e.g., Agardhbukta Fault – AF) under E-W**
 1640 **contraction during the Caledonian Orogeny, (c) reactivation as low-angle, brittle–ductile, normal–sinistral extensional**
 1641 **detachments and overprinting by high-angle normal–sinistral brittle faults during Devonian–Carboniferous, late–post-**
 1642 **Caledonian extensional collapse and rifting, (d) reactivation as brittle–ductile sinistral–reverse thrusts, overprinting by**
 1643 **high-angle sinistral–reverse brittle thrusts, and mild offset by reactivated top-west thrusts (e.g., Agardhbukta Fault – AF)**
 1644 **during E–W Eurekan contraction, and (e) renewed, recent–ongoing, sinistral–reverse reactivation and overprinting possibly**
 1645 **due to ongoing magma extrusion and transform faulting (ridge-push?) in the Fram Strait.**

1646



Formatted: Keep with next

1647

1648

1649

Figure 8: Paleogeographic reconstruction of the Svalbard Archipelago in the latest Neoproterozoic during the Timanian Orogeny and in the early–mid Paleozoic during the Caledonian Orogeny according to the present study.

Formatted: Font: (Default) Times New Roman, Bold, Not Italic

Formatted: Caption